THESIS

IMPROVING HYDROPHILICITY OF SILICONE ELASTOMER BY IPN FORMATION WITH HYALURONAN

Submitted by

Richard L. Koch

Graduate Degree Program in Bioengineering

In partial fulfillment of the requirements

For the Degree of Master of Science

Colorado State University

Fort Collins, Colorado

Summer 2016

Master's Committee:

Advisor: Susan P. James

Travis Bailey
Ketul C. Popat

ABSTRACT

IMPROVING HYDROPHILICITY OF SILICONE ELASTOMER BY IPN FORMATION WITH HYALURONAN

Soft contact lenses have been available to consumers for the past several decades. By far, the most popular form on the market today is the silicone hydrogel, with nearly 70% of the market share. However, many contact lens wearers still have issues which cause them to discontinue lens use. It is estimated that between 25-35% of people discontinue use permanently. This can be traced back to two main issues with modern hydrogel lenses: a lack of adequate oxygen permeability across the lens; and lens-induced dehydration of the cornea. The corneal epithelium lining the lens of the eye is an avascular environment. As such, the cells must get their oxygen by diffusion through the tear film, or any material covering the lens. The silicone hydrogel SCLs have reduced oxygen gas permeability compared to traditional silicone elastomers. Additionally, when the hydrogel lenses lose water to evaporation, they pull water from the wearer's eye, contributing to dryness. Beyond simple discomfort, these issues can lead to pathologies such as hyperemia and even corneal cell death in severe cases. It was determined that a solution to these issues would be a new ocular lens material which had superior oxygen gas permeability and was hydrophilic without containing water in its bulk. The aim of this research was to create an interpenetrating polymer network (IPN) materials of poly(dimethyl siloxane) (PDMS) and hyaluronan (HA) with such properties. The results in this work indicate the successful synthesis of these HA-PDMS IPN materials. These elastomeric materials had improved hydrophilicity compared to untreated PDMS. Additionally, new chemical species (ATR/FTIR and XPS

spectroscopy) and surface morphologies (SEM imaging) indicated the introduction of HA into the PDMS. Furthermore, analysis of the oxygen gas permeability showed no significant change for the treated samples as compared to the PDMS base material. As silicone materials have use in many biomedical fields, the material was also tested for platelet adhesion/activation and whole blood clotting. However, studies showed unfavorable results as the treated samples still caused platelet activation and blood clotting. Additionally, overall optical transmittance of the treated materials was significantly decreased. Further refinement of the treatment methods may yield more favorable results in the areas of thrombogenicity and platelet adhesion.

ACKNOWLEDGEMENTS

I would like to thank my academic advisor, Dr. Susan P. James, for all the support, guidance, knowledge, and her invaluable time that she has shared with me throughout my career. Even as an undergraduate worker, before I became her graduate student, she showed an exceptional level of commitment to my professional and personal development. I would also like to thank my committee members, Dr. Travis Bailey and Dr. Ketul C. Popat, as well for their extensive guidance in this work, particularly in the areas of polymeric materials and blood contacting materials. In addition to having them as committee members, I also had the pleasure of learning much from the classes they taught. Although he is not an official member of my committee, I would like to acknowledge Dr. David Prawel for his time, lab management, valuable advice, and general contribution to my development as an academic and professional.

Several other persons and groups deserve acknowledgement, and my sincere thanks, due to their technical contribution to this work, in terms of skills utilized and/or equipment furnished: Dr. Arun Kota and his lab for the (frequent) use of both their contact angle goniometer and their spin coating system and the guidance for the aforementioned equipment; Nicole Dixon, PBT and the other technicians at the Colorado State University Health Center Laboratory for their assistance in drawing blood; Dr. Patrick McCurdy and the others in the Central Instrument Facility for the many instruments and associated hours of training they supplied; Rachael Simon-Walker for her guidance in cell and blood studies; Alyssa Winter for the creation of the gas permeation apparatus used in this study as well as the instruction of its use; and the entire Biomaterials Research and Engineering Laboratory (BREL) group whose assistance on many levels made much of this work possible.

TABLE OF CONTENTS

CHAPTER 1: INTRODUCTION AND OVERVIEW

1.1 Motivation for Research

For decades, contact lenses have served as a convenient alternative to prescription eye glasses for many people. As of 2014, there were nearly 40 million wearers of contact lenses in the United States [1]. However, symptoms of discomfort due to lens use results in an estimated 24.1% to 35% of soft contact lens wearers to permanently discontinue use. This discomfort can be attributed to two main contact lens effects: corneal drying; and a reduction in oxygen reaching the corneal epithelial cells [2-4]. Beyond simple discomfort and the discontinuation of use, these two factors can also result in serious pathologies in some cases. The majority of these pathologies are discussed in more detail in a later section. Many variations in contact lenses have been developed to improve comfort, safety, and general consumer satisfaction. Currently, the dominant form of contact lenses is soft contact lenses (SCLs) made of silicone hydrogel, which accounts for an estimated 68% of all contact lenses sold to consumers in 2014 [1]. Silicone hydrogel SCLs come in many forms, but are characterized by a significant portion of their bulk containing water. While these SCL materials are hydrophilic and generally lubricious, research and surveys have found that they tend to contribute to dryness and discomfort with certain users. It has been documented that hydrogel lenses such as these will lose water from evaporation to the environment and subsequently remove water from the surface of the wearer's eye to compensate [3]. This can be especially problematic in arid climates, dry atmospheres (such as due to winter heating), and for users already suffering from dry eyes. A general concern with any type of cornea contacting material is oxygen permeability of the material; i.e. how well does oxygen gas diffuse through the material. This is because the cells on the cornea are in an avascular

environment and they must get their oxygen via diffusion through the atmosphere and tear film. Therefore, a lens material must have sufficient oxygen gas permeability to avoid discomfort or damage to the tissue. Conventional silicone hydrogels have reported oxygen permeability coefficients (Dk) as high as 160 Barrer [3, 4] for high-end day and night use SCLs whereas traditional silicone elastomer films, which contain no significant water in their bulk, have reported Dk values as high as 800 Barrer [5]. It is clear that the contact lens users would benefit from a contact lens that does not cause dryness and has superior oxygen gas permeability. Thus, this research aimed to develop a method for the creation of hydrophilic silicone elastomers to produce a material for contact lens use with superior oxygen gas permeability. In particular, the research focused on making interpenetrating polymer networks (IPN) of poly(dimethyl siloxane) elastomers and hyaluronic acid, a hydrophilic biopolymer found in many mammalian tissues. The following literature review is a concise overview of corneal physiology, current technologies for contact lenses, their problems and possible pathologies, and the select chemistry relevant to the research discussed in later chapters.

1.2 Literature Review

1.2.1 Cornea physiology

The outer, exposed surface of the eye can be divided into two regions: the cornea and the sclera. The sclera is a structure of opaque, mostly white connective tissue that serves to protect the eye, provide structure, provide ocular muscle attachment, and is highly vascularized. The cornea, while also having some protective role, is clear, crucial in light transmittance and vision, and is avascular. A drawing of the cornea can be seen in Figure 1.1 as the upper most structure in the image. The anterior surface of the cornea is lined with a layer of epithelial cells which reside in the avascular environment; because of this, they must receive their nourishment and oxygen

via diffusion through the surrounding fluids and atmosphere [6, 7]. This anterior surface is also the surface on which a typical contact lens would rest. The region between the cornea and the lens is called the Anterior Chamber and is filled with fluid which is rich in proteins, nutrients, and oxygen. Posterior to the lens is a larger chamber called the Posterior Chamber, which is filled with vitreous humor containing hyaluronic acid.

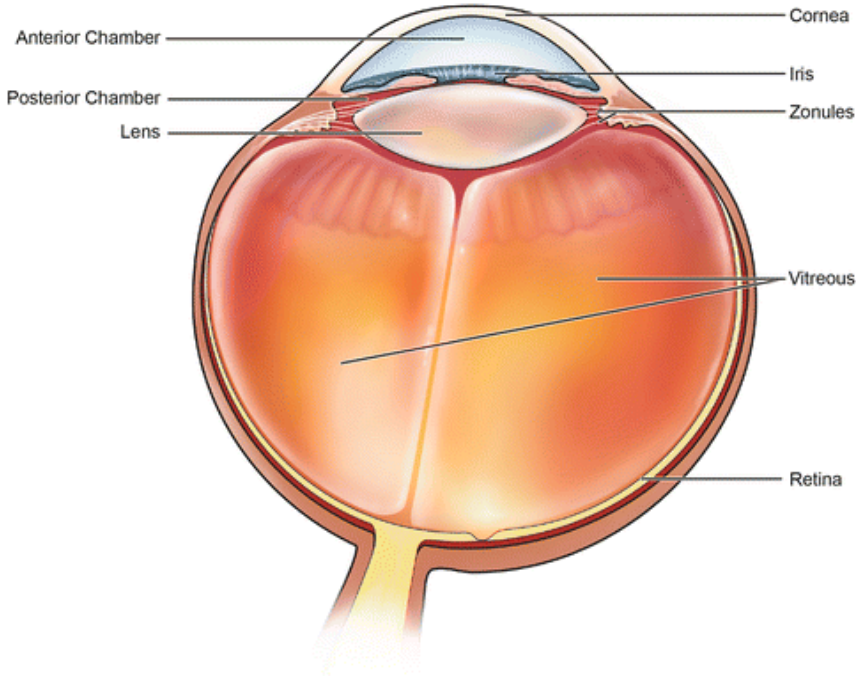

Figure 1.1: A sagittal cross-section of the human eye [7].

1.2.2 Pathologies of the cornea

The effect that any membrane (such as a contact lens) has on the health of the corneal epithelium has been studied for a long time. Two major areas of study have been in: determining the amount of oxygen permeability a film on the corneal surface must have to avoid pathologies; and the drying effect that some hydrogel lenses can have on the eye.

1.2.2.1 Hypoxia and Related Disease States

As mentioned previously, the epithelium on which the film rests is in an avascular environment and must get its oxygen from diffusion from the atmosphere and through the tear film. The oxygen gas permeability or transmissibility of a material describes how well oxygen gas can diffuse through the material. Permeability coefficients, Dk, for ocular lens applications are often presented in units of Barrers (10^{-11} (cm^3 O_2) cm cm^{-2} s^{-1} $mmHg^{-1}$) named after Richard Barrer. Work by Holden and Mertz demonstrated that any material which covers the lens must have a minimum oxygen transmissibility of 87 Barrer/mm to prevent corneal edema (corneal swelling) [8, 9]. That is, that the material must have a minimum of oxygen permeability 87 Barrer per millimeter of material thickness (Dk/t). However, a more recent study performed by Harvitt, et al. suggests an even higher minimum threshold of 125 Barrer/mm in order to avoid any serious effects of hypoxia on the corneal surface [10].

When a material restricts the amount of oxygen that reaches the corneal epithelium below a critical amount, it can induce a state of hypoxia. Over short periods of time, there is usually no damage to the tissue. However, when the epithelium is subjected to hypoxia for extended periods and/or chronically, discomfort or even disease states can occur [11]. This discomfort commonly affects users who regularly wear contact lenses for the majority of the day, or over multiple days, and is commonly referred to as "end-of-day contact lens discomfort" by many in the industry. Disease states which can develop due to lens induced corneal hypoxia include: edema; hyperemia (excessive vascularization of the conjunctiva); and the development of corneal mircocysts in extreme cases [8, 11, 12].

As a side note, a literature search shows no documented serious corneal pathologies associated with high oxygen conditions, "hyperoxia."

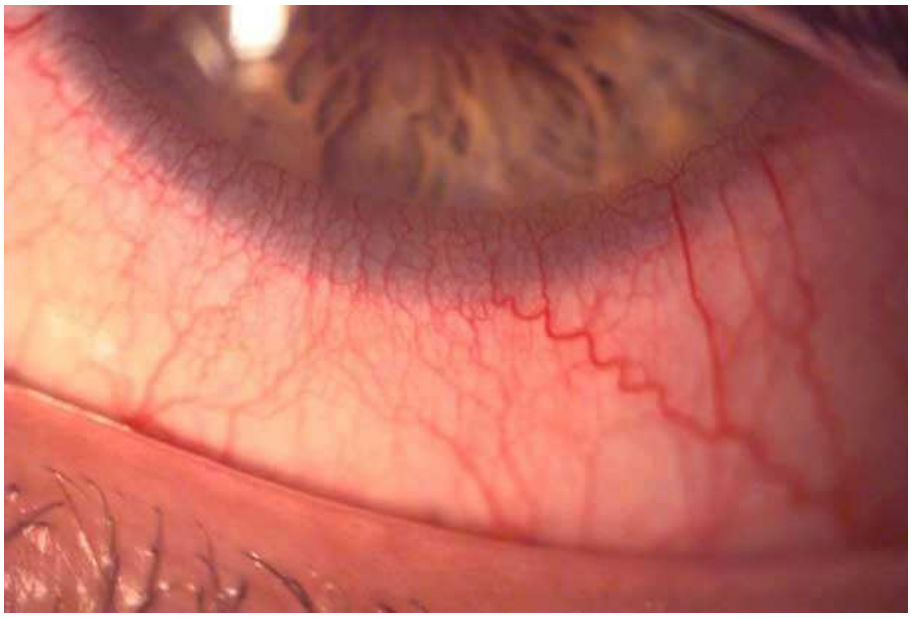

Figure 1.2: Patient's sclera suffering from hyperemia [13]

1.2.2.2 Corneal Dehydration and Related Disease States

Concerns have increased over the last couple decades about the corneal dehydration tendencies of some current hydrogel contact lenses. As discussed earlier in this chapter, many hydrogel contact lenses have the tendency to remove water from the wear's eye to replace water lost from the lens due to evaporation. This can result not only in discomfort but also in disease states if it is severe enough. Irritation and sensations of dryness due to contact lens wear have been reported by as many as half the users. Additionally, discomfort resulting from lens induced dryness is one of the leading causes for contact lens discontinuation [3, 14].

Apart from user discomfort, a pathology known as corneal epithelial staining (named after its detection technique) is the major concern with lens induced dryness. Damage to the corneal epithelial cells, including cell death, can result from this dehydration. This cell damage or death is commonly seen clinically by staining with a fluorescent agent (e.g. fluorescein) that enters damaged membranes or fills gaps of epithelial cells on the corneal surface (hence the name). An example corneal staining of a patient's eye can be seen in Figure 1.3.

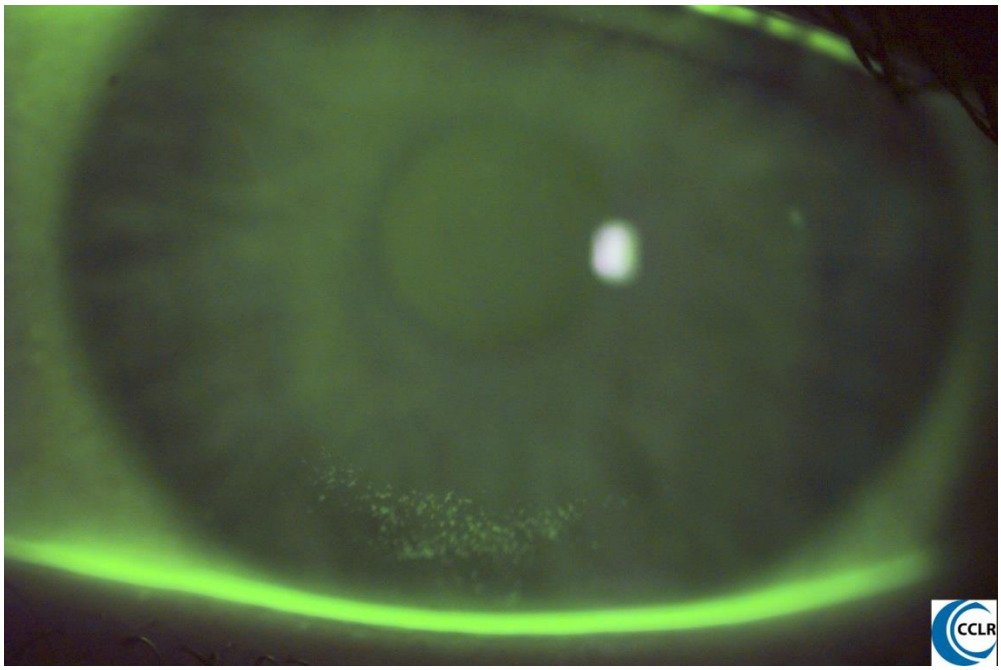

Figure 1.3: Example of corneal staining of a patient's eye. The corneal staining near the bottom of the cornea indicates a damaged epithelium [15].

1.2.3 Current Contact Lens Technologies

Contact lenses have been used to correct vision since the late 1800s. The original lenses were made from glass and were quite large compared to standard lenses today [9]. Since then, various technologies have emerged, notably: rigid gas permeable lenses made from stiff plastic; non-hydrogel soft contact lenses (SCLs); and hydrogel soft contact lenses. Lens technology has evolved over time in an effort to create lenses that are both more comfortable and can be safely worn longer without pathologies such as those discussed earlier. In the last decade, the dominant form of contact lens emerged as silicone hydrogels. While rigid gas permeable lenses are still used by a portion of lens wearers today, they account for less than 10% of the market [1]. Therefore, the remaining discussion will be focused on soft contact lenses (SCLs).

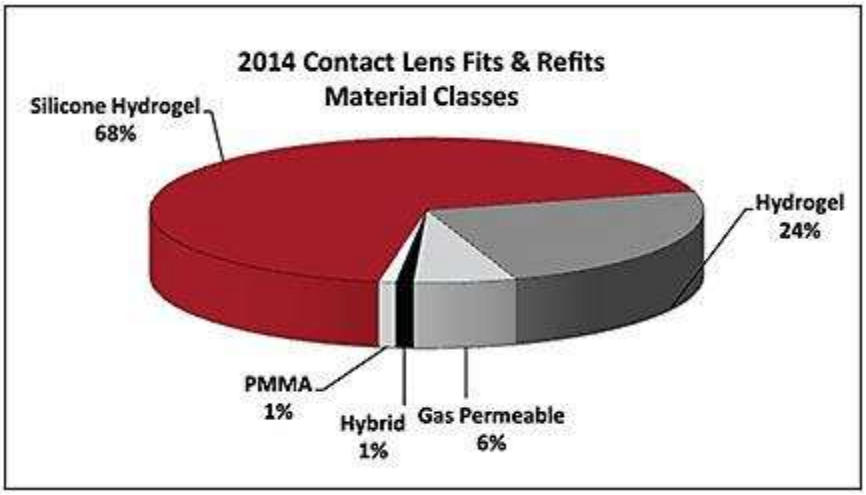

Figure 1.4: Distribution of material types for contact lenses based on clinical prescriptions [1].

1.2.3.1 Soft Contact Lenses (SCLs)

Hydrogels are distinguished from other polymers in that they are water-swollen polymeric materials that maintain their shape and do not dissolve when in water [16]. Hydrogel soft contact lenses (SCLs) have been commercially available since 1970. Wichterle is credited with leading the development of the technology for these first SCLs which were made of poly-hydroxyethylmethacrylate (pHEMA) and could be fabricated by lathing zero-gels as well as direct spin casting [9]. Since the introduction of this new form of lens material, the market has exploded with many varieties of hydrogel SCLs and has become a multi-billion dollar industry [17].

Some examples of current commercially available hydrogel SCLs are: ACUVUE OASYS (Senofilcon A, Johnson & Johnson; New Jersey, USA); Air Optix (lotrafilcon B, Alcon; Texas, USA); ACUVUE 2 (etafilcon A, Johnson & Johnson; New Jersey, USA); DAILIES AquaComfort Plus (nelfilcon A, Alcon; Texas, USA); and Biofinity (comfilcon A, CooperVision; California, USA). The previous list represents the top five "most popular" products from a well-known contact lens vender: 1800-Contacts (Utah, USA) [18]. The

aforementioned commercial SCLs have water contents ranging between 33 and 69% of the material by mass according to their respective product data sheets from the manufacturers.

However, a report published by Holden, et al. in 1984 about the requirement of oxygen transmissibility shook the industry. In this report it was declared that a minimum transmissibility of 87 Barrer/mm was needed to avoid corneal edema for any overnight contact lenses. At the time, no SCL hydrogel material was commercially available that met this requirement [8, 9]. To make things more difficult for the industry, a more recent report by Harvitt, et al suggested a minimum transmissibility of 125 Barrer/mm to completely avoid issues resulting from low oxygen conditions [10].

Silicone hydrogel SCLs were created in an effort to combat this issue of wearer discomfort due to low oxygen permeability of older hydrogel SCLs [9]. In the most general definition, silicone hydrogels are distinguished by the silicone component in the polymeric material. Silicone hydrogels benefit from higher oxygen gas permeability when compared to other older hydrogel SCL material with reported values as high as 160 Barrer for modern silicone hydrogel lenses [3, 4]. In the time since the development of the original SCLs, silicone hydrogel SCLs have risen to be the market dominant form since their introduction in the 1980s [1]. To illustrate the prevalence of silicone hydrogel SCLs, in the above list of five popular SCLs all but one are forms of silicone hydrogel; the only exception is the DAILIES AquaComfort Plus (nelfilcon A) which is a polyvinyl alcohol (PVA) based hydrogel [19].

1.2.3.2 Limitations of Current Technology

Silicone hydrogels, which lead the market as the most prevalent SCL material, are not without their issues. While the silicone hydrogels do have superior oxygen gas permeability coefficients (Dk) when compared to other hydrogels, they still possess a decreased Dk when

compared to elastomeric, non-water containing forms such as poly(dimethyl siloxane) (PDMS). Dk values for commercial SCLs have been reported to be as high as 160 Barrer whereas PDMS has values as high as 800 Barrer [3-5]. As discussed earlier in this chapter, it is important for eye health that any cornea contacting material to have at least a certain degree of oxygen permeability: 125 Barrer/mm [10]. While some of these thinner silicone hydrogel SCLs can meet this requirement to avoid pathologies, there is still considerable consumer dissatisfaction that can be traced back to a lack of oxygen transfer across the lens. The effect of this reduced oxygen transmissibility is exacerbated in lower oxygen environments such as higher altitudes and by those who already have issues with sensitivity of the eyes [2, 14, 20].

In addition to complications related to oxygen transmissibility, there is also concern related to the tendencies of these hydrogel lenses to dehydrate the wearer's eyes. Research has linked this tendency to the high water content of the hydrogels. As water is lost from the lens material to the environment, the lens adsorbs water from the wearer's eyes. This issue is only made worse in arid climates or artificially dry environments (e.g. due to winter heating). Similar to above, this is also worse for those who already have naturally dry eyes [2, 14, 20].

Based on the above listed limitations of current soft contact lens technology, this work intended to create a new ocular lens material. This new material will be designed to contain no water in its bulk, have superior oxygen transmissibility, have similar surface wettability and similar optical clarity compared to current silicone hydrogel SCLs. The material chosen for this work was an IPN of HA and a silicone elastomer, poly(dimethyl siloxane), as the latter possess extraordinarily high oxygen gas permeability among polymers and contains no water in its bulk [4]. The host polymer in this sequential IPN is PDMS (99%) and the guest polymer is HA.

1.2.4 PDMS elastomers

Silicones are a category of polymers which are characterized by a backbone of alternating oxygen-silicon bonds with functional groups attached to the silicon. Silicones have found a myriad of different uses in the modern world. Variations in chemistry and curing conditions can produce materials with a wide variety of physical properties and forms: liquids; gels; hydrogels; rubbers; and resins/solids. Beyond having the ability to be formed with desired mechanical properties, silicones also exhibit a number of properties contributing to a high overall biocompatibility: chemical inertness; thermal stability; antimicrobial properties; and excellent oxygen permeability [5, 21]. Historically silicones have seen use in the biomedical device field as breast implants, facial prostheses, catheters, drug delivery systems, small joint implants, and soft contact lenses [22-24].

Possibly the most basic example a silicone elastomer is poly(dimethyl siloxane) (also known as "PDMS"). Figure 1.5 shows the simple chemical structure of uncrosslinked PDMS. The functional groups are methyl groups in this case.

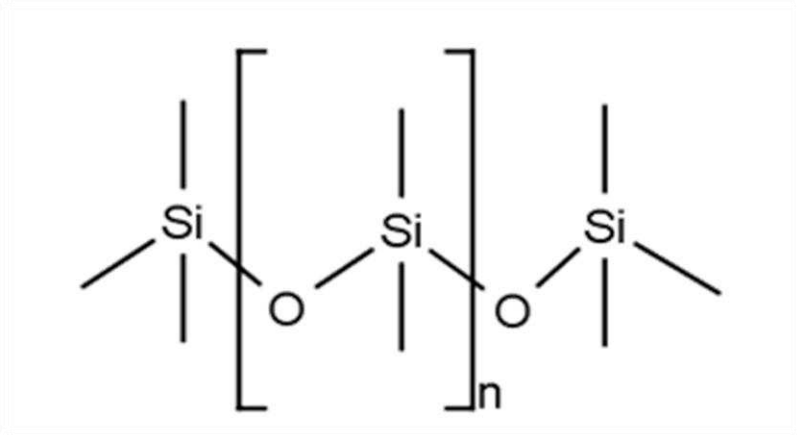

Figure 1.5: Chemical structure of poly(dimethyl siloxane). The unlabeled groups off the silicon are methyl groups. Original work.

PDMS can be processed in a variety of ways to have a material with desired properties. The individual chains can be made to various lengths, can be cross-linked to each other, and/or filler (usually silica) can be added to change the material properties of the final product. By modifying these parameters, this simple polymer can be made into anything from oils to stiff rubbers. PDMS is also known as being exceptionally permeable to oxygen even among the other silicone polymers [5].

However, despite its other biocompatible aspects, surface properties of unmodified PDMS such as hydrophobicity and associated protein adsorption/adhesion have contributed to clinical complications when used as medical devices or implants [25, 26]. Many attempts have been made in the literature to modify PDMS materials through a variety of methods to overcome this issue. These modifications have ranged from grafting hydrophilic species to the outer surface backbone, chemically modifying the native outer surface (such as plasma oxidation/activation), complete modification of the chemical structure, and forming interpenetrating polymer networks (IPNs) with hydrophilic polymers [22, 26, 27]. It is this last synthesis method (IPNs) that this work focused on. A review of the formation of IPNs is contained in the following section.

1.2.5 IPNs

An interpenetrating polymer network (IPN) is a category of composite material in which there are two or more polymeric species whose networks are intimately entangled in such a way that they cannot be separated without breaking bonds but are, at the same time, not bound to each other [22, 28]. This is to say that with the distinct polymeric species A and B, there is no chemical binding of A-B, only A-A and B-B. These materials retain their form and properties solely by virtue of the physical entanglement of their respective cross-linked networks. Figure 1.6 below shows a simple cartoon which shows an example of this. One of the major benefits of

these IPN composites is the retention of desirable traits from both species: mechanical and/or surface interactions [29].

Figure 1.6: A simple cartoon depicting an example IPN. Note that the blue and yellow networks are not chemically bound to each other, only entangled [30].

Possibly the most simple, and common, method for forming IPNs such as these is referred to as the "monomer immersion" method [29]. In this method, a polymeric cross-linked network that is already formed serves as the host polymer. This host polymer is immersed in a solution containing the monomer of the polymer of interest. The monomers, once impregnated in the host polymer, are then polymerized and cross-linked to each other *in situ*. This network formed *in situ* is referred to as the guest polymer and a sequential-IPN is now made. These types of IPNs are referred to as "sequential" because their respective polymeric networks are formed in sequence (i.e. first the host polymer and then the guest polymer(s)) [29, 31].

It is this type of sequential-IPN which this work was inspired to create. With the many desirable properties of PDMS preserved, then inclusion of a hydrophilic guest polymer would result in a material with desired surface hydrophilicity and bulk properties. For this purpose, hyaluronan, a highly hydrophilic biopolymer common in mammals was chosen to act as the guest polymer. The following section contains a discussion of and background information on hyaluronan.

1.2.6 Hyaluronan and its Biomedical Applications

Hyaluronan, or hyaluronic acid (HA), is a biopolymer which has received much attention from the scientific community, especially in the area of biomaterials. This section is dedicated to the discussion of HA, its significance in biomaterials, and its derivatives used in this work.

1.2.6.1 Hyaluronan: An Overview

Hyaluronan (HA) is a biopolymer composed of disaccharide repeat units and is common in virtually all mammalian tissue, with especially high amounts in synovial fluid and the vitreous humor of the eye. HA is exceptionally hydrophilic, lubricous, and its ubiquitous presence in tissue has been linked to improved overall biocompatibility and acceptance of materials which have been modified to include HA [32, 33]. Figure 1.7 shows the chemical structure of the disaccharide repeat unit of which the HA polymer is composed. As can be seen from this figure, HA is a linear, unbranched polysaccharide.

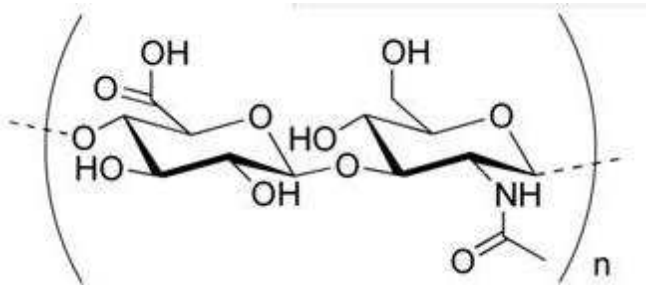

Figure 1.7: The chemical structure of a repeat unit of hyaluronan [34].

HA is not only hydrophilic, but will also retain water to swell to 1000 times its dry size when hydrated. This great increase in volume is due in part to the large molecular volume allowing HA domains to overlap and entangle [34, 35]. This large degree of swelling in the presence of water means that a relatively small amount of HA on a surface can have a great effect on overall hydrophilicity and lubricity of said surface. However, this high hydrophilicity also means that HA will dissolve in water if not properly anchored or bound to a surface. In

addition to this, the enzymes that degrade HA, hyaluronidases, are just as ubiquitous as HA. Both of these issues have been shown in past work to be avoidable or minimized by chemically cross-linking HA. Previous work with HA treated surfaces exposed to multiple levels of hyaluronidases by Zhang, Lowry, and Beavers demonstrated that chemical binding or cross-linking of HA greatly reduced the action of this enzyme on the treated material [35, 36].

Interestingly, the way in which cells respond to the presence of hyaluronan is, in part, determined by the molecular weight of the HA polymer. It has been observed that lower molecular weight HA (below $3.5x10^4$ Da) is involved in triggering ECM turnover and the inflammatory response. In contrast, higher molecular weight HA (above $2x10^5$ Da) has been shown to inhibit cell proliferation and angiogenesis [32, 37-39].

1.2.6.2 Chemical Modifications of Hyaluronan

Chemical modification of hyaluronan used in this work is discussed in more detail in Chapter 2 and is based on the work of Zhang [40]. In brief, trimethyl silyl groups (Me_3Si-) were substituted for the existing hydroxide groups on the HA structure, producing a hydrophobic polymer whose network has the capability of being swelled by the organic solvent xylenes, which also expands the polymeric network of the silicone elastomer. This is accomplished in two main stages: conversion of water soluble HA to the DMSO soluble HA-CTA complex; then the HA-CTA complex is converted to the xylenes soluble silyl-HA-CTA. Figure 1.8 below shows the change in chemical structure as these conversions happen as outlined by Zhang.

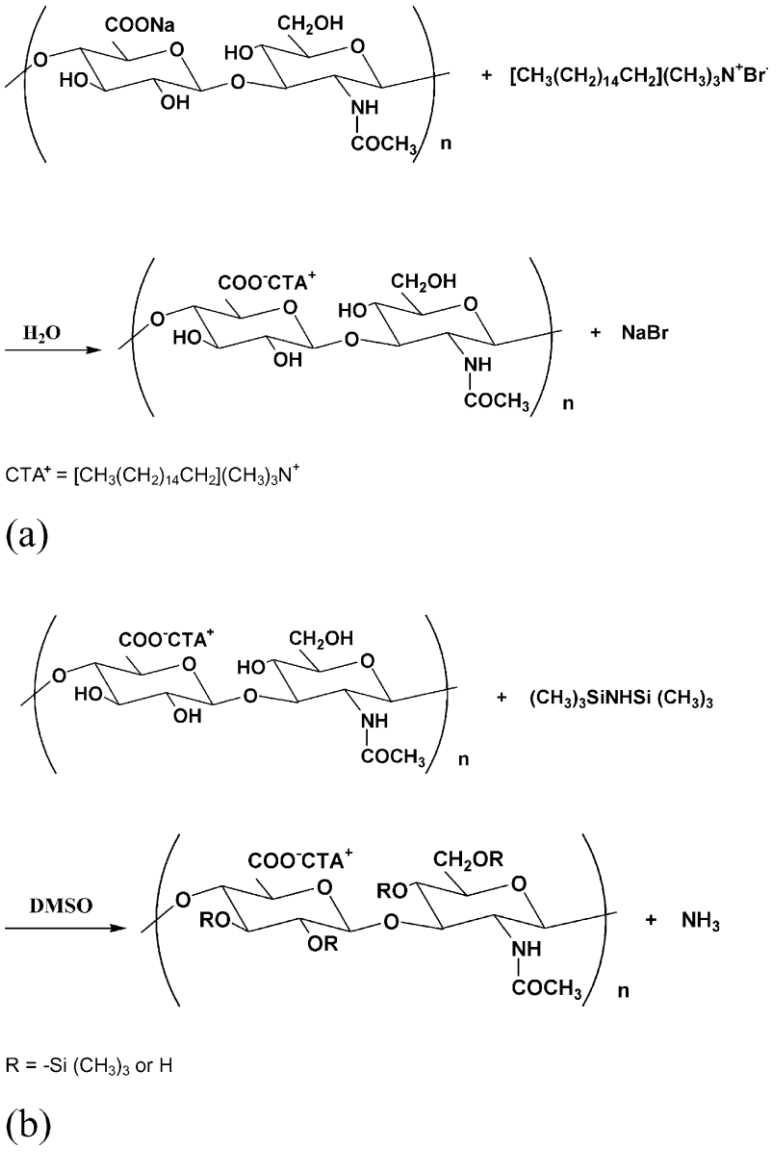

Figure 1.8: Schematic of the conversion of Na-HA to HA-CTA (a) and then from HA-CTA to silyl-HA-CTA (b) [40]

1.2.6.3 Prior Work with Combining HA and Synthetic Plastics for Biomedical Applications

Hyaluronan (HA) has seen use in many different applications in the biomedical field due to its many desirable properties and biological interactions. HA has been formed into cross-linked hydrogel matrices, chemically grafted onto material surfaces, and used as direct injections into tissues just to name a few prevalent uses [32, 41-43]. However, integration of HA into

hydrophobic, synthetic polymeric materials presents its own unique challenges and is of particular interest to this work.

Such examples include work done by Zhang, et al. and Dean, et al. In these works, HA was used to modify the surfaces of ultra-high molecular weight polyethylene (UHMWPE) and linear low density polyethylene (LLDPE), respectively. In the former, a microcomposite was created by adding small amounts of HA to the UHMWPE bulk material [35]. This work would later go on to drive the creation of a commercially available synthetic articular cartilage repair product: BioPoly (Schwartz Biomedical; Indiana, USA). However, the present work differs from Zhang's both in that their material was a microcomposite (not an IPN), made with a very different manufacturing approach, and that their material was a rigid, opaque polymer for weight bearing applications.

1.3 Material selection

As mentioned earlier in this chapter, silicone materials possess exceptionally high oxygen gas permeability as well as a breadth of processing possibilities. Additionally, silicone materials can be made such that they are optically clear while still maintaining good mechanical and handling properties. Based on this, poly(dimethyl siloxane) (PDMS) was chosen to be the base material for the HA-silicone IPN creation. PDMS materials used in this work were obtained via commercially available two-part liquid silicone rubber (LSIR) kits and were made on site. The LSIR kit used for the majority of this work was the P-125 kit (Silicones, Inc; North Carolina, USA). This product is a platinum-catalyzed, addition cure, room temperature vulcanizing (RTV) LSIR two-part kit. This means that the curing of the mixed components requires no heat or extra additives.

More detail about the selection and characterizing of the base materials considered for this study can be found in Chapter 2.

1.4 Thesis Objectives and Specific Aims

While soft contact lenses (SCLs) have made significant strides since their appearance on the market, they are still not without their issues. Efforts into making more comfortable lenses lead to the development of the first hydrogel SCLs made of pHEMA. When discovery of a high degree of oxygen transmissibility was made [8, 10], silicone hydrogels rose to the scene to address this issue. Satisfactions surveys and clinical visits chronicled over the last decade have begun to enlighten the industry and scientific community to two remaining major issues: that the high water content of some of the most popular SCLs may be contributing to discomfort and pathologies; and that, despite improvements in oxygen transmissibility of modern hydrogels, there appears to still be an unmet need for more oxygen permeable lenses [2-5]. These remaining issues have proven significant enough to prevent many people from being able to continue wearing SCLs. The goal of the presented work is to address these issues by synthesizing a new ocular lens material which is hydrophilic, highly oxygen permeable, and does not contain water in its bulk. The material chosen for this new material was an interpenetrating polymer network (IPN) of poly(dimethyl siloxane) (PDMS) and hyaluronan (HA). PDMS is an elastomeric silicone material which has superior oxygen gas permeability and hyaluronan is a highly hydrophilic biopolymer common in mammals. Silicones are commonly used as biomaterials in a wide range of applications so in addition to characterizing the new materials for use as SCLs, the cytotoxicity and hemocompatibility of the new materials will also be investigated. The focus of this work was on the development of a synthesis method for these HA-PDMS IPNs and their characterization.

1. Specific Aim 1: Development of a method for the synthesis of HA-PDMS IPN materials
    a. Hypothesis: PDMS elastomers can be impregnated with a modified hyaluronan derivative (silyl-HA-CTA), via a mutual swelling solvent, which can then be cross-linked in place, thereby forming an IPN.
2. Specific Aim 2: Evaluation of the materials created in Aim 1 in terms of hydrophilicity (CAG) and surface chemical/morphological analyses (ATR/FTIR, SEM, XPS)
    a. Hypothesis: Successful HA-PDMS IPN materials will have more hydrophilic contact angles (CAG), will demonstrate the presence of chemical groups and elements which are native to HA but not PDMS (ATR/FTIR and XPS), and will possess a smooth surface on the micron scale (SEM).
3. Specific Aim 3: Evaluation of materials created in Aim 1 in terms of select properties relevant to their use as contact lens material and general bio-compatibility. Success in this aim will be in terms of oxygen gas permeability, optical transmittance, cytotoxicity, whole blood clotting, and platelet adhesion/activation studies.
    a. Hypothesis: Successful HA-PDMS IPN materials will: have a high oxygen gas permeability compared to market SCLs; be highly optically transmitting; non-cytotoxic; non-thrombogenic; and, will have decreased platelet response when compared to virgin PDMS.

REFERENCES

[1] J.J. Nichols, 2014 Annual Report, Contact Lens Spectrum 30(January 2015) (2015) 22-27.

[2] K. Richdale, L.T. Sinnott, E. Skadahl, J.J. Nichols, Frequency of and Factors Associated With Contact Lens Dissatisfaction and Discontinuation, Cornea 26(2) (2007).

[3] L. Jones, C. May, L. Nazar, T. Simpson, In vitro evaluation of the dehydration characteristics of silicone hydrogel and conventional hydrogel contact lens materials, 25(3) (2002) 147-156.

[4] N. Efron, P.B. Morgan, I.D. Cameron, N.A. Brennan, M. Goodwin, Oxygen Permeability and Water Content of Silicone Hydrogel Contact Lens Materials, Optometry & Vision Science 84(4) (2007).

[5] G. Erdodi, J.P. Kennedy, Water-swollen highly oxygen permeable membranes: Analytical technique and syntheses, 43(16) (2005) 3491-3501.

[6] C.E. Willoughby, D. Ponzin, S. Ferrari, A. Lobo, K. Landau, Y. Omidi, Anatomy and physiology of the human eye: effects of mucopolysaccharidoses disease on structure and function – a review, Clinical & Experimental Ophthalmology 38 (2010) 2-11.

[7] R.S. Koplin, E.I. Wu, D.C. Ritterband, J.A. Seedor, The scrub's bible: How to assist at cataract and corneal surgery with a primer on the anatomy of the human eye and self assessment, Springer New York, New York, NY, 2013.

[8] B. Holden, G. Mertz, Critical oxygen levels to avoid corneal edema for daily and extended wear contact lenses., Investigative Ophthalmology and Visual Science 25 (1984) 1161-1167.

[9] P.C. Nicolson, J. Vogt, Soft contact lens polymers: an evolution, Opthalmic Special Issue 22(24) (2001) 3273-3283.

[10] D.M. Harvitt, J.A. Bonanno, Re-Evaluation of the Oxygen Diffusion Model for Predicting Minimum Contact Lens Dk/t Values Needed to Avoid Corneal Anoxia, Optometry & Vision Science 76(10) (1999).

[11] L. Keay, I. Jalbert, D.F. Sweeney, B.A. Holden, Microcysts: clinical significance and differential diagnosis, 72(7) (2001) 452-460.

[12] F. Stapleton, S. Stretton, E. Papas, C. Skotnitsky, D.F. Sweeney, Silicone Hydrogel Contact Lenses and the Ocular Surface, 4(1) (2006) 24-43.

[13] MyAlcon.com, Limbal Hyperemia. <https://www.myalcon.com/education/academy-eye-care-excellence/cclm/limbal-hyperemia.shtml>, (accessed 2015-09-01.).

[14] D. Fonn, Targeting Contact Lens Induced Dryness and Discomfort: What Properties Will Make Lenses More Comfortable, Optometry & Vision Science 84(4) (2007).

[15] Contactlensupdate.com, Corneal staining. <http://contactlensupdate.com/2012/03/08/corneal-staining/>, 2012 (accessed 2015-09-01.).

[16] J. Kopecek, Hydrogels: From soft contact lenses and implants to self-assembled nanomaterials, 47(22) (2009) 5929-5946.

[17] K.L. Maki, D.S. Ross, A NEW MODEL FOR THE SUCTION PRESSURE UNDER A CONTACT LENS, Journal of Biological Systems 22(02) (2014) 235-248.

[18] 1800-Contacts, MOST POPULAR [Contact lenses]. <http://www.1800contacts.com/lenses/mostpopular>, 2016 (accessed 2016-06-19.).

[19] N. Bühler, H.-P. Haerri, M. Hofmann, C. Irrgang, A. Mühlebach, B. Müller, F. Stockinger, Nelfilcon A, a New Material for Contact Lenses, 53(6) (1999) 269-274.

[20] N. Efron, P.B. Morgan, Hydrogel Contact Lens Dehydration and Oxygen Transmissibility, Eye & Contact Lens 25(3) (1999).

[21] J.E. Mark, Some Interesting Things about Polysiloxanes, Accounts of Chemical Research 37(12) (2004) 946-953.

[22] F. Abbasi, H. Mirzadeh, A.-A. Katbab, Modification of polysiloxane polymers for biomedical applications: a review, Polymer International 50(12) (2001) 1279-1287.

[23] A.B. Swanson, Disabling Arthritis at the Base of the Thumb TREATMENT BY RESECTION OF THE TRAPEZIUM AND FLEXIBLE (SILICONE) IMPLANT ARTHROPLASTY, 54(3) (1972) 456-471.

[24] D.P. Clark, C. William Hanke, N.A. Swanson, Dermal implants: Safety of products injected for soft tissue augmentation, 21(5, Part 1) (1989) 992-998.

[25] M.B. Habal, The biologic basis for the clinical application of the silicones: A correlate to their biocompatibility, 119(7) (1984) 843-848.

[26] H. Chen, M.A. Brook, H. Sheardown, Silicone elastomers for reduced protein adsorption, 25(12) (2004) 2273-2282.

[27] S. Pinto, P. Alves, C.M. Matos, A.C. Santos, L.R. Rodrigues, J.A. Teixeira, M.H. Gil, Poly(dimethyl siloxane) surface modification by low pressure plasma to improve its characteristics towards biomedical applications, 81(1) (2010) 20-26.

[28] L.H. Sperling, Polymeric multicomponent materials: an introduction, Wiley-Interscience1997.

[29] J.S. Turner, Y.L. Cheng, Preparation of PDMS−PMAA Interpenetrating Polymer Network Membranes Using the Monomer Immersion Method, Macromolecules 33(10) (2000) 3714-3718.

[30] POLYMERICS, "IPN Technology". <http://www.polymerics.de/technology/ipn_en.html>, 2002 (accessed 2015-05-20.).

[31] H. Liu, L. Zhang, Structure and properties of semiinterpenetrating polymer networks based on polyurethane and nitrochitosan, 82(12) (2001) 3109-3117.

[32] D.D. Allison, K.J. Grande-Allen, Review. Hyaluronan: A powerful tissue engineering tool, Tissue Engineering 12(8) (2006) 2131-2140.

[33] R.A. Oldinski, C.N. Cranson, S.P. James, Synthesis and characterization of a Hyaluronan-polyethylene copolymer for biomedical applications, Journal of Biomedical Materials Research Part B: Applied Biomaterials 94B(2) (2010) 441-446.

[34] N.R. Lewis, *HYALURONIC ACID ENHANCEMENT OF EXPANDED POLYTETRAFLUOROETHYLENE FOR SMALL DIAMETER VASCULAR GRAFTS* Master's Thesis, Colorado State University, Fort Collins, CO, Summer 2014.

[35] M. Zhang, *Surface modification of ultra high molecular weight polyethylene with hyaluronan for total joint replacement application*, Ph.D. Dissertation, Colorado State University, Fort Collins, CO, 2004.

[36] K.M. Lowry, E.M. Beavers, Resistance of hyaluronate coatings to hyaluronidase, Journal of biomedical materials research 28(8) (1994) 861-864.

[37] D. West, S. Kumar, Hyaluronan and angiogenesis, The biology of hyaluronan 143 (1989) 187-207.

[38] C.M. McKee, M.B. Penno, M. Cowman, M.D. Burdick, R.M. Strieter, C. Bao, P.W. Noble, Hyaluronan (HA) fragments induce chemokine gene expression in alveolar macrophages. The role of HA size and CD44, Journal of Clinical Investigation 98(10) (1996) 2403.

[39] C. Tempel, A. Gilead, M. Neeman, Hyaluronic Acid as an Anti-Angiogenic Shield in the Preovulatory Rat Follicle, Biology of Reproduction 63(1) (2000) 134-140.

[40] M. Zhang, S.P. James, Silylation of hyaluronan to improve hydrophobicity and reactivity for improved processing and derivatization, Polymer 46(11) (2005) 3639-3648.

[41] Y. Luo, K.R. Kirker, G.D. Prestwich, Cross-linked hyaluronic acid hydrogel films: new biomaterials for drug delivery, 69(1) (2000) 169-184.

[42] D. Campoccia, P. Doherty, M. Radice, P. Brun, G. Abatangelo, D.F. Williams, Semisynthetic resorbable materials from hyaluronan esterification, 19(23) (1998) 2101-2127.

[43] G.N. Smith, S.L. Myers, K.D. Brandt, E.A. Mickler, Effect of intraarticular hyaluronan injection in experimental canine osteoarthritis, Arthritis & Rheumatism 41(6) (1998) 976-985.

CHAPTER 2: SYNTHESIS AND CHARACTERIZATION OF PDMS-HA IPN MATERIALS

2.1 Introduction

In this chapter specific aims 1 and 2 are addressed. Elastomeric silicone materials such as poly(dimethyl siloxane) (PDMS) tend to be very hydrophobic but can possess many desirable mechanical and physical properties. It is no wonder that silicone materials have been used as medical materials for decades, but have encountered bio-interaction complications. Therefore, it was the goal of this study to combine the hydrophobic PDMS elastomers with hydrophilic hyaluronan (HA) in an interpenetrating polymer network (IPN) wherein the materials are largely silicone with a small percentage of HA. Wherein the resulting materials exhibit the desirable properties of silicone elastomers but with improved surface hydrophilicity.

The silicone materials selected for use were treated with a modified form of hyaluronan: silylated hyaluronan complexed with an ammonium salt (silyl-HA-CTA) as described elsewhere by Zhang and James [1]. The treatment was carried out via mutual swelling of the PDMS network and silyl-HA-CTA in xylenes. This was followed by swelling of the material in a xylenes solution containing a crosslinking agent: poly(hexamethylene diisocyanate) (pHMDI). Once the impregnated silyl-HA-CTA was crosslinked inside the PDMS network and an IPN formed, a hydrolysis procedure to return the modified hyaluronan to its native, hydrophilic form was performed. The details and parameters of the described treatment were subject to variation and refinement through the course of the study. These details are discussed in more detail later in this chapter.

Characterization tests were performed on treated samples as well as virgin materials for comparison. Samples were characterized for changes in: hydrophilicity/phobicity; surface morphology; and presence of chemical species.

2.2 Materials

2.2.1 Silicone materials

While various silicone materials were evaluated during the early stages of this work, the bulk of the work was done using a commercially available two-part liquid silicone rubber kit – P-125 from Silicones, Inc (North Carolina, USA). This product is a platinum-catalyzed, addition cure, room temperature vulcanizing (RTV) liquid silicone (LSIR) rubber two-part kit. These kits created crosslinked elastomeric networks of poly(dimethyl siloxane) (PDMS). These kits were mixed, spin-cast, and cured on-site and into films of average thickness 0.1905mm (0.0075in). The details of the method for creating these spin-cast films are discussed in a later section.

2.2.1.1 Selection of silicone materials

Basic material selection was influenced largely by gas permeability as review of literature indicated this to be a major are for improvement of current contact lens technologies [2, 3]. In this respect, silicone elastomers, particularly PDMS, are well known for their exceptionally high oxygen gas permeability among polymers [4]. Based on this, PDMS was chosen as the base material for this work. In the course of this study, various PDMS elastomer materials were considered and evaluated based on their material and optical properties, handling, processing options, and receptivity to treatment. As the motivation for this work lies in producing a new soft ocular lens material, the initial selection of material/optical properties were aimed at similarities to soft contact lens materials. This meant a material which would be optically clear and have

good handling properties when formed into a relatively thin film [5]. Typical center thicknesses of commercially available soft contact lenses can range from 60 to 118 μm [6].

Specifically perusing materials that would be suitable as ocular lens material, the properties of interests which guided initial silicone selection included: optical clarity; tear strength; durometer; and the ability to be processed into films of thickness as described above [7]. Initial searching focused on obtaining premade films of silicone elastomers. However, finding factory extruded films at the thickness desired while still being optically clear proved to be challenging. Furthermore, in the few cases where these premade films met the above requirements, the variability in thickness by this manufacturing method was unacceptably large (in some cases ±50% of the target thickness) according to technical staff at the film manufacturer.

Consideration then turned to two-part silicone kits, which could be processed to a desired thickness while still having predicable properties. The main downside being that they had to be made in small batches on an as-needed basis. However, a side benefit was that with low temperature curing kits we could explore the introduction of HA before the silicone was fully cured (i.e. simultaneous IPNs). While an unsuccessful effort, this is discussed later in this chapter. Several silicone kits were found to meet the requirements for our base material and are summarized in Table 2.1 below. All of these kits produced optically clear silicone elastomers over a range of durometers and tear strengths. The P-125, XP-536, and XP-565 kits were products of Silicones, Inc (North Carolina, USA). The LSR 7030 kit was procured from Momentive, Inc (New York, USA).

Table 2.1: Summary of silicone kits used and example properties as reported by the manufacturers.

Product name	P-125	XP-536	XP-565	LSR 7030
Durometer, Shore A	40	22±2	16±2	30
Tear Strength [N/mm]	15.8 ±2.6	15.8 ±2.6	7 ±1.8	3

While all of the above kits were involved in early treatments, ultimately the P-125 kit (Silicones, Inc) was chosen as the primary base material for the remainder of the study. Final selection of this kit was based on its handling properties during treatment, degree and rate of swelling in xylenes (the treatment solvent), and general success of the treatment.

2.2.2 Hyaluronan and modification to silyl-HA-CTA

In its native, hydrophilic form, hyaluronan is soluble only in water, and thus, is not soluble in any solvent that also expands/swells the PMDS network to a significant degree. Therefore, it must be chemically modified to be soluble in xylenes (a common solvent which also swells PDMS materials). This is a two-step process: first from Na-HA to HA-CTA; then from HA-CTA to silyl-HA-CTA. The stages of the process of modifying hyaluronan to silyl-HA-CTA for use in this work are outlined here, but more detail can be found elsewhere in a publication by Zhang and James [1]. Additionally, a protocol for this process is included in the appendix section detailing this process.

Hyaluronan was obtained from Lifecore Biomedical (Minnesota, USA) in the form of sodium-hyaluronate (Na-HA) at an average molecular weight of 750kDa. The Na-HA was dissolved in room temperature DI water for at least 15 hrs. Cetyltrimethylammonium bromide

(CTAB) was then dissolved in DI water at 40C for 10-15 min. The CTAB solution is then slowly poured into the HA solution. The mixture is allowed to stir at room temperature for up to two days. During this time the HA complexes with the CTAB, forming HA-CTA, and then precipitates out of solution. This precipitate is then separated from the remainder of the solution, rinsed with DI water four times, and then dried for 3 days (50C, -25inHg (gage)). Once dried, the now clumpy white compound is ground into a fine powder using a freezer mill chilled with liquid nitrogen. This powdered HA-CTA is dried again as water contamination can compromise the next steps.

The powdered HA-CTA complex is swollen to a gel-like state in dimethyl sulfoxide (DMSO) at room temperature in a sealed round bottom flask purged with dry nitrogen gas. Heat, 50C, is then introduced until the HA-CTA is fully dissolved in the DMSO. Then hexamethyldisilazane (HMDS) is added to the flask via cannula transfer with dry nitrogen gas. The DMSO phase and HMDS phase are immiscible so the reaction of HA-CTA to silyl-HA-CTA takes place at the phase interface. Therefore the mixture is stirred vigorously to create HMDS-DMSO emulsions for greater phase interface area. As the HA-CTA is converted to silyl-HA-CTA it will move from the DMSO phase to the HMDS phase, where it remains dissolved.

The silyl-HA-CTA is recovered from the HMDS phase via evaporation of the HMDS until the silyl-HA-CTA is left behind. The silyl-HA-CTA is dried (50C, -25inHg (gage)) for 3 days before use or storage. When stored, the water-sensitive silyl-HA-CTA is stored in vacuum desiccators. Figure 2.1 outlines the changes to the chemical structure to HA during this process.

This modification results in an HA derivative which will swell in xylenes and impregnate the swollen PDMS network. The modified HA is later returned to its natural, hydrophilic state via a hydrolysis procedure which is described later in this chapter.

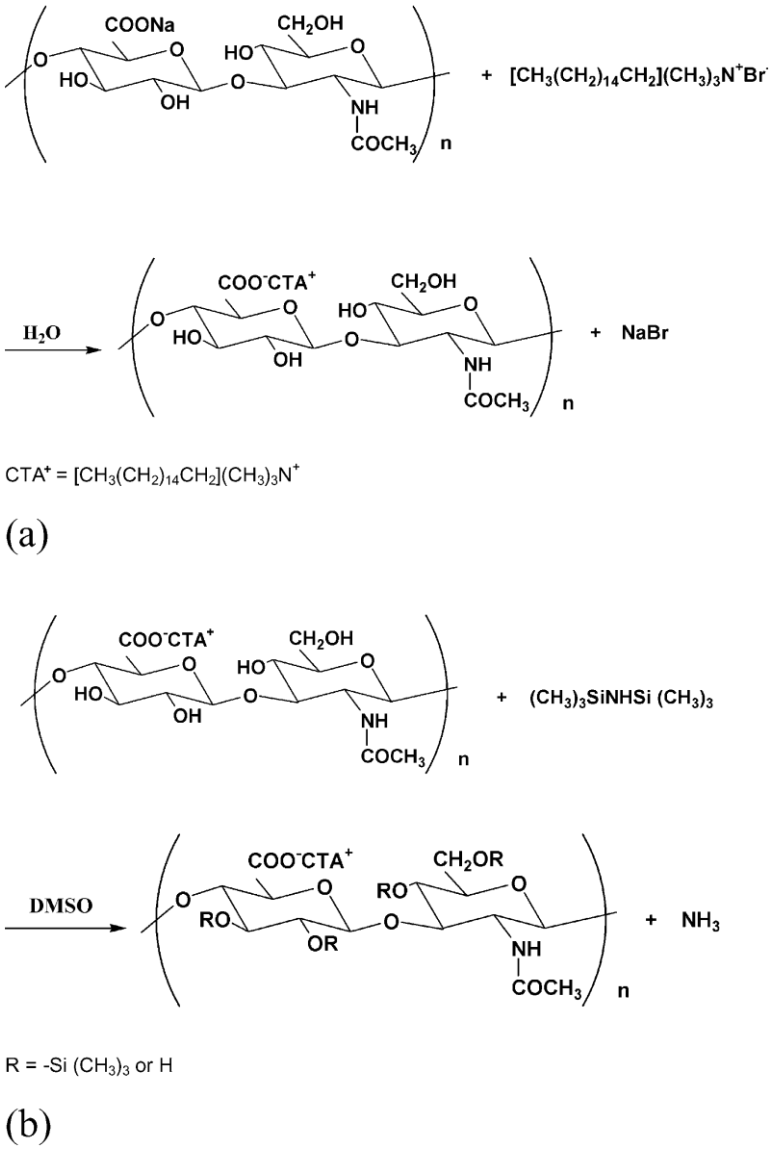

Figure 2.1: Schematic of the conversion of Na-HA to HA-CTA (a) and then from HA-CTA to silyl-HA-CTA (b) [1].

2.2.3 Crosslinking agent (pHMDI)

The chemical crosslinking agent used for hyaluronan impregnated in the PDMS elastomer was poly(hexamethylene diisocyanate) (pHMDI, viscosity 1300-2200 cP, Sigma Aldrich). Figure 2.2 shows the chemical structure of pHMDI. This cyclic trimer of isocyanates crosslinks the silyl-HA-CTA to itself or other similar polymers by reacting at the O-Si$(CH_3)_3$ groups or residual non-silylated alcohol groups [8]. This crosslink results in both intra- and inter-

molecular crosslinking of the HA. Sham treated samples were exposed to pHMDI during this work and were found to be unaffected, demonstrating that the crosslinker does not react with the base silicone material. This crosslinking between like-guest polymers and not between the host polymer (PDMS) and the guest (silyl-HA-CTA) results in an interpenetrating polymer network (IPN).

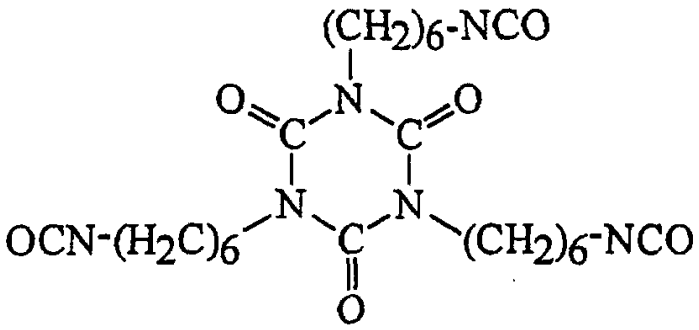

Figure 2.2: Chemical structure of the chemical crosslinker used in this work, poly(hexamethylene diisocyanate). [9]

2.2.4 Solvents

The xylenes used in this work were a racemic mixture of ortho-,meta-, and para-xylene isomers that was obtained from EMD Millipore (ACS grade). Xylenes were used as the treatment solvent for their ability to expand the PDMS crosslinked network and dissolve both silyl-HA-CTA and pHMDI [10]. This mutual solvent property allows for simultaneous expansion of the PDMS network and introduction of the dissolved hyaluronan derivative or crosslinker. Additionally, xylenes were used to clean the PDMS films prior to treatment.

Xylenes were purified of water contamination prior to use as treatment solvents. This purification consisted of drying over molecular sieves and then distillation. The xylenes were first dried over molecular sieves (Type 3A, 8-12 mesh beads, EMD Millipore) for a minimum of 24hrs in order to reduce the water contamination to trace levels. This was followed by a

distillation processes using vacuum, hot oil baths, and a West condenser. The system is demonstrated in Figure 2.3 below. Distillation was performed primarily to separate the solvent from microscopic sieve particulates which entered suspension during drying over the sieves. These particulates were found to contaminate samples which used solvents that had not been distilled (unpublished work). All transfers of liquid were performed in a controlled (dry) atmosphere. Following purification, solvents were tested with a water testing kit to determine the new water content.

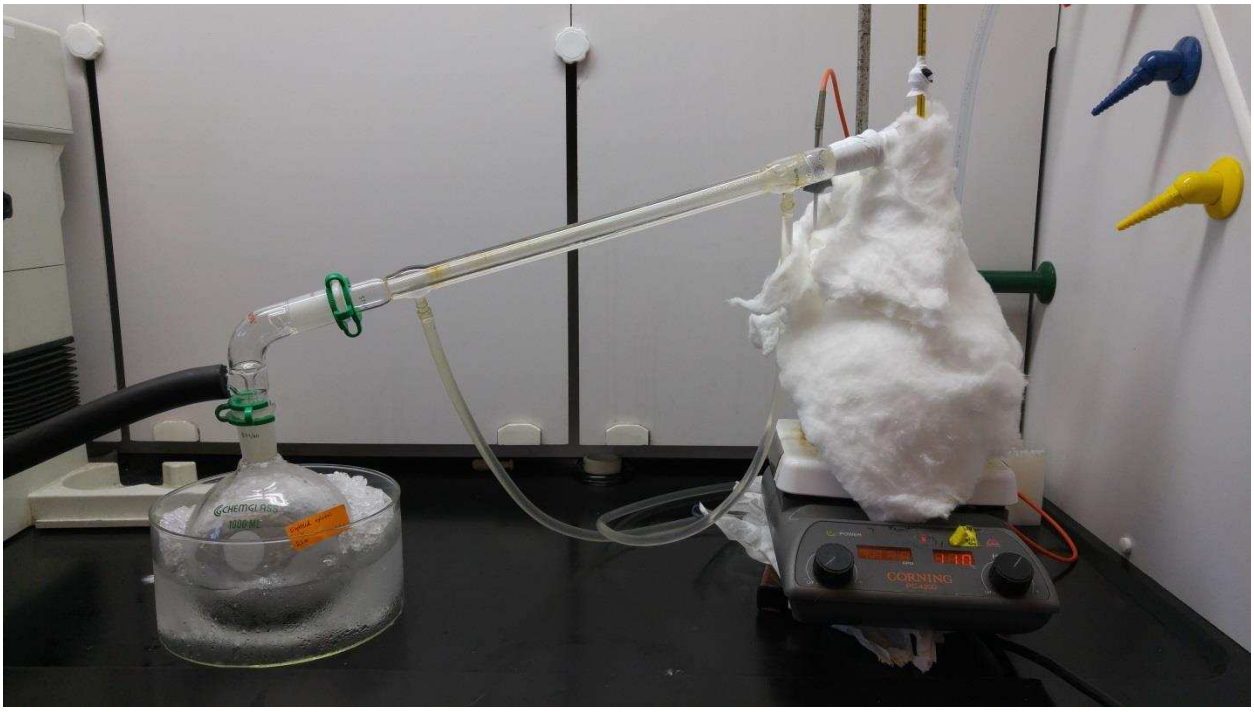

Figure 2.3: Distillation setup used for xylenes purification. The donating flask (containing the initial solvent) is wrapped in cotton for insulation to speed up the distillation process.

Other solvents which were used as-received include: acetone (ACS reagent ≥99.5%, Sigma-Aldrich); ethanol (Absolute anhydrous ACS/USD grade, PHARMCO-AAPER); and hexamethyldisilazane (HMDS, reagent grade, ≥99.9%, Sigma Aldrich).

2.2.5 Other Special Materials

Acrylic slabs (5x10x0.158 cm, SACR.062CEF, Professional Plastics) were used as curing surfaces for the PDMS films. Acrylic was used for this purpose due to the ease of removing the cured films from these surfaces. It was found that the kits used would bond irreversibly to glass surfaces during curing. This could be reduced by silylating the glass surface prior to contact. However, the cured material retained some tendency to stick firmly to the glass surfaces, sometimes still destructively.

2.3 Methods – Sample synthesis

2.3.1 PDMS film creation

PDMS films made from the P-125 kit (Silicones, Inc) were created as described here. The kit components (activator and base) were mixed according to the manufacturer recommended ratio – 1:10 activator:base. Six mL of base and 0.6mL of activator were dispensed into and mixed in a disposable container. The mixture was stirred vigorously for one minute before being placed on a chilled aluminum brick in a vacuum chamber, at -25inHg (gage), to degas for up to 10 minutes or until no bubbles were noticeable. Two grams of the mixture were scooped onto an acrylic slab and lightly spread to create a shallow oval-shaped deposit. This was repeated for a second acrylic slab substrate. Both substrates were returned to the vacuum chamber, on a new chilled aluminum brick, to degas for up to another 15 minutes or until no bubbles were observable in the mixture. Once degassed for the second time, the mixtures and their substrates were spin cast using a spin coating system (Spin processor WS-650MZ-23NPP, Laurell Technologies Corporation). The spin casting settings used were 2500rpm for 37.5s of which 10s were used as an acceleration period. The films were then moved to heat (50˚C) where they were allowed to cure for a minimum of 6 hours.

After being allowed to cure the films were removed from their acrylic substrates and both mass and thickness were measured using a digital scale and calipers respectively. At this time the films were also inspected for surface imperfections that may have occurred during creation. Following this, the films were placed in a 250mL Erlenmeyer flask with 200mL of xylenes at 50˚C for a minimum of 24hrs. This step was used to wash out lower molecular weight (LMW) species formed during curing which did not become part of the elastomer's crosslinked network. Films were dried and their mass and thickness recorded again. It is not unusual with a two-part kit such as this to lose up to 15% of the initial mass in this wash. This washing step is therefore crucial in determining the change in mass due to treatment; which would be obscured by these LMW species leaving. Additionally, it is suspected that this sizeable egress of LMW species would inhibit the entry of the desirable species during treatment.

After processing, films are stored, dry, in plastic containers until just before use. Shorty prior to use in treatment the larger films (5x10cm rectangles) are cut into smaller test sizes of 2.5x1.5cm rectangle samples. After portioning into the smaller test sizes, one final shape modification was made: with the face of the film that was exposed to air during curing, a small notch is cut from the upper left corner of the film. This is done so that the orientation of the film can always be known during future characterizations. The portioning and shaping of the films are outlined in Figure 2.4 below. In the sketch, the side of the film facing the viewer is the side that was exposed to air during curing. Due to the rectangular shape of the film, with the air exposed side facing the viewer is the only orientation in which that notched corner will be in the upper left. This ensures that the orientation of the test film can always be determined.

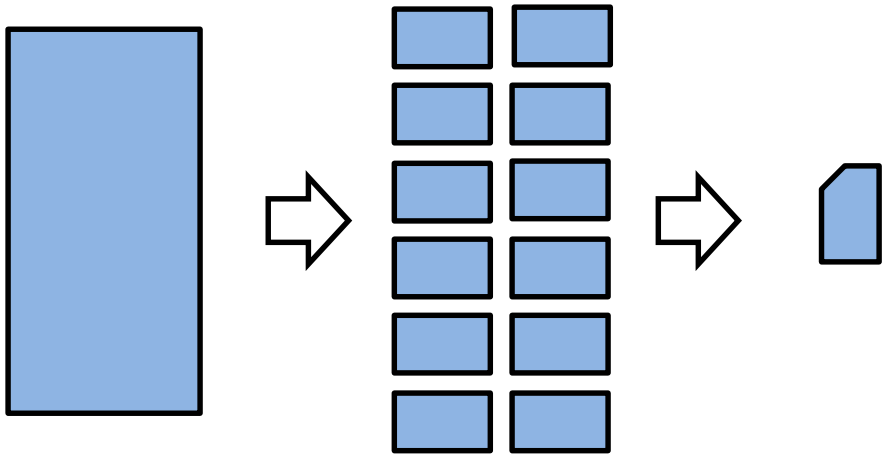

Figure 2.4 Simple outline of portioning and notching of the PDMS test films. The notch in the upper left corner of the test film ensures that the film's orientation can always be known.

2.3.2 Swelling of PDMS in xylenes

All of the PDMS elastomers considered in this study were able to be swollen significantly by xylenes. The extent to which varied based on the kit used, which produced elastomers of different densities and stiffness. The rate and extent of swelling in xylenes was determined by swelling portions of the PDMS elastomers in xylenes for predetermined amounts of time and recording the mass while still wet (swollen). When massing, samples were removed from the xylenes and quickly blotted dry of surface liquid and then immediately measured for mass on a digital scale. Assuming constant density of both xylenes and the elastomer, the change in volume of the elastomeric network can be determined according to Equation 2.1 below. In this equation, ρ_{PDMS} and $\rho_{xylenes}$ are the densities of the elastomer (prior to swelling) and xylenes respectively, $m_{swollen}$ is the mass of the swollen elastomer (and xylenes contained therein), and $m_{PDMS,0}$ is the mass of the non-swollen elastomer.

$$\Delta V = \frac{m_{swollen}}{\rho_{PDMS}+\rho_{xylenes}} - \frac{m_{PDMS,0}}{\rho_{PDMS}} \qquad \text{(Eq 2.1)}$$

The density of the PDMS elastomer, ρ_{PDMS}, was determined by modeling the film as a thin rectangular sheet and dividing the measured mass by the volume (calculated from the measured lengths and thickness). The density of xylenes was listed in the product data sheet provided by the manufacturer and was 0.87 g/mL (at 25C) (EMD Millipore).

2.3.3 Synthesis of HA-treated PDMS materials

The general treatment of the PDMS films occur over five major events: swelling of the PDMS elastomer network; introduction of silyl-HA-CTA into the PDMS network; introduction of the crosslinker into the PDMS network; crosslinking of the silyl-HA-CTA impregnated in the PDMS network; and hydrolysis of the modified hyaluronan to return it to its native, hydrophilic form.

Two major variations on this set of events were explored. The most significant distinction between these two methods lies in the manner in which the modified hyaluronan and crosslinker are swollen into the PDMS elastomer. In one method, the modified hyaluronan and crosslinker were swollen into the elastomer in separate, sequential steps; this method is referred to as the "sequential swelling" method. In the other, the modified hyaluronan and crosslinker were swollen into the elastomer in a single, simultaneous step; this method is referred to as the "simultaneous swelling" method. In both cases, since the PDMS network is formed before any other species are introduced, the resulting IPN is still considered to be a "sequential IPN." Both treatment methods are described in further detail in this section.

2.3.3.1 Sequential swelling of silyl-HA-CTA and pHMDI

Since the hyaluronan derivative, silyl-HA-CTA, and the cross-liking agent, pHMDI, both readily react with water, certain precautions against water contamination were taken. All glassware used in the treatment process was heated in a glass drying oven (120C) overnight and

then pre-silylated shortly before use to minimize any residual water contamination. Additionally, xylenes which had been dried over molecular sieves (3Å) and distilled were used. Finally, all solutions were mixed inside of a dry, controlled environment – i.e. a glove bag filled with dry nitrogen gas.

PDMS films were prepared as described earlier in the chapter. Before treatment, the initial mass of all samples was recorded. Silyl-HA-CTA was swollen into the PDMS elastomer network via a swelling solution consisting of 2.5% (m/V) silyl-HA-CTA in dry xylenes in an Erlenmeyer flask, covered. The xylenes were added to the silyl-HA-CTA in a dry environment and allowed to mix at room temperature for 2hrs prior to use. Similarly, the pHMDI swelling solution consisted of 2.5% (V/V) pHMDI in dry xylenes in an Erlenmeyer flask, covered. The pHMDI was combined with xylenes in a dry environment and allowed to mix at 50C for 2hrs prior to use. Samples were first allowed to swell in the silyl-HA-CTA swelling solution in a 20mL scintillation vial for 1hr at room temperature. Samples were then moved immediately, without drying, to fresh scintillation vials containing the pHMDI swelling solution and allowed to swell at 50C for 1 hr. Following this, samples were placed in a vacuum oven, 50C and -25inHg (gage), overnight to allow the samples to dry and ensure completion of the crosslinking reaction. The following day, the mass of the samples were recorded and then placed in an acetone bath for 5 minutes to dissolve any residual surface pHMDI. The samples were again dried and had their mass recorded. Samples were then underwent a hydrolysis procedure to return the modified hyaluronan to its native, hydrophilic form. This hydrolysis procedure is discussed in detail later in the chapter.

2.3.3.2 Simultaneous Swelling of silyl-HA-CTA and pHMDI

The "simultaneous swelling" method differs from the "sequential swelling" method in that temperature was determined to be a significant factor. This is because the crosslinker is highly active, even at room temperature, and silyl-HA-CTA may not be able to impregnate the PDMS well enough before crosslinking advances too far. One solution was to chill everything as well as possible. This included having custom machined aluminum blocks which could be placed in a freezer (-20C) for the scintillation vials. Since the hyaluronan derivative, silyl-HA-CTA, and the cross-liking agent, pHMDI, both readily react with water, certain precautions against water contamination were taken. All glassware used in the treatment process was heated in a glass drying oven (120C) overnight and then pre-silylated shortly before use to minimize any residual water contamination. Additionally, xylenes which had been dried over molecular sieves (3Å) and distilled were used. Finally, all solutions were mixed inside of a dry, controlled environment – i.e. a glove bag filled with dry nitrogen gas.

PDMS films were prepared as described earlier in the chapter. Before treatment, the initial mass of all samples was recorded. Aluminum blocks with holes milled for 20mL scintillation vials were placed in a -20C freezer overnight. The scintillation vials were placed in the cooling blocks 1 hr prior to treatment to chill. Silyl-HA-CTA was swollen into the PDMS elastomer network via a swelling solution consisting of 2% (m/V) silyl-HA-CTA in dry xylenes in an Erlenmeyer flask, covered. The xylenes were added to the silyl-HA-CTA in a dry environment and allowed to mix at room temperature for 2hrs prior to use. Similarly, the pHMDI swelling solution consisted of 1.33% (V/V) pHMDI in dry xylenes in an Erlenmeyer flask, covered. The pHMDI was combined with xylenes in a dry environment and allowed to mix at 50C for 2hrs prior to use. Prior to use, of the aforementioned master solutions were chilled in a

refrigerator (0C) for 1hr. Solutions were mixed (via benchtop vortexer for ~15s) in individual treatment vials immediately before addition of PDMS test film into solution. Scintillation vials were returned to the cooling block immediately after adding solution and film. Once all solutions were mixed and the films added, the temperature of the block (via infrared thermometer) was noted and block placed in refrigerator (0C) for 45min. Following this, samples were placed in a vacuum oven, 50C and -25inHg (gage), overnight to allow the samples to dry and ensure completion of the crosslinking reaction. The following day, the mass of the samples were recorded and then placed in an acetone bath for 5 minutes to dissolve any residual surface pHMDI. The samples were again dried and had their mass recorded. Samples were then underwent a hydrolysis procedure to return the modified hyaluronan to its native, hydrophilic form. This hydrolysis procedure is discussed next.

2.3.3.3 Hydrolysis of modified hyaluronan

A hydrolysis reaction converted the hyaluronan derivative, silyl-HA-CTA, back into its native, hydrophilic form, Na-HA. The hydrolysis procedure is carried out via a series of solvent baths in an ultrasonic bath. The solutions were comprised of sodium chloride (NaCl, Certified ACS, Fisher-Scientific), ethanol (Absolute anhydrous ACS/USD grade, PHARMCO-AAPER) and DI water. Table 2.2 below summarizes each step in the hydrolysis procedure. This procedure is based on one developed elsewhere [10] with some modifications. Since the water in the ultrasonic bath heated up during each run, it was replaced with fresh, cool water between each sonication run.

Samples first were placed in a solution of 1:1 (by volume) DI water:ethanol with 0.2M NaCl and subjected to an ultrasonic bath. This was repeated two more times for a total of three identical baths per sample. Samples were then allowed to steep in an identical solution overnight

(at least 12 hours). Following this soak, samples were placed in a solution containing DI water and 0.2M NaCl in an ultrasonic bath for 1 hour. Samples were then allowed to soak in a mixture of 3:2 DI water:ethanol overnight (at least 12 hours). Finally, samples were allowed 30 min in an ultrasonic bath in DI water only. Samples were then stored in a fresh volume of DI water in clean scintillation vials until characterized. Samples were kept in a hydrophilic environment as much as possible after treatment due to the surface rearrangement tendencies of the treated samples. It was determined in preliminary work that treated samples which had been left in a hydrophilic environment tested differently than those which were left dry in certain tests (e.g. wet-stored samples demonstrated more hydrophilicity on contact angle measurements). Samples were dried for 6-12 hours in a vacuum oven at 50C and -25inHg (gage) when necessary for subsequent characterization (e.g. scanning electron microscopy).

Table 2.2: Summary of the solution baths and times for the hydrolysis procedure.

Step	Bath composition	Duration
1	1:1 DI Water:Ethanol + 0.2M NaCl	1hr sonication
2	1:1 DI Water:Ethanol + 0.2M NaCl	1hr sonication
3	1:1 DI Water:Ethanol + 0.2M NaCl	1hr sonication
4	1:1 DI Water:Ethanol + 0.2M NaCl	Overnight soak
5	DI Water + 0.2M NaCl	1hr sonication
6	3:2 DI Water:Ethanol	Overnight soak
7	DI Water	0.5hr
8	DI Water (sterile)	Storage

2.4 Early work

This section is dedicated to discussion of early work or pilot studies which helped to guide the rest of the work in an indirect way. This includes smaller studies which yielded useful information as well as some select treatment attempts which proved ineffective in some way and were no longer pursued.

2.4.1 Adding silyl-HA-CTA Before PDMS Curing

Before making the sequential IPNs as described above, a simultaneous IPN reaction was explored. It was observed in early work that silyl-HA-CTA and the PDMS material would phase separate from each other even when strongly diluted in a mutual solvent – xylenes (unpublished work). This was observed as the two initially clear solutions formed an opaque/cloudy mixture within seconds after combining which did not clear up with mixing and processing. Figure 2.5 shows an example of an early attempt at making one of these simultaneous IPNs, which were far too opaque to be used in an ocular lens application.

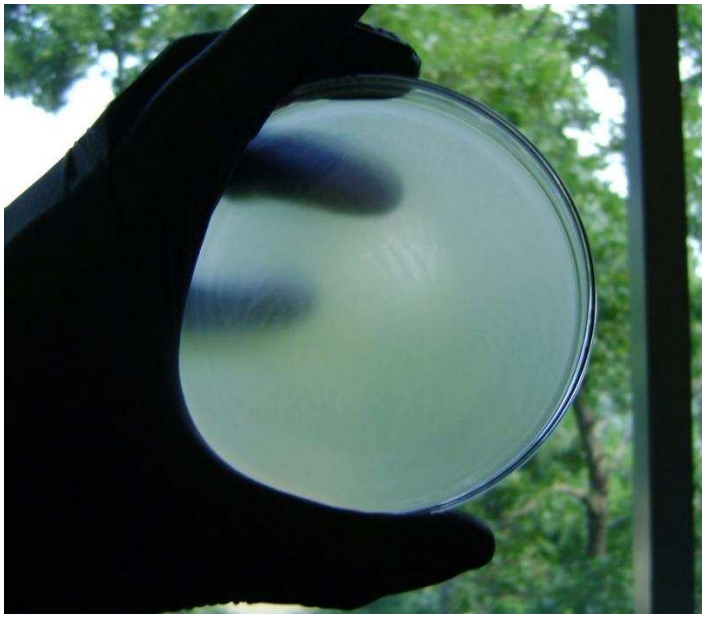

Figure 2.5: Picture of an early attempt at making a simultaneous IPN between PDMS and HA. Sample is held in front of window to demonstrate severity of opacity.

This approach was explored in the hopes that thorough dispersion of the silyl-HA-CTA in the PDMS network could be guaranteed.

2.4.2 PDMS Pucks

Prior to the development of a successful thin film creation protocol, early work involved thicker PDMS pucks cured in plastic culture dishes. These were commonly 5 cm in diameter and 0.5 cm thick. For treatment, these were typically cut into four smaller square portions. These pucks were also used in the initial evaluation of the various kits and development of base material fabrication protocols. Treatments later focused on thin spin cast films in an effort to work with a base material form that more closely resembled soft contact lenses. It was noted that the films behaved differently from the thicker pucks. Not surprisingly, the thin films swelled with xylenes far more quickly than the thicker pucks and equilibrium swelling of silyl-HA-CTA took less time. Because of this, the films would deform more quickly when swelling than the pucks. This made some earlier treatment methods not viable with the films. One example of which was referred to as the "Sponge swelling" approach as it involved dispensing a predetermined amount of solution onto the substrate surface and allowing it to soak in. This is discussed briefly later in this section.

2.4.3 Abandoned Treatment Variations

Many treatment variations were explored before coming to the ones described later in this chapter. However, some of these methods showed little promise or presented too many complications and were not pursued in favor of the others. One worth mentioning is the "Sponge swelling" approach. This is approach is named after the idea of a sponge soaking up liquid placed on it. Briefly, in this approach a pre-calculated amount of solution (silyl-HA-CTA or pHMDI in xylenes) was dispensed directly on the substrate surface and allowed to soak in. The

idea of this method was to encourage a strong concentration gradient of silyl-HA-CTA at the surface.

This method had some amount of success with the thicker PDMS pucks but had issues when applied to PDMS films. While the thicker pucks tended to arch upwards when the solutions were placed on their surface due to only one side swelling, they could be successfully treated this way. On the other hand, the thinner films would deform and wrinkle so severely and quickly that a successful treatment could not be done this way. An attempt at correcting this included sandwiching the films between metal washers to hold it tight. However, the films would expand to such a degree that this just created a sagging film holding a puddle of solvent. Figure 2.6 shows examples of slabs from pucks (left) and films (right) undergoing this "sponge swelling" treatment method.

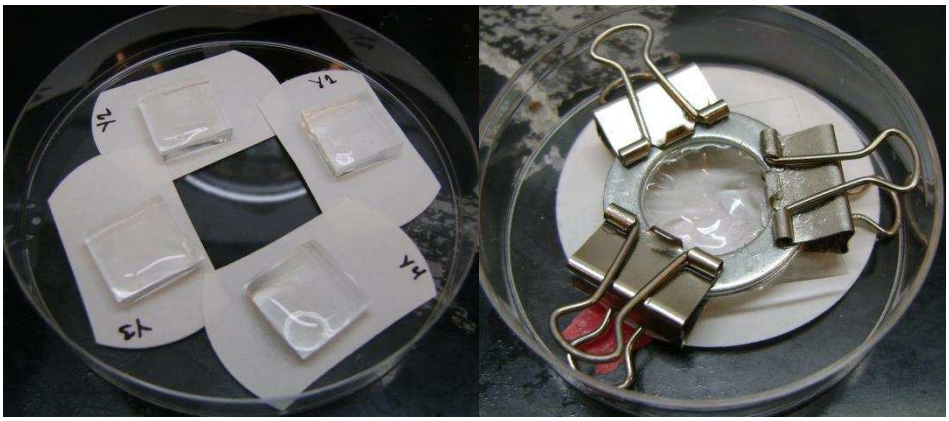

Figure 2.6: Samples undergoing the "Sponge swelling" approach. Pictured are square slabs cut from pucks (left) and a thin film in its holder (right).

Unfortunately, due to the deformation of both the slabs and films during this treatment approach, the surfaces were left with uneven deposits of crosslinked hyaluronan. Furthermore, the films remained permanently wrinkled. Figure 2.7 below shows examples of this for slabs

(left) and films (right). Due to the aforementioned reasons, this treatment approach was ultimately abandoned in favor of the others discussed in detail later in this chapter.

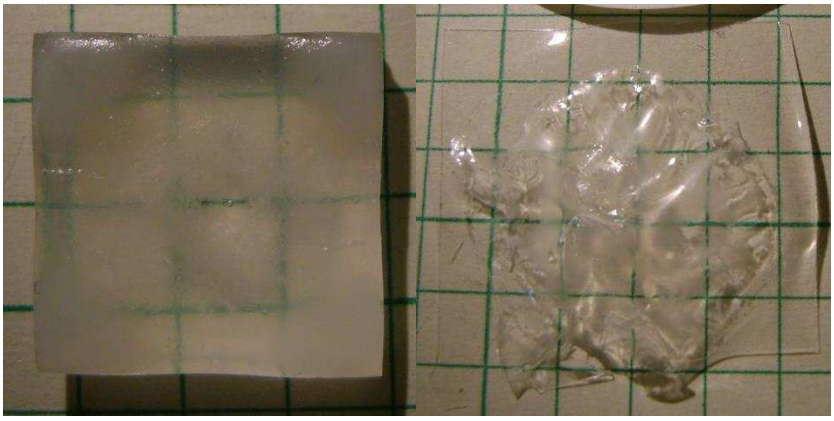

Figure 2.7: Examples of the uneven surfaces left behind by the "Sponge swelling" approach on a slab cut from a puck (left) and a thin film (right).

2.4.4 Contact Angle Differences on the Films

During the course of this work, it was determined that the different sides of the PDMS films showed different water contact angles. For the sake of discussion, the face which was in contact with the acrylic substrate during curing will be referred to as the "down" side and the face which was exposed to air during curing will be referred to as the "up" side. This difference was discovered after it was noticed that some treatments would have a binary distribution of contact angles which agreed well with each other in their respective binary group. Figure 2.8 below shows the static captive bubble contact angle of plain PDMS samples taken before this knowledge. In the plot it can be clearly seen that there are two groupings of contact angles that have good intra-group agreement. These two groups correspond to either the up or down side of the films. This data was obtained before considering that the sides mattered and no effort to keep track of which side was measured was made. It can be seen from the plot that there can be as much as a 15 degree difference in contact angle between the two sides.

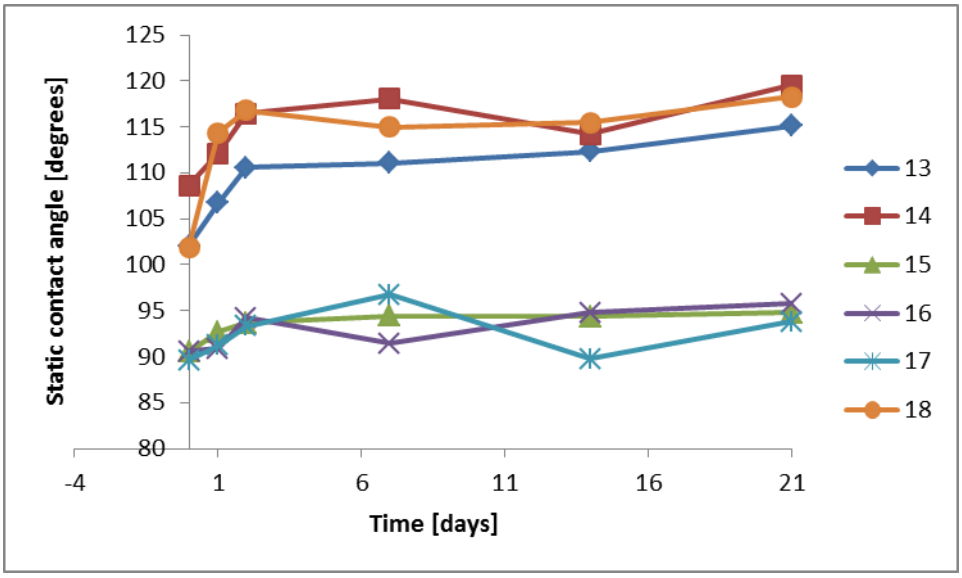

Figure 2.8: Plot of static captive bubble contact angles of plain PDMS films that clearly demonstrates a binary grouping. All samples were untreated PDMS.

This sparked the idea that there was a difference in the sides which presented itself in the contact angles. From this idea a study was performed to determine if this was some anomaly or something that legitimately warranted consideration going forward. The study consisted of analyzing PDMS films made under various conditions: exposed to air with heat (the normal method); in vacuum (-25inHg gage); and with/without heat. The analysis focused on observing differences in contact angles but also included SEM imaging and ATR/FTIR analysis to determine if there were any detectable differences on the surface. SEM imaging and ATR/FTIR could not show any difference between the two sides. However, there was a significant difference noticed in the contact angles between the up and down sides, especially so in the sessile receding angles. Table 2.3 below contains the summary of the difference in angles between the two sides. While it did vary, all samples showed higher sessile drop contact angles for static, advancing, and receding on the up side, compared to the down side. This difference is most obvious for receding contact angles.

Table 2.3: Table summarizing the difference (up - down) in contact angles.

Differences (raw) between up and down sides

Δ=(up - down)	1	2	3	4	Average across all samples
Δaverage(static)	0.511	8.26	4.74	6.84	5.09
Δadv	0.695	2.27	2.07	5.17	2.55
Δrec	15.6	20.3	13.4	26.0	18.9

The same trend was observed for films cured under vacuum, without heat, and when using different substrates (tissue culture polystyrene). Of note: the angles for the up sides did not vary significantly between when the films were cured in air and cured under vacuum. Based on the above, it was decided that only the up side of the films (treated or not) should be considered going forward.

2.4.5 Drying Between Swelling Steps

Previous work with other host polymers like polyethylene films or expanded polytetrafluoroethylene which guided the early stages of this work [11, 12] included a step for drying samples immediately after swelling in silyl-HA-CTA. Early treatments in this work followed this procedure. However, it was later determined that the complete exclusion of this drying step improved the success of treatment for the PDMS films. This was based on a small study which varied the amount of drying that was allowed between the two swelling steps. Drying groups were: 1 hr dry in vacuum oven; 7 min dry in vacuum oven; no drying at all (straight into crosslinking solution); and wet-drying in DMSO (DMSO wicks out xylenes but does not swell PDMS or silyl-HA-CTA). The resulting films were characterized via sessile drop contact angles. Figure 2.9 shows a plot summarizing the result of this characterization. The result was that not drying at all produced the samples with the lowest receding contact angles (i.e. most hydrophilic). The average receding contact angle for samples that were not dried at all was

statistically different ($p \leq 0.05$ at $\alpha = 0.05$) from all other drying variations. This is likely due to the fact that PDMS has a much lower glass transition temperature, greater chain mobility, and considerably more free volume than the host polymers studies by Dean and Lewis [11, 12].

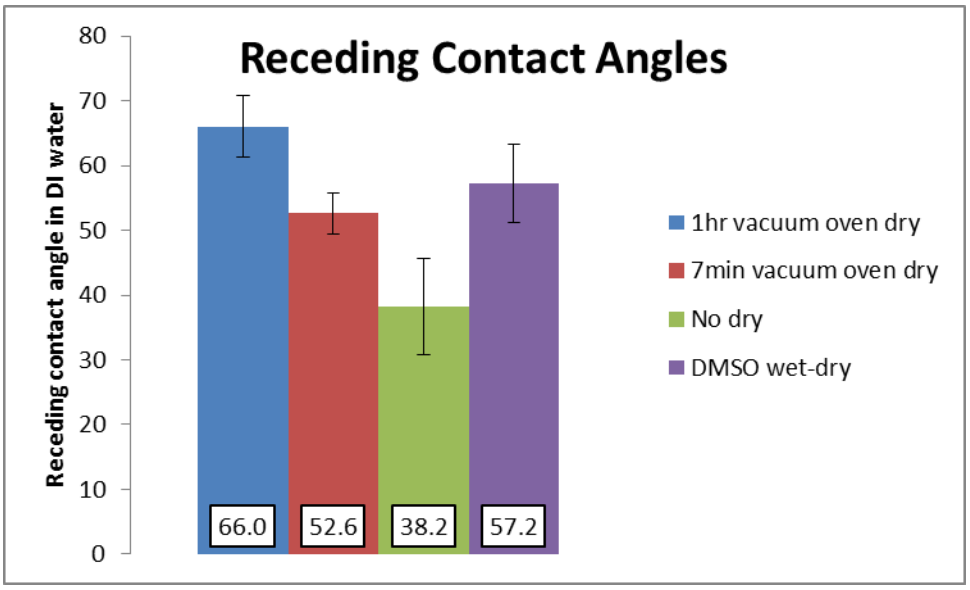

Figure 2.9: Plot summarizing the results of receding contact angles for samples of varied degrees of drying after swelling in silyl-HA-CTA.

2.4.6 Determination of Treatment Parameters for Simultaneous Swelling Method

During the early stages of developing the simultaneous swelling method, a study was designed to determine the optimal treatment parameters under this method. This study varied the three parameters thought to be most crucial to the success of treatment: swelling time (in treatment solution); ratio of silyl-HA-CTA to pHMDI (crosslinking agent); and solution concentration (with the previous ratio kept constant). Swelling time and silyl-HA-CTA:pHMDI ratio each saw 4 variations and solution concentrations saw 3 variations. Samples were all characterized under contact angle goniometry (CAG) for hydrophilicity and SEM imaging for changes in surface morphology. Table 2.4 below summarizes the treatment groups and parameter variations for the study.

Table 2.4: Summary of treatment groups and their variations in the study designed to explore treatment parameter variations for the simultaneous swelling treatment method. The values highlighted denote the variables which were chosen to be default values in groups where the respective parameter was not varied.

	Group 1	Group2	Group 3
Parameter varied	Swell time	Solution ratios (OH:NCO)	Solution concentration
Variation 1	15 min	1:1	1x (2% m/V silyl-HA-CTA | 1.33% V/V HMDI)
Variation 2	30 min	3:1	0.5x
Variation 3	45 min	5:1	2x
Variation 4	60 min	7:1	- -

The highlighted values represent the default value in groups where the respective parameter was not varied. The solution ratios were based on concentrations such that at 1:1 there would be a 1:1 ratio of crosslinkable groups on the silyl-HA-CTA to active NCO groups on the pHMDI. This set the solution concentrations as presented in the table above. The default swelling time of 45 minutes was determined from a pilot study in which solutions containing both silyl-HA-CTA and pHMDI were observed for the time that it took for a precipitate to fall out of.

The result of this study was that the optimal values were actually the values already selected as the default parameters (highlighted in the above table). This was determined by a combination of: CAG analysis; SEM imaging; changes to handling properties and clarity; evenness of treated surface (across the surface of any given sample); and the variability in treatment success (i.e. how reproducible the positive results were under those parameters).

CAG analysis showed decreasing sessile drop receding contact angle (increasing hydrophilicity) with increasing swell time, increasing solution concentrations, and with decreasing solution ratio (OH:NCO). Figures 2.10-2.12 below show the sessile configuration contact angle results for each group. The large error bars show the large standard deviation that existed in these samples. For some groups, there would be one or more samples which possessed a zero receding contact angle (successful treatment) as well as one or more than had relatively high receding contact angles (unsuccessful treatment) even when made in the same treatment batch. The inclusion of the advancing contact angles on the following plots helps to illustrate the large contact angle hysteresis resulting from surface rehydration and reconfiguration.

Differences between treatment parameters were also noted in handling and opacity. Both opacity and stiffness increased with increasing swell time, increasing solution concentration, and decreasing solution ratios (OH:NCO). Additionally, the 60 min swelling and 2x solutions concentration samples appeared to have a crusty deposit on their surfaces when dried. This was believed to be excessive crosslinked HA anchored to the surfaces. Furthermore, on some samples this layer would crack and dissociate from the sample during vacuum oven drying (50C, -25inHg gage). These samples showed unfavorable handling and stability of treatment on the surface.

SEM imaging showed trends of various surface morphologies and features for each group. Table 2.5 summarizes these features by using representative images for each respective

group. The most noteworthy features were spherical micro-globules (phase separated crosslinked HA) which were either loosely associated or adhered to each other to form larger three dimensional super structures. In increasing swell time, there was a larger presence of the superstructures and fewer independent micro-globules on the surface. This trend continued to the point where, at 60 min, the samples surface was covered in the superstructures and there was very little exposed PDMS surface. A similar trend was observed with increasing solution concentrations. At 2x solution concentrations, the samples were also covered in cracked plates formed of the superstructures. Another noteworthy observation was that these micro-globules became less spherical in shape as solution ratios increased (OH:NCO). The features were very spherical and regular at the 1:1 ratio level, but as the ratio approached 7:1 they became more irregularly shaped and deformed.

Based on hydrophilicity, handling properties, and opacity it was determined that the treatment parameters which produced the best samples most regularly were: 45 minute swelling time; and 2% (m/V) silyl-HA-CTA and1.33% (V/V) pHMDI in xylenes treatment solutions. Therefore, these were the treatment parameters used in the simultaneous swelling method for the remainder of the presented work.

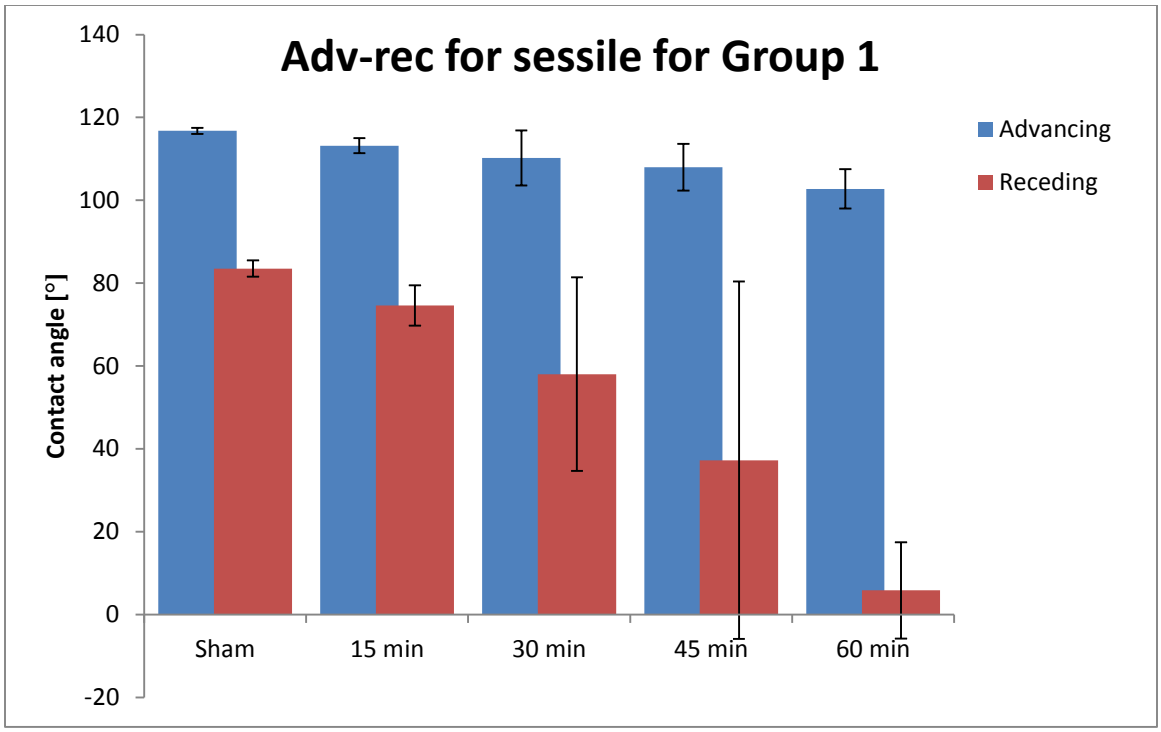

Figure 2.10: Sessile CAG results for Group 1

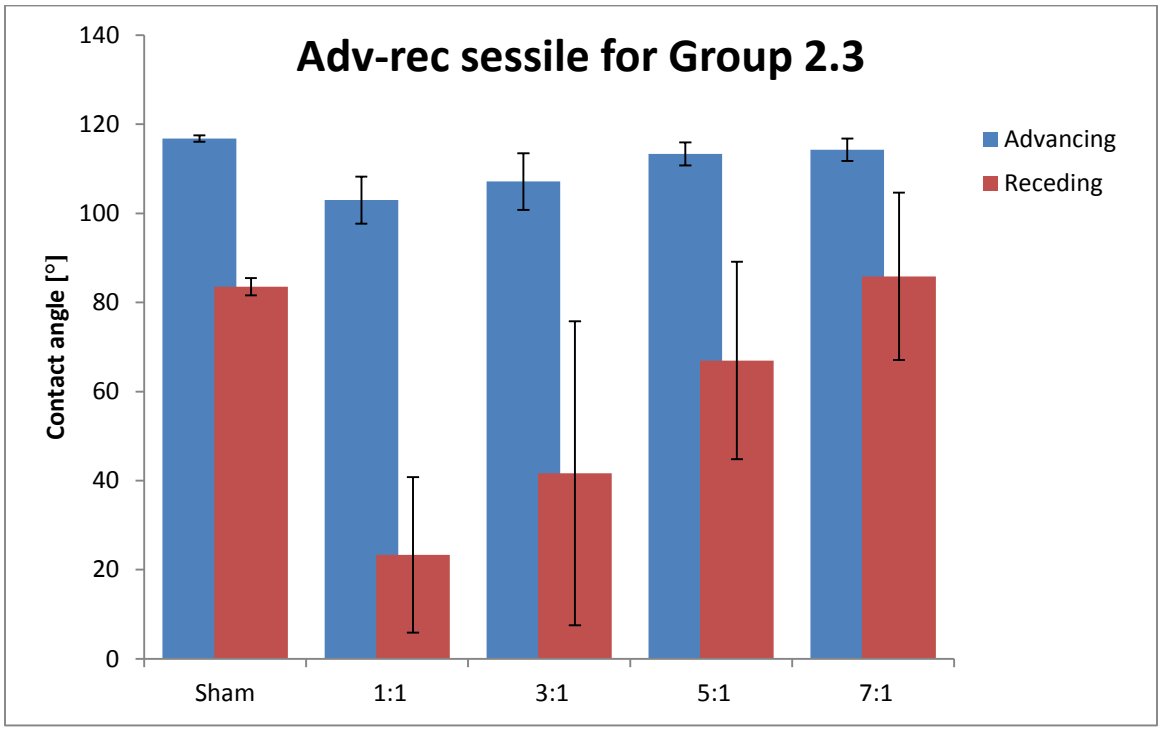

Figure 2.11: Sessile CAG results for Group 2

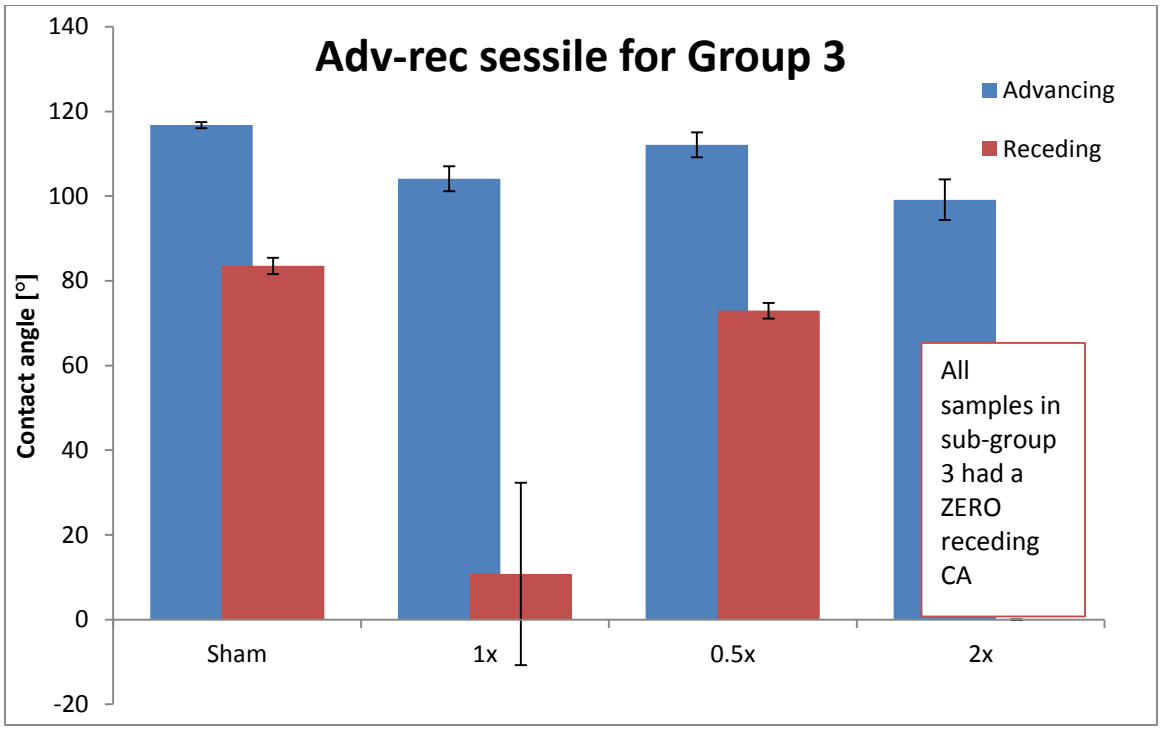

Figure 2.12: Sessile CAG results for Group 3

Table 2.5: SEM images for each of the parameter variations explored in the study designed to determine the treatment parameters of the simultaneous swelling method.

Group 1 (Swell time)	Group 2 (Solution ratio)	Group 3 (Solution concentration)
15 min	1:1	0.5x
30 min	3:1	1x
45 min	5:1	2x
60 min	7:1	

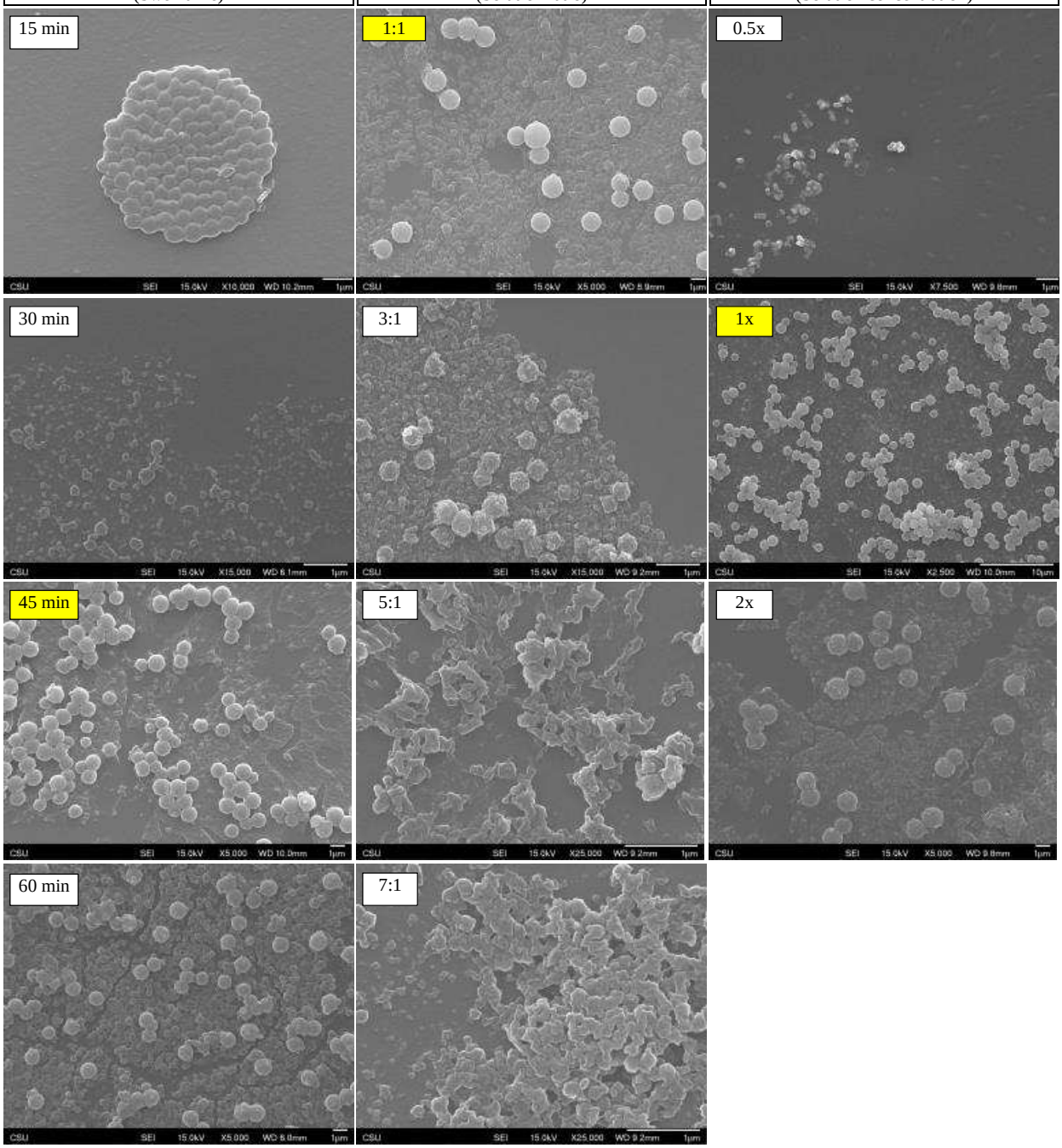

2.5 Methods – Sample characterization

The goal of the specific aims discussed in this chapter included synthesis of the HA-PDMS IPN material as well as the evaluation of the aforementioned materials based on hydrophilicity and surface chemistry/morphology. In this section the analytical techniques used to evaluate the materials are described. Hydrophilicity was evaluated via Contact Angle Goniometry and surface chemistry/morphology was evaluated via SEM imaging, ATR-FTIR spectroscopy, and XPS spectroscopy.

2.5.1 Contact Angle Goniometry (CAG)

Contact angle goniometry (CAG) is the measurement of the angles which a probe fluid makes when in contact with a substrate. Two basic but distinct variations exist for this analytical technique. One is the sessile drop method wherein a liquid is deposited onto an upright sample and the profile is used to determine the contact angle. Probably the most common form is that where the fluid whose contact angle being measured is water on a dry surface and air as the bulk medium. In this case, high contact angles imply a more hydro*phobic* substrate and low contact angles imply a more hydro*philic* substrate. Figure 2.13 below shows an example of each. The measured angles are higher on hydrophilic surfaces because the balance of free energies favors minimizing substrate-water contact. Conversely, the lower angles observed on a hydrophilic surface are because the balance of free energies favor maximizing substrate-water contact. This is the case for flat, homogeneous, nonreactive surfaces. In the case of a superhydrophilic surface, the water will spread across the surface completely and is said to have a zero contact angle.

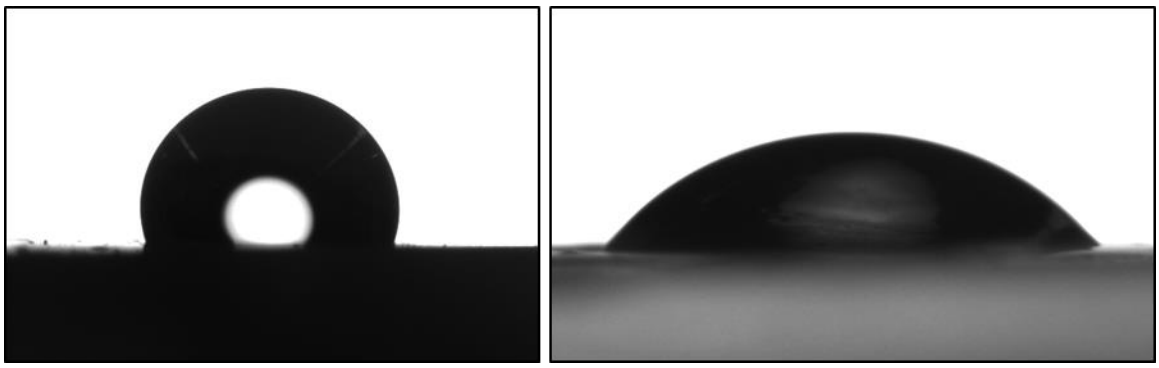

Figure 2.13: Example images of a water droplet on a hydrophobic surface (left) and a more hydrophilic surface (right) in a sessile drop arrangement. Original work.

The other basic technique for CAG is the captive bubble method. This method is named so because, unlike the sessile drop, the substrate is inverted and submerged in a liquid that is more dense than the probe fluid. The probe fluid (usually a gas or a less dense liquid such as an oil) is released under the substrate where buoyancy delivers it to the surface. Probably the most common arrangement is when the bulk fluid is water and the probe fluid is air. In this case, the reverse relationship between hydrophilicity and contact angle is observed as compared to sessile drop. A higher contact angle implies a more hydro*philic* substrate while a lower contact angle implies a more hydro*phobic* one. Figure 2.14 below shows an example of each situation. In the hydrophobic case, the balance of free energies seeks to minimize water-substrate contact and the bubble, therefore spreads more over the surface. In the hydrophilic case, the water-substrate contact is maximized, resulting in little air-substrate contact and a more spherical bubble. For superhydrophilic surfaces, the bubble may not actually make contact with the surface at all but be separated by a thin film of water. This case is generally harder to see in the profile but it can be noted by the bubble gliding freely under the substrate when gently agitated or tilted.

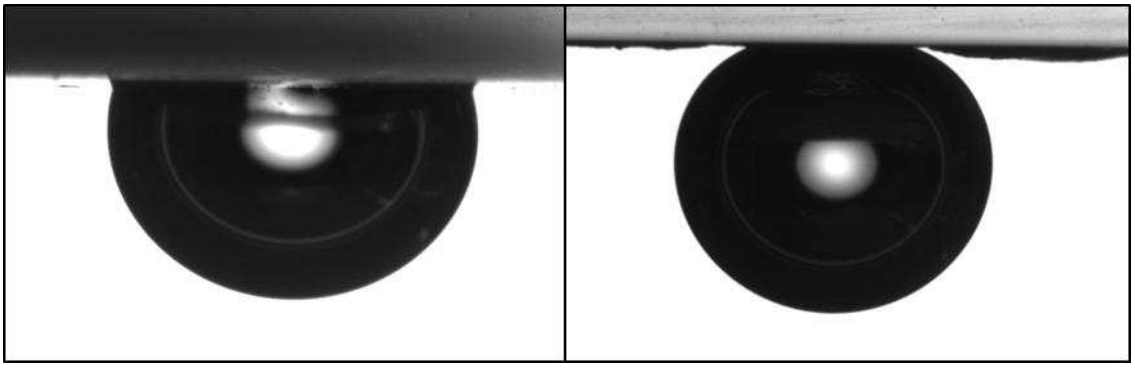

Figure 2.14: Example images of a water droplet on a hydrophobic surface (left) and a more hydrophilic surface (right) in a captive bubble arrangement. Original work.

In addition to the sessile drop and captive bubble arrangements, there are also two main ways in which the contact angles were observed – static and dynamic (advancing-receding) contact angles. In the former, the probe fluid is brought in contact with the substrate and measured as-is. In the latter, the probe fluid is brought into contact with the substrate and then probe fluid is added then retracted from the drop/bubble. As probe fluid is added/removed the drop/bubble will change in size and shape but the triple-phase interface (line where substrate, probe fluid, and bulk fluid all interface simultaneously) will remain "pinned" in place. The changing shape of the drop/bubble results in a change in contact angle.

Once the contact angle reaches a certain threshold, the triple-phase interface moves but maintains a constant contact angle. Depending on the configuration, this constant angle during interface movement is either the advancing or the receding contact angle. The advancing angle relates to how readily a surface becomes wetted, whereas the receding contact angle relates to the tendency of the surface to remain wetted. The difference between these two angles is referred to as the hysteresis. Large hystereses indicate a surface that somehow changes when exposed to the probe fluid, whether this is some reaction or surface rearrangement. Figure 2.15 below diagrams the advancing and receding contact angles in both a sessile drop and captive bubble

configuration. In the figure, two red circles have been added to highlight the triple-phase interface for demonstration. In the profile view, this interface appears as a single point on either side of the drop/bubble where the probe fluid contacts the substrate.

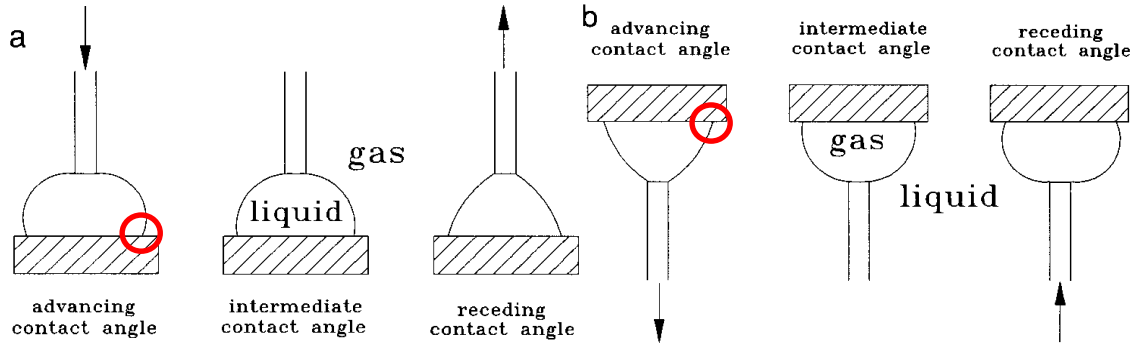

Figure 2.15: Diagram of static and dynamic contact angles in both sessile drop and captive bubble configurations. The red circles highlight a couple examples of the triple-phase interfaces. Adapted from Drelich, et al. [13]

The instrument used in this study to measure the contact angles is a ramé-hart Model 260 Standard Contact Angle Goniometer/Tensiometer (ramé-hart instrument co.) augmented with a manual tilt base (100-25-M, ramé-hart instrument co.). This apparatus included an adjustable sample platform, tunable fiber optic light source, camera (F4 series Firewire, ramé-hart instrument co.), and specialized image/video analysis software (DROPimage Advanced v2.7.01, ramé-hart instrument co.). Figure 2.16 shows the goniometry setup. Samples are placed on the sample platform and illuminated by the light source. A small amount of probe fluid was dispensed manually onto the sample surface by turning the dial on a calibrated syringe. The backlighting of the sample and probe fluid creates a contrast profile which is recorded by the camera which then feeds it to a computer as a monochromatic image for display and analysis. The images in Figures 2.13 and 2.14 were taken using this instrument and demonstrate the contrast profile image of the drop/bubble. Contact angles are calculated from the images in real-

time by the associated software and saved as text files. The text files are then exported into a Microsoft Excel spreadsheet for analysis.

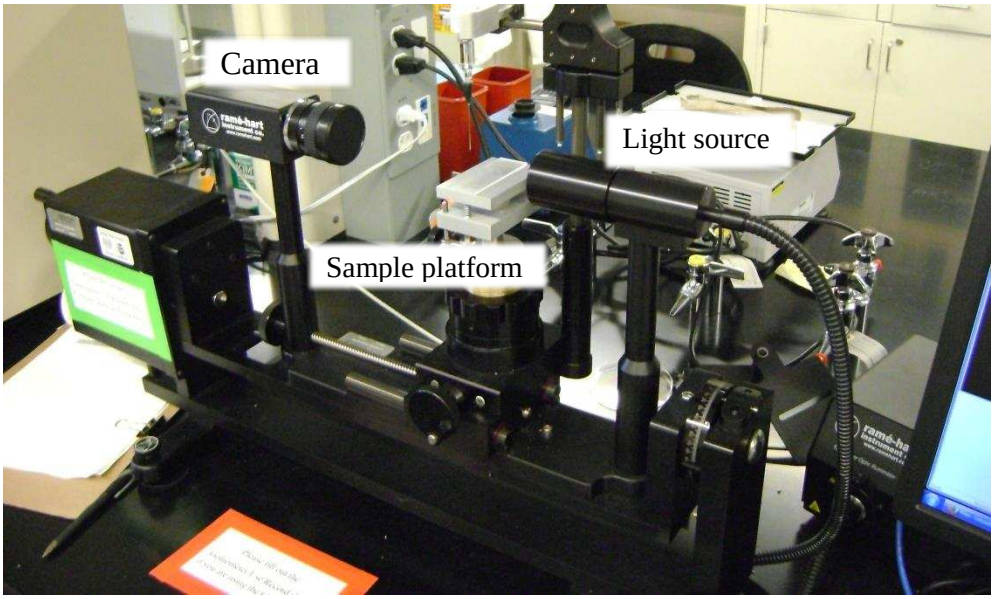

Figure 2.16: Pictured: the goniometry apparatus used in this work. The instrument components were manufactured by ramé-hart instrument co. Labeled are the camera, sample platform, and light source.

In the sessile drop configuration, each sample was tested in three locations for static, and two locations for advancing/receding contact angles. In the captive bubble configuration, only the three static angles were observed due to the difficulty in managing the bubble during adding/removing air. In each of the static contact angle cases, three measurements were taken in rapid succession and then averaged for each drop. For advancing/receding contact angles, the software was set to automatically record the contact angle at regular intervals of 5/sec as water was slowly added to and then removed from the drop on the sample surface. Data collection and water addition/removal continued for several seconds after the triple-phase interface moved and the contact angles stabilized. The analysis of the advancing-receding contact angle data was carried out by plotting the contact angles to aid in determining the regions where the upper and

lower plateaus occur; these correspond to the advancing and receding contact angles respectively. These constant value regions are where the triple-phase interface moved and the angle remained constant while adding or removing the water from the drop. Figure 2.17 illustrates an example of this plot for advancing-receding data. The advancing and receding contact angles are the averaged values of these constant value regions.

Values reported for captive bubble contact angles in the results and discussion section have been modified to be more comparable to sessile drop contact angles. This modification is simply subtracting the recorded values from 180°. It is important to note that this modification only makes the relationship between reported contact angle and hydrophilicity more comparable. The values themselves are still not directly comparable. Contact angles recorded by the software for the captive bubble configuration have a positive relationship with hydrophilicity: larger angles imply greater hydrophilicity. In contrast, contact angles recorded by the software for the sessile drop configuration have a negative relationship with hydrophilicity: smaller angles imply greater hydrophilicity. Thus, the contact angles reported for the captive bubble configuration have been modify by 180° to make their trends comparable to those of the sessile configuration: smaller reported angles implies greater hydrophilicity for both configurations under this modification.

The samples characterized under CAG were stored in DI water for a minimum of 6 hrs before testing. Samples were gently blotted dry with a Kimwipe prior to testing.

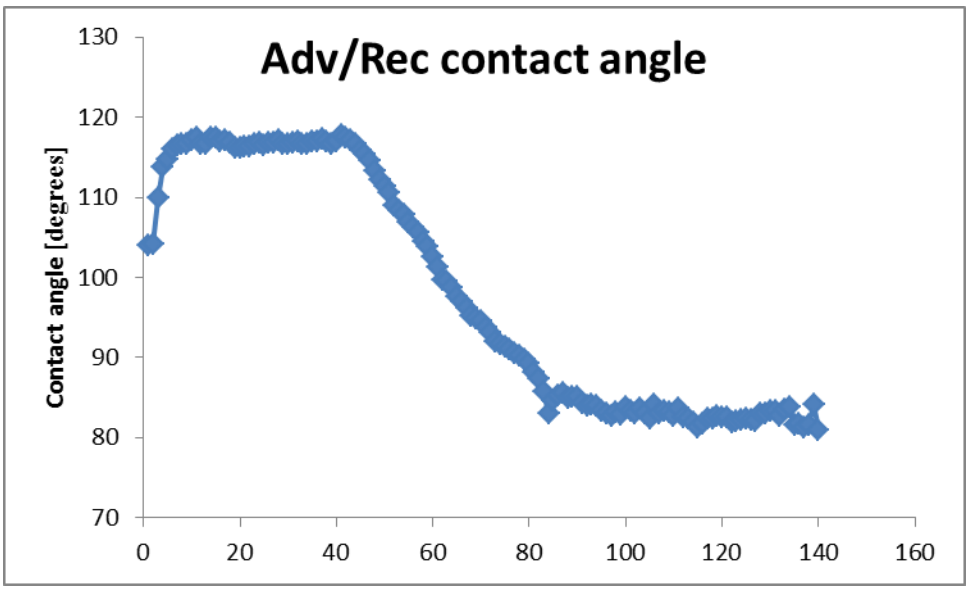

Figure 2.17: An example plot of advancing-receding contact angle data for a PDMS film. The upper and lower plateaus correspond to the advancing and receding contact angles, respectively. Original work.

2.5.2 Attenuated Total Reflectance Fourier Transform Interferometry (ATR-FTIR)

Surface chemistry of the test samples was evaluated via Fourier Transform Interferometry (FTIR) with Attenuated Total Reflectance. This analytical technique is useful for observing changes in or introduction of chemical bonds within 200nm to 1μm of the substrate surface [14]. The instrument used was a Nicolet SX-60 FTIR spectrometer with ATR-ZnSe (Thermo Scientific) and the output was analyzed using a specialized software suite (OMNIC software, Thermo Scientific).

Samples were placed directly on top of the crystal and a pressure was applied with an attached lever arm to ensure good sample-crystal contact. Samples were analyzed over a spectrum of 600-4000cm^{-1} with a resolution of 5 and 64 scans. Before each scan, the crystal was wiped clean with a Kimwipe damp with ethanol to remove any residue which may have been left on the crystal due to the pressure of the lever arm. This was determined to be necessary for

PDMS samples as minute amounts of material could leak out under the pressure applied and remain on the crystal to contaminate following scans (unpublished work). Backgrounds were taken at the beginning of each session and after every 4 spectra collections. Backgrounds were automatically subtracted from the collected spectra by the program.

Spectra were obtained for untreated PDMS, sham PDMS (i.e. underwent entire treatment with the exception of silyl-HA-CTA steps), treated PDMS, and sodium hyaluronate (Na-HA, as received from manufacturer, Lifecore Biomedical LLC) for comparison. In the case of PDMS films, the samples were laid on the platform in contact with the crystal and the lever arm engaged to apply pressure. In the case of the Na-HA, a small amount of the powdered material was piled and packed onto the crystal before lowering the lever arm to compress it against the crystal. All sample materials were dried (50C, -25inHg (gage)) for at least 12 hours before testing.

2.5.3 Scanning Electron Microscopy

Scanning Electron Microscopy (SEM) was used to visualize and characterize changes to surface morphology of the sample materials. SEM testing portions were cut out of larger test films via an 8mm biopsy punch. Since silicone is an insulating material, samples were adhered to a conductive (aluminum) platform via carbon tape and coated with 5nm of gold prior to imaging. Additionally, samples were dried (50C, -25inHg (gage)) for at least 12 hours prior to imaging and kept in a portable vacuum desiccator until just before imaging. This was found to greatly decrease the required for the instrument to return to a low vacuum pressure. Silicone is generally highly gas permeable material [4] it is believed that the decrease in pump-down time is likely that the films off-gas in the instrument when not properly stored prior to testing.

The instrument used was a JEOL JSM-6500F field emission scanning electron microscope (FESEM) with associated proprietary software for both instrument control and image

analysis (JEOL USA, Inc). Samples were analyzed at 15kV and a working distance of 5.0-10.0mm depending on the sample. Images were taken at multiple magnifications and locations for each sample. Care was taken to obtain image of anomalies of interest as well as representative portions of the samples.

2.5.4 X-ray Photoelectron Spectroscopy

X-ray Photoelectron Spectroscopy (XPS) was used to characterize the elemental composition of the surface of samples. This differs from the characterizations obtained via ATR-FTIR in that XPS primarily gives information on elemental composition whereas ATR-FTIR primarily gives information on chemical bonds. Additionally, XPS is generally more surface sensitive than ATR/FTIR [14]. XPS testing portions were cut out of larger test films via an 8mm biopsy punch. Additionally, samples were dried (50C, -25inHg (gage)) for at least 12 hours prior to imaging and kept in a portable vacuum desiccator until just before imaging. This was found to greatly decrease the required for the instrument to return to an ultra-low vacuum pressure. Silicone is generally highly gas permeable material [4] it is believed that the decrease in pump-down time is likely that the films off-gas in the instrument when not properly stored prior to testing.

The instrument used was a 5800 ESCA/AES system with the monochromatic Al Kα X-ray source (1486.6 eV, Physical Electronics PHI) and associated software (Multipak, Physical Electronics). In addition to full spectrum survey scans, high resolution scans were taken focusing on the elements carbon (C), oxygen (O), silicon (Si), and nitrogen (N). These elements were of interest because of their presence in hyaluronan and/or PDMS. The output was analyzed using the Multipak software and SG5 smoothing was performed. Percent elemental composition of the sample surfaces was also obtained using Multipak. For generic PDMS, $[SiO(CH_3)_2]_n$, the

expected elemental ratio for C:Si:O is 2:1:1. Any changes in this ratio and/or the inclusion of nitrogen were of particular interest because HA contains N and silicone does not.

Samples analyzed included: untreated PDMS films, sham PDMS films (i.e. exposed to all treatment step with the exception of those involving silyl-HA-CTA), treated PDMS films, and sodium hyaluronate (Na-HA, as received from manufacturer, Lifecore Biomedical LLC) for comparison.

2.5.5. Statistics

All comparisons were done with at least a sample size (n) of 3. Where quantifiable differences are concerned, statistical significance was determined by use of a paired t-test with $\alpha=0.05$ and $p<0.05$ unless otherwise noted.

2.6 Results and discussion

The results and observations of the previously described treatment and characterizations are discussed in this section. This begins with observations and comments regarding the synthesis, processing, and swelling of the base silicone film materials. This is followed by observations and comments regarding the treatment of said films. Finally, the results and observations of the characterization of the treated materials' hydrophilicity and surface chemistry/morphology are discussed in detail.

2.6.1 PDMS Film Creation and Processing

The films used for the majority of this work came from the P-125 kit (Silicones-Inc). The kit had a listed gel time (time past which the mixture has cured beyond the point of flowing freely) of about 1 hour at room temperature. The use of chilled aluminum blocks significantly increased the time that the mixtures were workable and any imperfections were able to be removed. With the process described previously in this chapter, it was found that if the mixtures

were not spin cast before 45min after first introducing the A and B components that there was a very high probability that the film would not be useable. The flow properties of these mixtures were so different from the initial mixture that the resulting films often had such severe surface blemishing or textures that they were not usable. This was most commonly seen as a crater-like feature outlining the shape of the original deposited mixture. This is often accompanied by radial ridges originating from the center of the film and radiating outwards. These features were sometimes so significant that they could easily be felt by hand.

However, films that were mixed, degassed, and spin cast in less than 35 minutes from initial mixing were nearly entirely free of noticeable surface blemishes and features (save for the occasional particle of dust that had fallen onto the surface before the films had fully cured). Barring any unusual complications, films cast under the method outlined earlier in this chapter were relatively uniform. These films had an average initial mass of 0.850g and an average thickness of 0.1905mm (0.0075in) as measured with a digital scale and calipers, respectively. This increase in film quality is very likely due to the fact that the crosslinking reaction had not yet proceeded as far and the still curing mixture could flow more freely in these more quickly made films.

Following curing, films were washed of any residual lower molecular weight species (LMWs) which were not a part of the larger crosslinked network. A loose positive relationship was observed between the time taken to make the films and the amount of mass lost during this washing step. It is believed that this can be explained in part by the fact that these films were still being processed and exposed to forces (i.e. during spin casting) while they are no longer able to freely flow but not yet fully cured. This results in more material which has yet to be incorporated into the larger network to be moved to a location in which it cannot fully integrate.

2.6.2 Treatment observations

In this section, observations of changes in samples noticed by the experimenter(s) are discussed. This begins with observations shared between both treatment methods and is followed by a more detailed discussion for observations specific to each respective method.

In both major treatment variations described earlier in the chapter – sequential and simultaneous swelling methods – there was a noticed decrease in clarity of the samples after treatment. In all cases, this decrease in clarity was lessened when the material was wetted (i.e. submerged in DI water). This change in clarity is measured and discussed in more detail in Chapter 3. This decrease in clarity seemed to correlate to increasing hydrophilicity (as determined by contact angle goniometry) for most samples.

Additionally, treated samples were noticeably more rigid. It is important to note that the samples were still flexible and elastic, but had a noticeably increased bending stiffness. The treated samples had less of a tendency to fold over on themselves when compared to untreated films. This is mentioned here only as a subjective observation from handling the samples in question and no quantifiable data has yet been obtained related to it.

One final subjective observation about the change in sample handling after treatment relates to the treated films' tendencies to cling to glass and itself. The untreated films possess a great tendency to cling statically to glass and other silicone surfaces (i.e. themselves); whereas the treated samples had a noticeable reduction in static attraction to glass and other silicone surfaces. This difference was even more noticeable when the samples were wetted. When a thin film of water was placed between the films and a glass surface, the treated films would glide more freely across the surface than the untreated (reduced apparent friction under these conditions). This was noticed even for treated films which did not retain water films across their

surface. This is mentioned here only as a subjective observation from handling the samples in question and no quantifiable data has yet been obtained related to it.

The change in mass of the sample after treatment as compared to its initial mass was calculated, using Equation 2.2, for each treated sample and averages for each treatment method are reported in Table 2.6.

$$\%change = \frac{m_{final} - m_{initial}}{m_{initial}} * 100\% \qquad \text{(Eq 2.2)}$$

Increases in mass indicate the introduction of new material into the PDMS film. It was not unusual for a film to lose some small amount (<0.5%) of mass after swelling in xylenes during the treatment process.

Table 2.6: Values given as: average ± standard deviation. Values are in units of %-change with respect to initial mass.

	Simultaneous	Sequential
%change	1.78±0.57	2.39±0.46

Sham samples showed no statistically significant ($p<0.05$) change in mass regardless of treatment method. Furthermore, sham samples in both treatment methods showed no noticeable differences in clarity, handling, or stiffness when compared to plain PDMS. This implies that the exposure of the PDMS material to pHMDI (chemical crosslinker) or any other step of the treatment process is not responsible for the changes observed but that it is due to the presence of hyaluronan.

2.6.2.1 Comparison between Sequential and Simultaneous Swelling Methods

The most noteworthy differences between samples made from these two methods relate to the reliability of successful treatment. While the most hydrophilic samples observed in this

work were made under the simultaneous swelling method, not all samples treated in this way would be hydrophilic (as observed by CAG analysis). This is to say that samples under the simultaneous swelling method were treated with varying degrees of success between each batch of treated samples. This is believed to be due, in part, to lack of precise control of environmental factors such as humidity and temperature. Both silyl-HA-CTA and pHMDI are sensitive to humidity and the crosslinking reaction is sped up as temperature increases. Because of this, water contamination and temperature fluctuations had detrimental effects on some treatment batches but not on others. It is believed that with greater control over humidity and temperature that this batch-to-batch variability could be reduced.

In contrast, the sequential swelling method produced samples which were more consistent but never quite as hydrophilic as some of the better films made under the simultaneous swelling method. These samples had predictable increases in hydrophilicity and handling properties from batch-to-batch.

2.6.3 Characterizations

The following section addresses specific aim 2 and contains the presentation and discussion of the results of the characterizations performed. Hydrophilicity was evaluated with contact angle goniometry and surface chemistry/morphology was evaluated using SEM, ATR-FTIR, and XPS.

2.6.3.1 Contact Angle Goniometry

Contact angle goniometry (CAG) was used to evaluate the hydrophilicity of the surface of the materials. The configurations of this test are discussed earlier in this chapter. Different trends were noted between the different treatment methods, specifically in the variability of water film retention and contact angles.

Table 2.7 below contains the average values for CAG for control, sham, and treated silicone films. Note: the captive bubble measurements have been adjusted by 180°. Refer to the methods section for more information. “Adv” and “Rec” refer to the advancing and receding angles, respectively. Following Table 2.7 are Figures 2.18 and 2.19 which contain the plots for the data in the table.

*Table 2.7: Summary of contact angles for the methods and samples in this work. Values reported as: average ± standard deviation. *The highlighted cell draws attention to the average being smaller than the standard deviation; this is due some samples having a zero receding contact angle in that category.*

Sequential swelling				
	sessile			Captive bubble
	Static	Adv	Rec	Static
Control	105.20 ±2.29	113.92 ±1.53	83.77 ±3.92	89.74 ±0.55
Sham	106.62 ±1.38	117.00 ±2.02	82.38 ±2.33	88.67 ±2.35
Treated	99.64 ±7.86	96.42 ±18.1	38.23 ±7.45	77.96 ±5.00

Simultaneous swelling				
	sessile			Captive bubble
	Static	Adv	Rec	Static
Control	105.20 ±2.29	113.92 ±1.53	83.77 ±3.92	89.74 ±0.55
Sham	107.42 ±2.24	116.77 ±0.72	83.52 ±1.95	91.06 ±1.76
Treated	94.57 ±5.75	102.76 ±4.73	*5.83 ±11.65	36.25 ±13.71

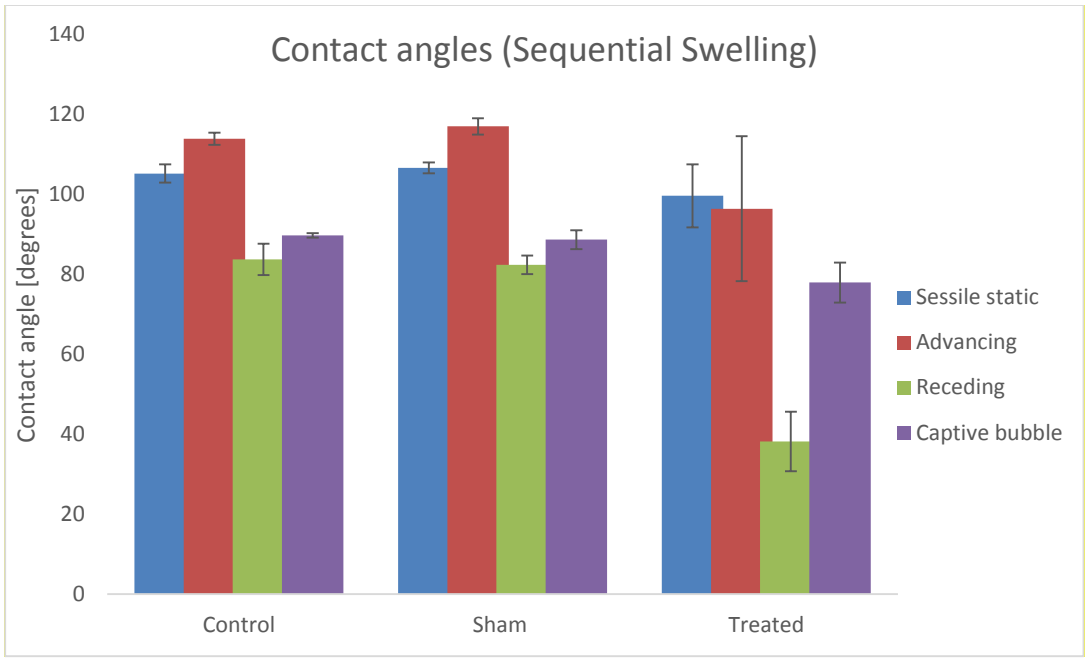

Figure 2.18: Plot displaying the comparison made in Table 2.7 for sequential swelling samples.

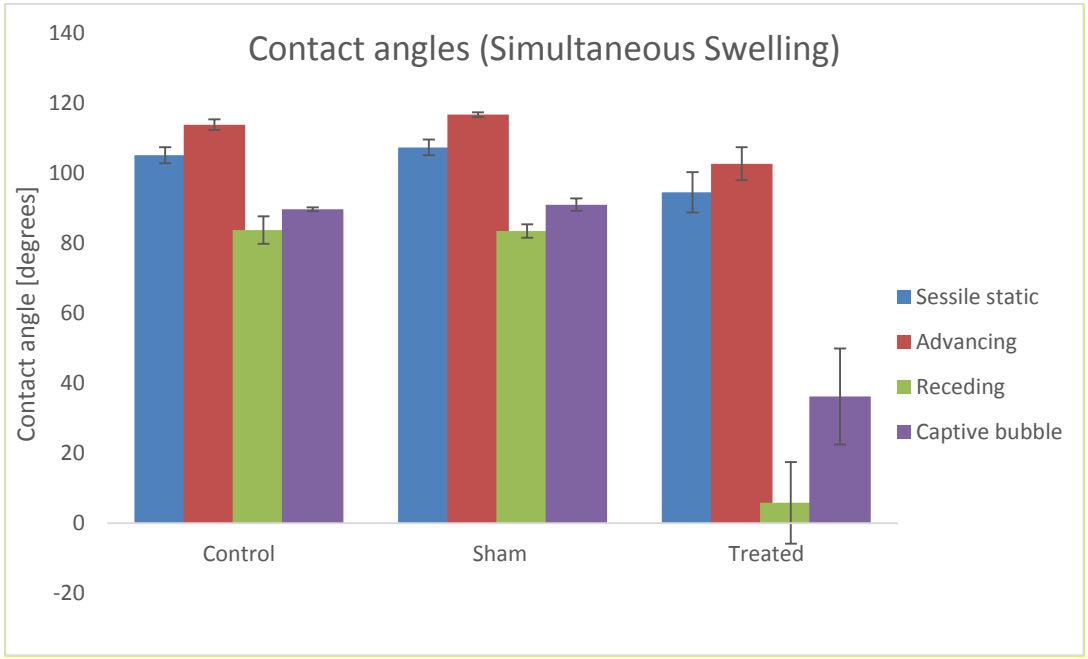

Figure 2.19: Plot displaying the comparison made in Table 2.7 for simultaneous swelling samples.

It can be seen from this data that the largest difference between plain and treated samples occurs in the receding contact angles. Because the receding contact angle relates to the substrate's tendencies to retain water once wetted, this is where the biggest differences due to treatment tended to be seen. These hystereses are largely due to surface rearrangement or reconfiguration once rehydrated. It is also in these receding contact angles that the differences between the results of the sequential and simultaneous methods become most evident. The samples made under the simultaneous swelling method had lower average contact angles (some even fully wetted the sample surface), but higher standard deviations (more inconsistency between samples) when compared to those made under the sequential swelling method.

In summary, both treatment methods proved to be capable of producing films that were more hydrophilic than untreated silicone. This improvement was especially evident in the receding contact angles. While the simultaneous swelling method produced samples that were more hydrophilic on average, there appears to still be refinement of the method needed to decrease the variability.

2.6.3.2 ATR/FTIR

ATR/FTIR analysis of the samples qualitatively demonstrated the introduction of absorbance peaks about 3400 cm^{-1} (OH bonds) and a series of peaks around 1600 (carbonyl stretch bands) [1]. These peaks are of particular importance because thay are found in crosslinked HA, but not in the untreated PDMS films. Therefore, the introduction of these new peaks suggests the presence of hyaluronan in the treated silicone samples. Furthermore, the sham samples (exposed to all treatment steps excluding HA) had spectra that were indistinguishable from those of plain PDMS.

Additionally, it was noted that samples treated under different methods showed different intensities of the above mentioned peaks. Specifically, the more opaque samples, such as those had more intense peaks about the ranges mentioned above.

Figure 2.20 shows three FTIR absorbance spectra. From top to bottom: plain PDMS; HA treated PDMS; and pure sodium hyaluronate (Na-HA, the form as received from the manufacturer).

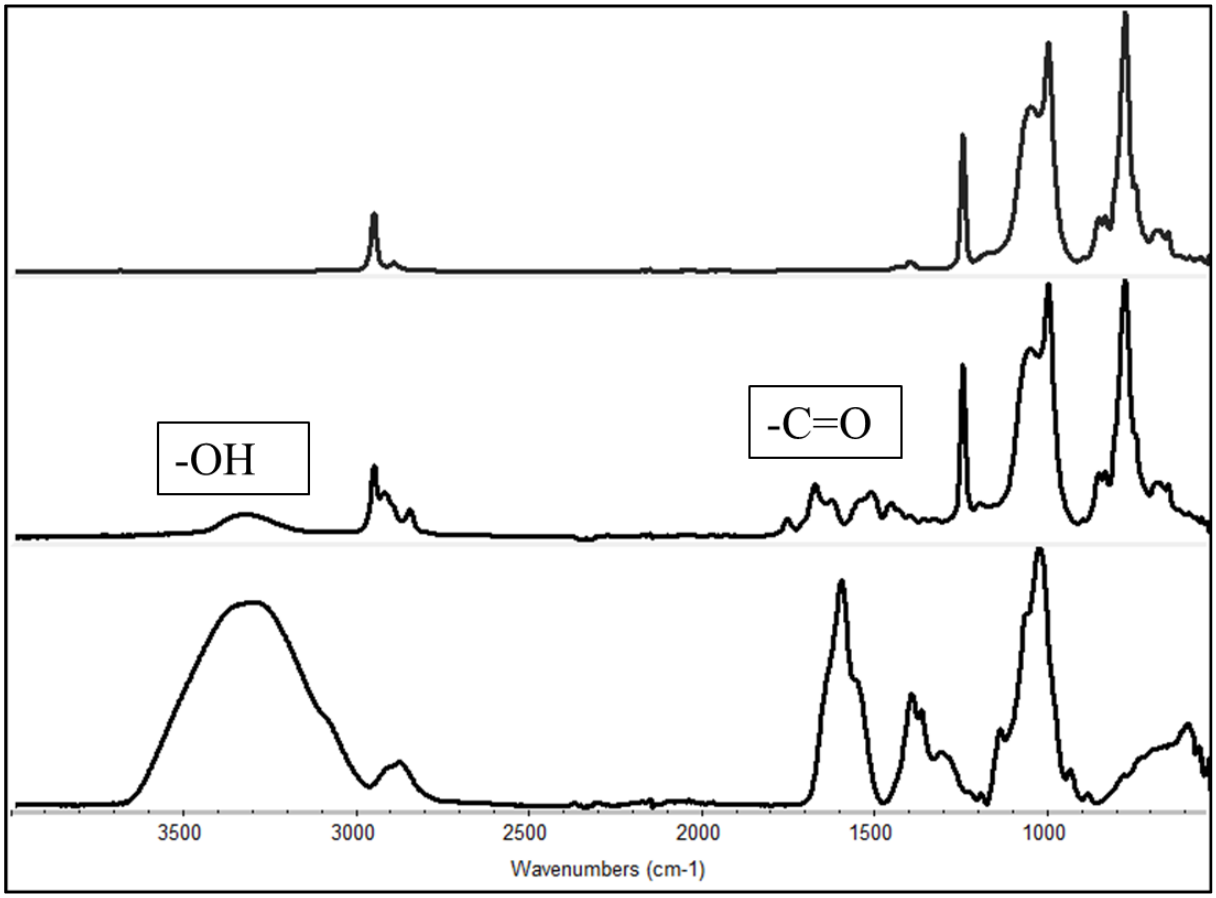

Figure 2.20: From top to bottom: control PDMS; HA treated PDMS; and pure sodium hyaluronate (Na-HA, the form in which we receive our HA from the manufacturer).

2.6.3.3 SEM Imaging

SEM imaging was used to characterize the surface morphology of treated and untreated PDMS films. Various trends were observed based on the treatment method, but one feature that appeared commonly on all treated samples but not on untreated samples was the presence of spherical micro-globules; see Figure 2.21 for examples. These entities are believed to be phase-separated domains of crosslinked hyaluronan that formed during treatment. The spherical globules were generally uniform in size, 1μm in diameter, and appeared both as independent features and as parts of larger superstructures which ranged in size and shape. These can be seen in Figures 2.22 and 2.23 respectively.

In the samples which showed more uniform hydrophilicity across the surface, the globules were more evenly spaced out and integrated with the background material (PDMS substrate), such as seen in Figures 2.22 and 2.24. Also worthy of mention is that the samples which had more superstructures or an unusually high density of independent globules tended to be more opaque. This seems to indicate that the opacity taken on by the samples after treatment can be attributed to these spherical micro-globules. It is therefore reasonable to assert that better control over the formation and distribution of these micro-domains among the surface would result in more hydrophilic films which are also more transparent than those created to date.

SEM images of untreated PDMS films and sham treatment samples showed nothing of interest. The surfaces were smooth and featureless with the exception of the occasional surface blemish (incurred during curing) or particle of dust contamination.

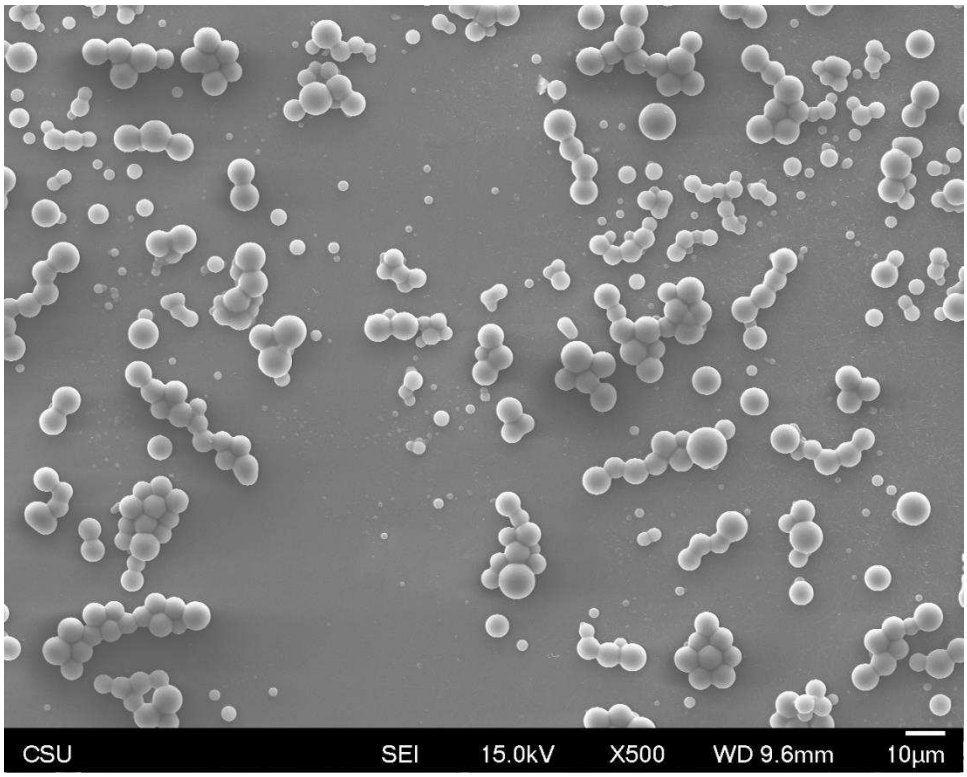

Figure 2.21: SEM image of the surface of a PDMS film treated with hyaluronan. Pictured is a film treated under the sequential swelling method.

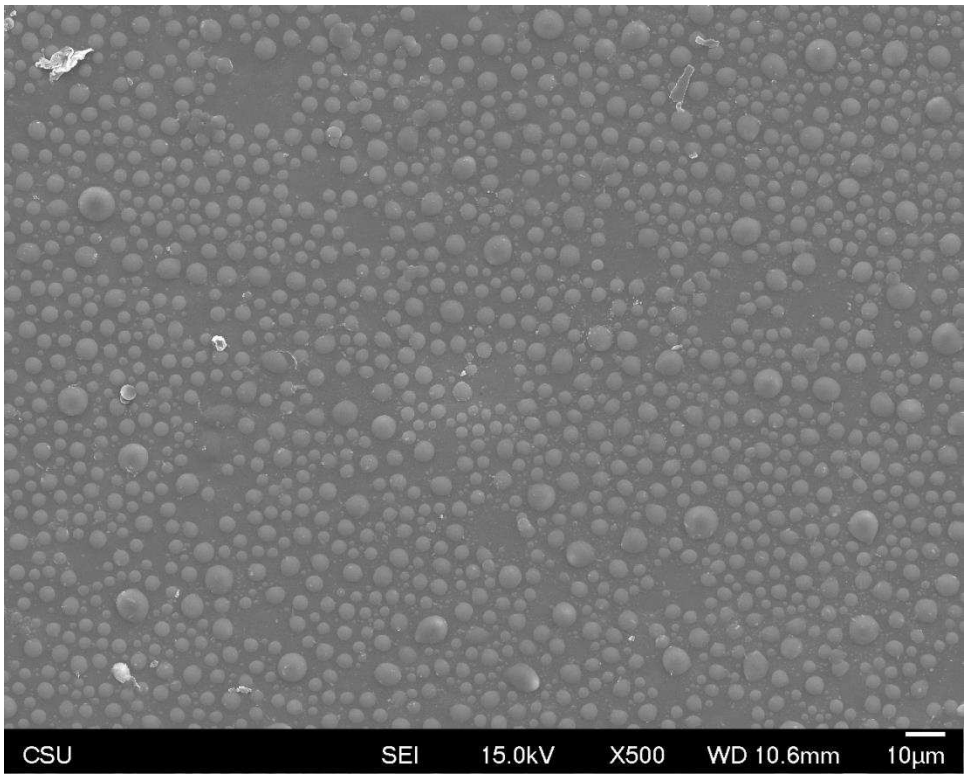

Figure 2.22: SEM image of the surface of a PDMS film treated with hyaluronan. Pictured is a film treated under the sequential swelling method.

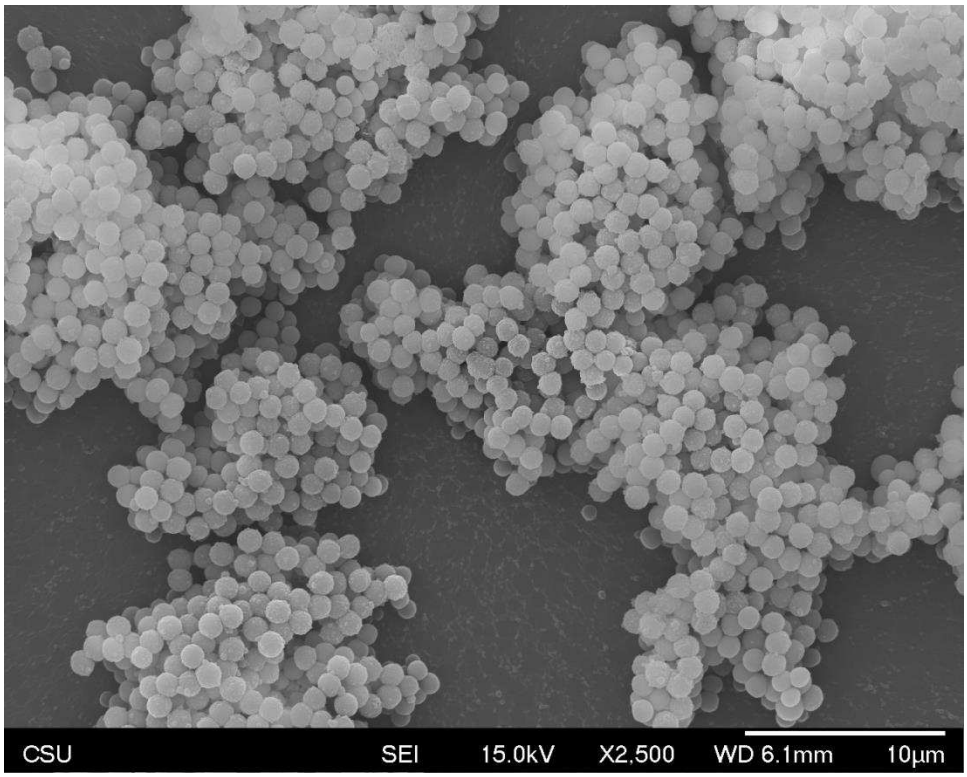

Figure 2.23: SEM image of the surface of a PDMS film treated with hyaluronan. Pictured is a film treated under the simultaneous swelling method.

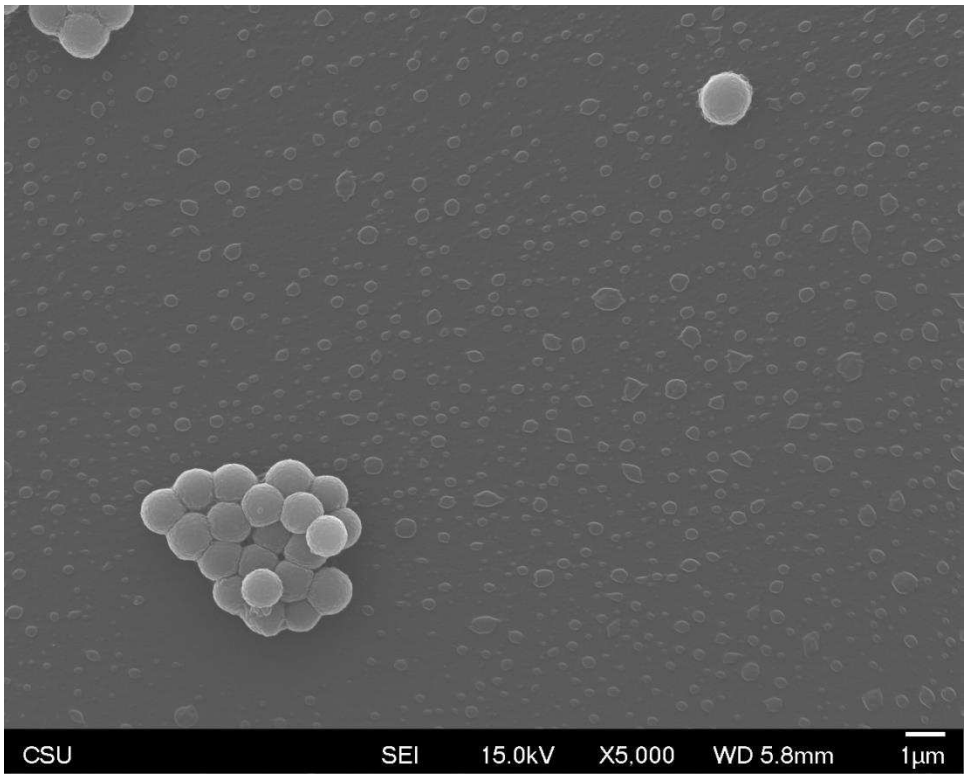

Figure 2.24: SEM image of the surface of a PDMS film treated with hyaluronan. Pictured is a film treated under the simultaneous swelling method.

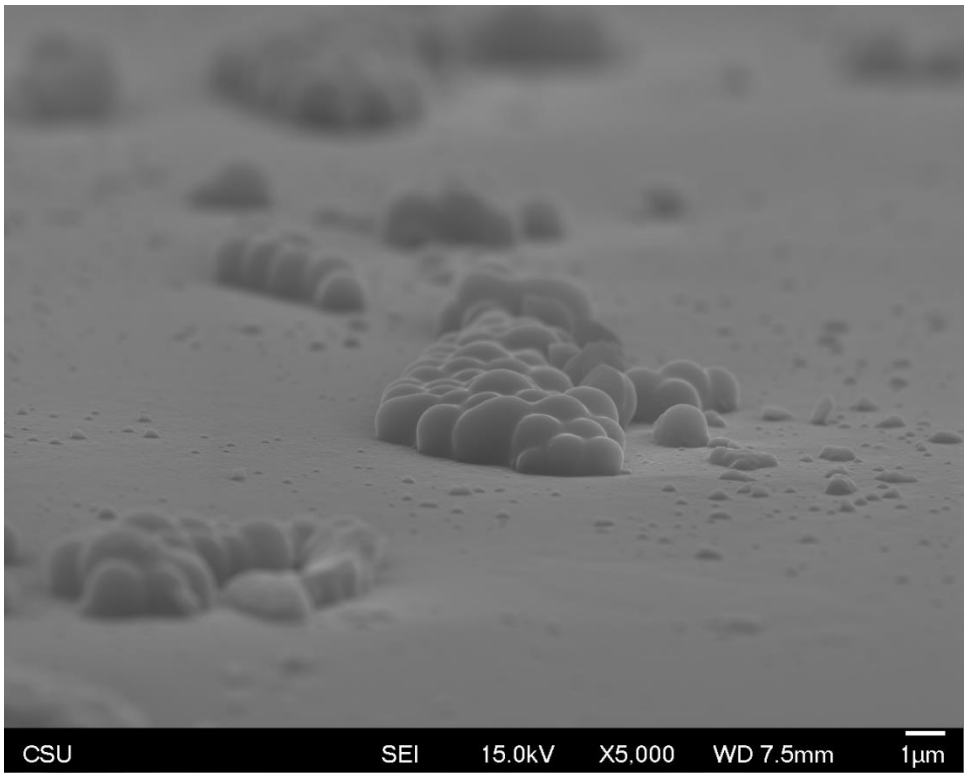

Figure 2.25: SEM image of the surface of a PDMS film treated with hyaluronan. The sample was tilted in the imaging chamber to get an idea of how the micro-globules interface with the substrate. Pictured is a film treated under the sequential swelling method.

2.6.3.4 XPS

XPS analysis was used to determine changes to surface elemental composition. The molecular formula for generic PDMS is $(SiO(CH_2)_2)_n$. So the expected ratio of atomic components on the surface is 2:1:1 (C:O:Si) in control and sham silicone samples. Some small variation in this ratio could be due to surface rearrangement/inversion or measurement noise.

Changes in surface elemental composition were observed for treated samples when compared to virgin PDMS films. Specifically, changes in the C:O:Si ratio and the presence of nitrogen were observed. On the untreated and sham samples, the ratio was approximately 2:1:1 with some deviation due to noise. Additionally, there was no appreciable presence of nitrogen on the untreated and sham samples. The treated samples had a different C:O:Si ratio with a higher elemental composition of carbon and oxygen along with the presence of nitrogen. Specifically,

the treated sample in Figure 2.27 had a C:O:Si:N ratio of 51.7:27.7:17.9:2.7 as compared the to the sham sample which had a ratio of 49.1:26.1:24.1:0.8 where the small nitrogen content is believed to be just contamination. When normalized to silicon content this change is more evident: these normalized ratios are 2.03:1.08:1:0.03 for the sham and 2.89:1.55:1:0.15 treated PDMS samples respectively. This change in C:O:Si:N ratio is as would be expected from the introduction of HA since it contains carbon, oxygen, and nitrogen but no silicon.

Figures 2.26-2.28 show example binding energy curves for survey scans of untreated PDMS, treated PDMS, and sodium hyaluronate (Na-HA) powder. The plots shown here have been recreated for better visibility in print (using Microsoft Excel). The labeled original spectra as displayed by the MultiPak software have been included in Appendix II of this chapter.

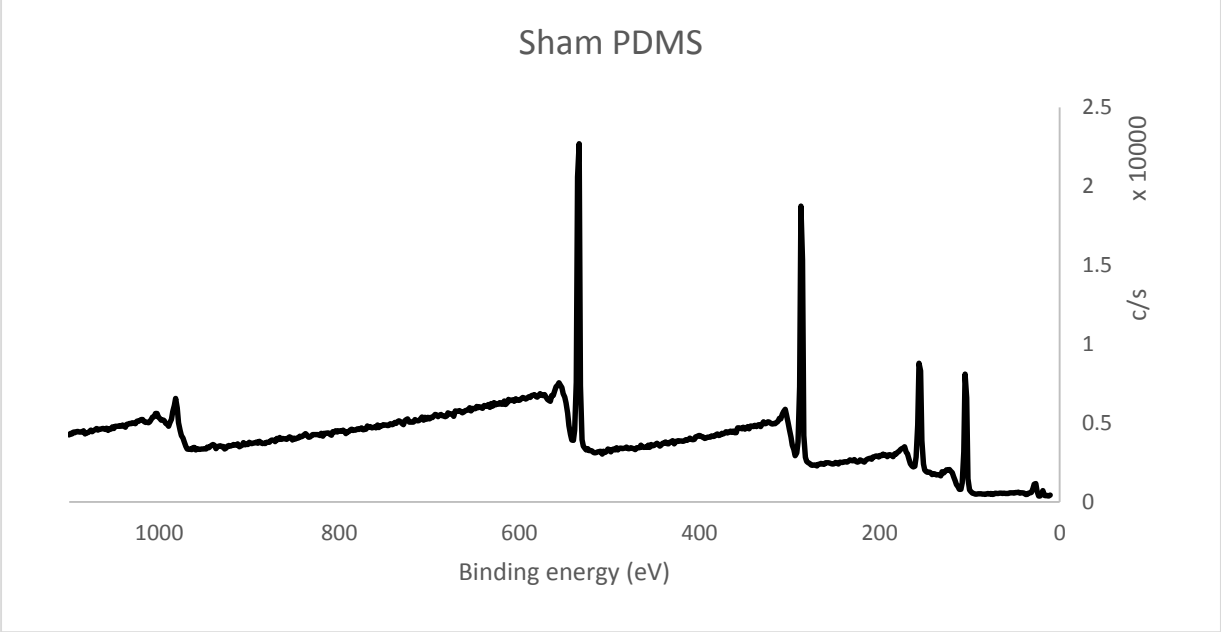

Figure 2.26: Binding energy curve for a sham silicone film. The approx. 2:1:1 ratio of C:O:Si is expected and implies a lack of modification to the sample.

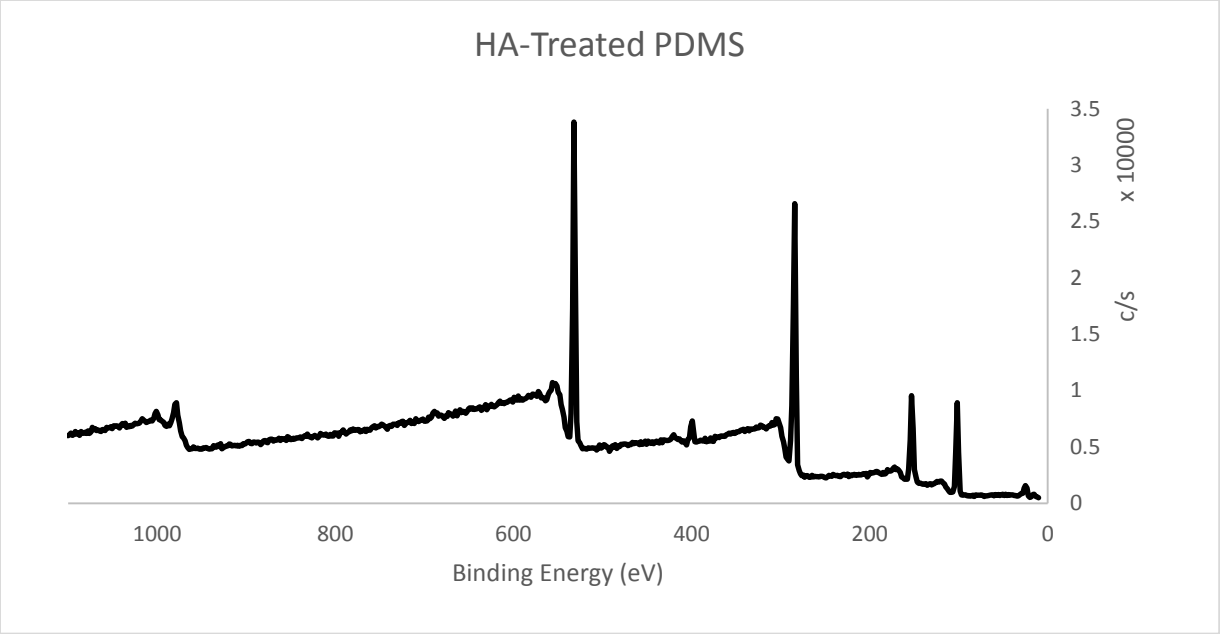

Figure 2.27: Binding energy curve an HA treated silicone film. Note shift in the C:O:Si atomic ratio in favor of more carbon and oxygen, as would be expected from the inclusion of hyaluronan. Additionally, the presence of nitrogen also indicates HA inclusion to the surface.

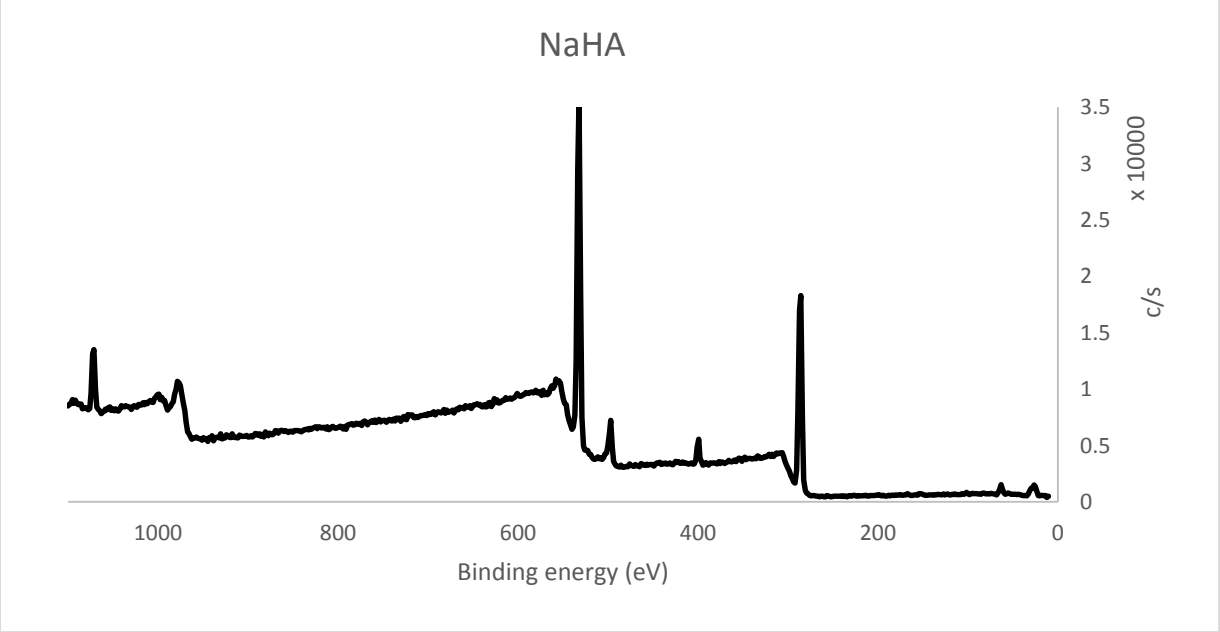

Figure 2.28: Binding energy curve for pure powdered sodium hyaluronate, as received by the manufacturer (Lifecore Biomedical, LLC).

2.7 Conclusions

Chapter 2 addressed specific aims 1 and 2 of this thesis. Herein the processes for synthesizing and evaluating the surface chemistry/morphology and hydrophilicity of hyaluronan treated PDMS IPN materials have been discussed. This has been followed by an in-depth discussion of the results and observations of the aforementioned processes. Treatment success was determined by increases in hydrophilicity, inclusion of new chemical species, surface elements, and changes to surface morphology.

Contact angle goniometry (CAG) demonstrated improvement in hydrophilicity, specifically in terms of receding contact angle. ATR/FTIR demonstrated the presence of new chemical bonds on the treated PDMS films which corresponded to those found in hyaluronan. XPS further confirmed the inclusion of new chemical species by showing that the treated PDMS films, specifically as an increase in the presence of carbon, oxygen, and nitrogen relative to silicon. Lastly, SEM imaging showed new features on the surface of the treated PDMS films in the form of micro-globules which were independent or formed superstructures. Additionally, correlations were noticed between hydrophilicity, opacity, and these spherical micro-domains. When the micro-domains were mostly contained in tightly packed superstructures, the materials were hydrophilic, but also strongly opaque. This is in comparison to samples which had these micro-domains more evenly distributed across the surface in looser communities. These samples demonstrated good hydrophilicity while being notably clearer than the former.

Additionally, the combination of these characterizations reveals even more trends. Samples with the micro-globules more evenly distributed across the surface had more hydrophilic contact angles and were less opaque than samples which had more superstructures seen under SEM imaging. It can therefore be concluded that PDMS-HA materials have been

made which are more hydrophilic than plain PDMS materials. And, with further refinement of the treatment process, treated materials can achieve both greater hydrophilicity and clarity as compared to those made in the present work. Suggestions of how to achieve this are briefly discussed in Chapter 4.

Specific aim 3 involves the evaluation of optical clarity, oxygen gas permeability, cytotoxicity, and hemocompatibility studies of the materials made in specific aim 1. This work is discussed in detail in Chapter 3.

REFERENCES

[1] M. Zhang, S.P. James, Silylation of hyaluronan to improve hydrophobicity and reactivity for improved processing and derivatization, Polymer 46(11) (2005) 3639-3648.

[2] K. Richdale, L.T. Sinnott, E. Skadahl, J.J. Nichols, Frequency of and Factors Associated With Contact Lens Dissatisfaction and Discontinuation, Cornea 26(2) (2007).

[3] L. Jones, C. May, L. Nazar, T. Simpson, In vitro evaluation of the dehydration characteristics of silicone hydrogel and conventional hydrogel contact lens materials, 25(3) (2002) 147-156.

[4] G. Erdodi, J.P. Kennedy, Water-swollen highly oxygen permeable membranes: Analytical technique and syntheses, 43(16) (2005) 3491-3501.

[5] G.D. Friends, J.F. Kunzler, R.M. Ozark, Recent advances in the design of polymers for contact lenses, Macromolecular Symposia 98(1) (1995) 619-631.

[6] N. Efron, P.B. Morgan, I.D. Cameron, N.A. Brennan, M. Goodwin, Oxygen Permeability and Water Content of Silicone Hydrogel Contact Lens Materials, Optometry & Vision Science 84(4) (2007).

[7] L. Jones, N.A. Brennan, J. González-Méijome, J. Lally, C. Maldonado-Codina, T.A. Schmidt, L. Subbaraman, G. Young, J.J. Nichols, The TFOS International Workshop on Contact Lens Discomfort: Report of the Contact Lens Materials, Design, and Care SubcommitteeTFOS International Workshop on CLD, 54(11) (2013) TFOS37-TFOS70.

[8] M. Zhang, *Surface modification of ultra high molecular weight polyethylene with hyaluronan for total joint replacement application*, Ph.D. Dissertation, Colorado State University, Fort Collins, CO, 2004.

[9] D.D. May, Aqueous emuslions comprising fluorocarbon-containing isocyanate derivatives as soil-resist agents, Google Patents, 2002.

[10] D.A. Prawel, H. Dean, M. Forleo, N. Lewis, J. Gangwish, K.C. Popat, L.P. Dasi, S.P. James, Hemocompatibility and Hemodynamics of Novel Hyaluronan–Polyethylene Materials for Flexible Heart Valve Leaflets, Cardiovascular engineering and technology 5(1) (2014) 70-81.

[11] H. Dean, *Development of BioPoly® materials for use in prosthetic heart valve replacements* Master's Thesis, Colorado State University, Fort Collins, CO, Spring 2012.

[12] N.R. Lewis, *HYALURONIC ACID ENHANCEMENT OF EXPANDED POLYTETRAFLUOROETHYLENE FOR SMALL DIAMETER VASCULAR GRAFTS* Master's Thesis, Colorado State University, Fort Collins, CO, Summer 2014.

[13] J. Drelich, J.D. Miller, R.J. Good, The Effect of Drop (Bubble) Size on Advancing and Receding Contact Angles for Heterogeneous and Rough Solid Surfaces as Observed with Sessile-Drop and Captive-Bubble Techniques, 179(1) (1996) 37-50.

[14] C.Y. Tang, Y.-N. Kwon, J.O. Leckie, Probing the nano- and micro-scales of reverse osmosis membranes—A comprehensive characterization of physiochemical properties of uncoated and coated membranes by XPS, TEM, ATR-FTIR, and streaming potential measurements, 287(1) (2007) 146-156.

CHAPTER 3: EVALUATION OF HA-PDMS IPN MATERIALS AS AN OCULAR LENS MATERIAL

3.1 Introduction

In this chapter specific aim 3 is addressed. Under specific aim 3, the characterizations that specifically related to the new material's suitability for ocular applications are explored and discussed here. These characterizations are: optical transmittance; oxygen gas permeability; platelet adhesion/activation; and cytotoxicity. Due to the hydrophobic nature of unmodified poly(dimethyl siloxane) (PDMS) it tends to exhibit some undesirable interactions in a biological environment. This hydrophilicity is linked to the tendency of this material to have high protein adhesion [1, 2]. Because biological fluids, such as lacrimal fluid and blood, tend to have high amounts of proteins in them, this is an area of concern for any ocular device. Adhesion of proteins to ocular devices can cause user discomfort and can even lead to infection in severe situations [3, 4].

However, previous work has suggested that otherwise hydrophobic surfaces treated with immobilized hyaluronan (HA) are more hydrophilic and experience reduced protein adhesion and thrombogenicity [5, 6]. Because silicones are commonly used for biomaterials but have thrombogenic tenancies, the effect that the presence of HA has on blood clotting on the PDMS materials was also of interest. Based on this, it was determined that the HA-treated silicone materials (HA-PDMS) would be tested for changes in protein adsorption and thrombogenicity. Additionally, as the initial goal of the presented work is to make a new ocular lens material, the optical clarity and oxygen gas permeability were measured. The results of these characterizations

for the treated films were compared both to those for untreated silicone and commercially available silicone hydrogel soft contact lenses (SLCs).

3.2 Materials and Methods

The materials being characterized in the following studies were: untreated PDMS; HA-treated PDMS; and, when applicable, tissue culture polystyrene (TCPS) to serve as a reference. HA-treated samples were treated under the "sequential swelling" method as described in Chapter 2. For optical transmittance, a commercial silicone hydrogel SCL was used for comparison (Biofinity, Coopervision). This lens was only evaluated in its wetted state.

3.2.1 Optical transmittance

As a candidate for a new ocular lens material, clearly optical clarity/transmittance is an important factor. The effect that the treatment had on the PDMS films is mentioned in Chapter 2 only in subjective terms. In this section, the procedure used to evaluate the optical transmittance of the films is described.

Samples were cut out of larger films with an 8mm biopsy punch. Samples were then placed in the bottom of the wells in a clear 48-well plate compatible with a UV-vis plate reader (BMG Labtech). A single 8mm diameter sample occupied each well. The 48-well plate was then loaded into the plate reader and the absorbance of each sample/well was measured over the visible light spectrum (400-700 nm wavenumber). The analysis parameters used were: continuous spectrum over 400-700 nm with a resolution of 5 nm. The absorbance values were converted to %-transmittance values in the associated analysis software, OMEGA (BMG Labtech).

Samples were analyzed both in dry and hydrated (submerged in DI water) states. For spectra obtained on hydrated samples, 1 mL of DI water was added to the wells. Empty wells

and wells with only 1 mL of DI water served as the “blanks” for the dry and wet state spectra, respectively. These blanks were automatically corrected for in the associated software. The output from the software was a Microsoft Excel spreadsheet with %-transmittance values for each sample at each wavelength observed. These values were plotted against each other to demonstrate differences. Additionally, average %-transmittance values for the entire spectrum (400-700 nm) were calculated as singular representative values.

Three groups of material were analyzed: untreated PDMS; HA-treated PDMS; and a commercial silicone hydrogel SCL. The silicone hydrogel SCL was only evaluated in its wetted state.

3.2.2 Oxygen gas permeability

As discussed in Chapter 1, possessing a high enough oxygen gas permeability has been a concern with contact lens materials since reports were first published in the 1980s. Work published by Holden, et al. and Harvitt, et al. described the effects of hypoxia on the corneal surface and both reported recommended minimum oxygen transmissibility values for contact lens materials. The more recent of which states this transmissibility threshold to be at least 125 Barrer/mm [7, 8]. Therefore it was critical to characterize the effect that the treatment had on the oxygen permeability and transmissibility of the HA-treated PDMS films.

Oxygen gas permeability was determined via the use of a *constant-volume variable-pressure apparatus*. As the name suggests, the premise of such an apparatus is that under a constant volume, the pressure of a volume of gas will change as gas is added to or removed from the volume. Two volumes are separated on either side of the membrane to be tested. The larger upstream (feed) volume contains the feed gas (in the case of this work, oxygen) at a higher pressure and the downstream (permeate) volume is evacuated to a low pressure via a vacuum

pump. The difference in pressure (high in the feed volume and low in the permeate volume) creates a driving force that results in the transport of matter (i.e. gas) across the membrane. This change in pressure is then measured by pressure transducers in each volume. The apparatus used was built in the Glover building at Colorado State University and was based on a similar one housed in the laboratory of Richard Noble (University of Colorado; Boulder, CO). Figure 3.1 shows the apparatus used in this work. The software used for data acquisition was a custom-made Labview script made by Alyssa Winter of Dr. Travis Bailey's lab group (Colorado State University; Fort Collins, CO). Figure 3.2 shows a screen capture of the user interface portion of this script. The user defines the file name and location and clicks the large "Record Data" button to begin recording data to the designated file.

The treated samples made under specific aim 1 were 1.5x2.5 cm rectangular films. However, the sample holder for this apparatus required samples of at least 4.5 cm in diameter. This issue was overcome by enfolding the treated samples in a foil mask. This foil mask was created by taking two 5.0cm disks of aluminum ducting tape, punching an aligned window into the both of them using a 7/16" (1.11125 cm) leather punch, and adhering the tape around the film. This was followed up by final trimming of the circumference of the foil disks. The resulting testing "cartridge" was a 4.6~4.8cm disk of aluminum foil with a 1.111 cm diameter window of exposed silicone sample.

Prior to testing, the PDMS films were dried overnight in a vacuum oven (50C, -25inHg gage). Once mounted in the sample holder, the entire system was allowed to vacuum down for a minimum of 3 hours. This was primarily to ensure that the films and plastic tubing had fully degassed such that this would not affect measurements and influence calculations. Following this system-wide vacuum period the feed and permeate volumes were closed off from the rest of the

system by turning the valves at the respective junctions. The feed gas was then introduced to the feed volume at 25psia and then purged by vacuuming down again for a total of 6 purges. Following the last purge, the feed volume was left pressurized to 25psia with oxygen gas and then isolated from the feed gas source. At this point, the apparatus was ready to begin collecting data.

To collect data, the "Record Data" button was clicked in the user interface of the Labview script and the feed volume was opened to the sample holder after 5s by turning the valve separating the two. This delay was to ensure that data acquisition had begun before exposing the sample to the feed volume. At this point, the feed side of the sample membrane is exposed to oxygen at 25psia and the permeate side is still at the vacuum pressure. As gas permeates across the membrane from the feed volume to the permeate volume, changes in pressure are observed in each respective volume.

Data acquired by this Labview script is stored in a text file. The data is converted to a Microsoft Excel document for ease of calculation, plotting, and analysis.

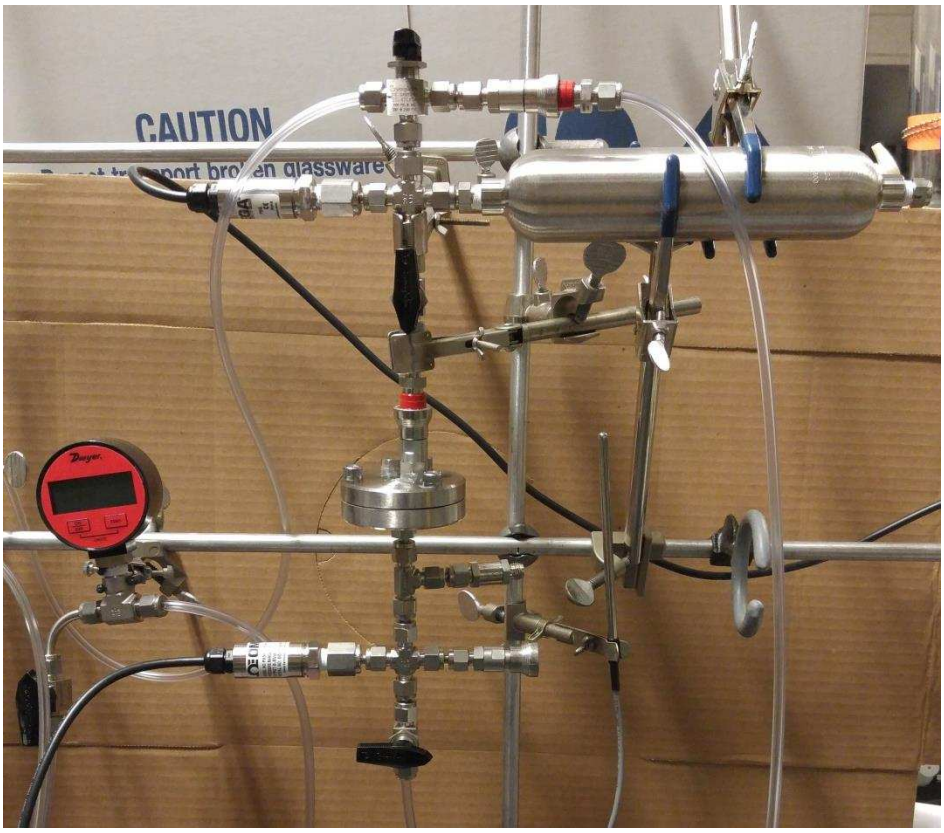

Figure 3.1: The constant-volume variable-pressure apparatus for evaluation of gas permeability used in this work is shown here.

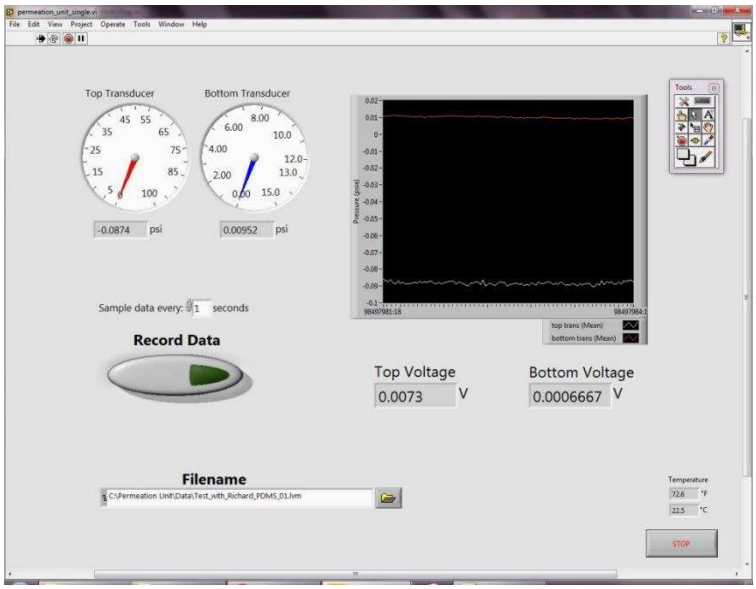

Figure 3.2: A screen capture of the Labview user interface for the gas permeability apparatus.

3.2.3 Platelet adhesion/activation

Characterization of platelet adhesion and activation were investigated with fluorescent staining and SEM imaging, respectively. The fluorescent stain used was calcein as it stains the intact cytoplasm of live cells only. Cytotoxicity, or cell death, was characterized in another study involving an LDH assay and is discussed later in this chapter. Calcein staining of the cells allows for visualization of the cells on the substrate surface when viewed with a fluorescent microscope.

For this study, tissue culture polystyrene (TCPS) was chosen as a control and reference material as it has well documented biocompatibility with many cell types. This was believed to serve as a good point of reference for the other samples.

Because this work involved incubation of live cells, it was performed in a sterile cell bio-safety hood. Plain PDMS, HA-treated PDMS, and tissue culture polystyrene (TCPS) pucks were sterilized in a 70:30 ethanol:DI water bath for at least 15 minutes. All other materials that were not provided in a sterile form (tweezers, carbon tape, 48- and 96-well plates, pipets, etc.) were sterilized under UV light exposure for 1 hr. Test samples were cut from larger films using sterile 8 mm biopsy punches. PDMS samples were anchored to TCPS pucks (8 mm diameter and 1 mm thick) using small portions of carbon tape to avoid samples floating in the plasma and other solutions. This was found to be necessary in early attempts as the films would float to the top of the plasma. Because TCPS pucks were used to anchor the samples, TCPS pucks in their own wells were used as controls and exposed to the plasma as well. Samples used in this study were treated and untreated PDMS films and TCPS pucks for control.

The cells exposed to the samples in this study were platelets in blood plasma isolated form whole blood (human donor). Blood was collected into 6 mL vacuum vials containing the anti-coagulant ethylenediaminetetraacetic acid (EDTA) by an experienced phlebotomist. The blood was

centrifuged at 150 times gravity for 7 minutes and then allowed to rest for 10 minutes to aid in separation of the plasma from the blood. The plasma was then extracted from the vials and pooled together in a single 50 mL conical tube and used immediately. Plasma, 500 μL, was added to each test well. The samples and associated plasma were then incubated at 37C on a horizontal shaker plate (100rpm) for 2 hrs [9].

Following the 2 hr incubation period, the sample wells were rinsed and aspirated with sterile PBS three times and then stained with calcein for fluorescent imaging or fixed with glutaraldehyde for SEM imaging.

3.2.3.1 Calcein staining

Fluorescent staining and imaging was carried out as described by Lezczak [9]. Due to the light sensitive nature of the stain, all soaking procedures and imaging were done in dark rooms. Samples were then incubated in a 2 μM solution of calcein-AM (Invitrogen; California, USA) for 20 minutes in a dark bio-safety hood. The samples were again rinsed and aspirated with sterile PBS and then imaged on a fluorescent microscope using the appropriate filter. With the setup used in this study, cells fluoresced bright neon green.

3.2.3.2 SEM fixing and imaging

SEM fixing was carried out as described by Lezczak [9]. The fixing process consisted of moving the samples through a series of baths. These baths began with a fixative solution and finished as gradual water removal steps with increasing ethanol concentration. Table 3.1 below summarizes the baths and their soaking times.

Table 3.1: Table summarizing the solutions used in SEM fixing of samples.

Step	Solution	Soak time
Fixative	3% gluteraldahyde + 1.1 M sodium cacodylate + 0.1 M sucrose in DI H2O	45 min
Buffer	1.1 M sodium cacodylate + 0.1 M sucrose in DI H2O	10 min
Dehydration	35% (v/v) ethanol in DI H2O	10 min
	50% (v/v) ethanol in DI H2O	10 min
	70% (v/v) ethanol in DI H2O	10 min
	95% (v/v) ethanol in DI H2O	10 min
	100% ethanol	10 min
	hexamethyldisilazane (HMDS)	10 min

Once the samples were fixed they were dried under vacuum (-25inHg) at room temperature for 12 hours. Since silicone is an insulating material, samples were adhered to a conductive (aluminum) platform via carbon tape and coated with 5nm of gold prior to imaging. The samples were then transferred to a portable vacuum desiccator for transport to the SEM instrument. This was found to greatly decrease the time required for the instrument to return to a low vacuum pressure. Silicone is generally highly gas permeable material [10], and thus the decrease in pump-down time likely means that the films off-gas in the instrument when not stored and transported in a desiccator prior to testing.

The instrument used was a JEOL JSM-6500F field emission scanning electron microscope (FESEM) with associated proprietary software for both instrument control and image analysis (JEOL USA, Inc). Samples were analyzed at 15kV and a working distance of 5.0-10.0mm depending on the sample. Images were taken at multiple magnifications and locations for each sample. Care was taken to obtain image of anomalies of interest as well as representative portions of the samples.

3.2.4 Cytotoxicity (LDH assay)

Cytotoxicity of PDMS and the HA-PDMS IPN materials was characterized using a commercial LDH assay kit (QuantiChrom LDH Cytotoxicity Assay Kit; BioAssay Systems). This assay measures cytotoxicity on the principle that when a cell dies or receives significant damage to its membrane, *lactate dehydrogenase* (LDH) is released [11]. The kit detects this with the reduction of a tetrazolium salt to a formazan dye in the presence of LDH. The amount of salt converted to dye is characterized by measuring the absorbance of the solution at 500nm. Therefore, the kit works on the principle that more absorbance at this wavelength implies more cell death. For this study, tissue culture polystyrene (TCPS) was chosen as a control and reference material as it has well documented lack of cytotoxicity with many cell types. This was believed to serve as a good point of reference for the other samples.

Because this work involved incubation of live cells, it was performed in a sterile cell bio-safety hood. Plain PDMS, HA-treated PDMS, and tissue culture polystyrene (TCPS) pucks were sterilized in a 70:30 ethanol:DI water bath for at least 15 minutes. All other materials that were not provided in a sterile form (tweezers, carbon tape, 48- and 96-well plates, pipets, etc.) were sterilized under UV light exposure for 1 hr. Test samples were cut from larger films using sterile 8 mm biopsy punches. PDMS samples were anchored to TCPS pucks (8 mm diameter and 1 mm thick) using small portions of carbon tape to avoid samples floating in the plasma and other solutions. This was found to be necessary in early attempts as the films would float to the top of the plasma. Because TCPS pucks were used to anchor the samples, TCPS pucks in their own wells were used as controls and exposed to the plasma as well. Samples used in this study were treated and untreated PDMS films and TCPS pucks for control.

The cells exposed to the samples in this study were platelets in blood plasma isolated form whole blood (human donor). Blood was collected into 6 mL vacuum vials containing the anti-coagulant ethylenediaminetetraacetic acid (EDTA) by an experienced technician. The blood was centrifuged at 150 times gravity for 7 minutes and then allowed to rest for 10 minutes to aid in separation of the plasma from the blood. The plasma was then extracted from the vials and pooled together in a single 50 mL conical tube and used immediately. Plasma, 500 μL, was added to each test well. The samples and associated plasma were then incubated at 37C on a horizontal shaker plate (100rpm) for 2 hrs [9].

After the plasma had been allowed to incubate on the samples, the well plates were moved back to the sterile bio-safety hood and the protocol provided by the manufacturer was followed [11].

Because of the person-to-person and even day-to-day differences, this is a relative assay. That is to say that the relationship between the absorbance values within a single study is more important than the raw values. Moreover, these raw values cannot be directly compared across studies and assays.

3.2.5 Whole Blood Clotting Study

Whole blood clotting kinetics was assessed using a whole blood clotting study. The protocol for this study was based on the one performed by Leszczak [9]. Human blood was drawn from a donor by an experienced phlebotomist into vacuum vials containing no anticoagulation agent. Test samples were cut from larger films using sterile 8 mm biopsy punches. Because the PDMS films have the tendency to float in water, they were anchored to the bottom of the wells in a clear 24-well plate using a small portion of carbon tape. DI water was placed in 3 wells to serve the time zero reference. Four time points were tested: 0 min, 15 min,

30 min, and 60 min. At the 0 min time point, 5 μL of blood was dispensed directly into DI water. Five μL of blood was placed onto the surface of each sample and allowed to remain in contact for the respective period of time. At the designated time points, 500 μL of DI water was added to the wells to release any unbound free hemoglobin. The liquid was agitated gently by pipetting up and down twice. The samples were then allowed to rest for 5 minutes to ensure that as much unbound free hemoglobin was released as possible. Liquid, 205 μ, from the sample wells for the given time point was transferred into the corresponding well in a clear 96-well plate.

Once all time points had passed and sample liquid for all samples had been collected, the 96-well plate containing the collected liquid was moved to a UV-vis plate reader (BMG Labtech). The absorbance was measured at 540 nm to determine the amount of free hemoglobin in the DI water. This analysis works on the premise that an increased absorbance at this wavelength corresponds to more free hemoglobin in the DI water. In turn, more free hemoglobin in the DI water implies that there was reduced clotting on the sample in question. Therefore, the measured absorbance at 540 nm is negatively correlated to the amount of blood clotted on the sample.

Samples analyzed included 3 untreated PDMS films and 3 treated PDMS films as well as wells containing only DI water for comparison. Samples were stored in DI water at least 12 hrs and were gently blotted dry with a Kimwipe before exposure to blood.

3.3 Results and Discussions

The following section presents and discusses the results from the characterization studies which comprise specific aim 3. Herein, the effects that the treatment has on the optical clarity, oxygen permeability, cytotoxicity, whole blood clotting, and platelet adsorption/activation of PDMS are presented and discussed.

3.3.1 Optical transmittance

The results for the characterization of the optical transmittance of the samples are presented and discussed here. Table 3.2, Figure 3.3, and Figure 3.4 summarize the results as averaged %-transmittance over the 400-700 nm range and plots of %-transmittance against wavelength, respectively. In the following table and figures, "seq_swell" and "simul_swell" refer to HA-PDMS IPNs made under the sequential swelling simultaneous swelling methods, respectively.

As can be seen from the table and figures below, samples treated under either method incurred a considerable reduction in optical transmittance. This aligns with observations made during treatment and briefly discussed in Chapter 2. Of note is that samples made under both treatment methods increased in optical transmittance when hydrated. In both dried and wetted cases, samples made under the simultaneous swelling method had a higher average %-transmittance than those made under the sequential swelling method.

Table 3.2: Summary of averaged transmittance values [%] over the range 400-700 nm.

Averaged %-transmittance	
Wetted samples	Avg transmittance [%]
Plain silicone film	98.69
Seq_swell	68.99
Simul_swell	73.01
CL in DI water	96.04
Dried samples	
Plain silicone film	99.25
Seq_swell	53.19
Simul_swell	66.13

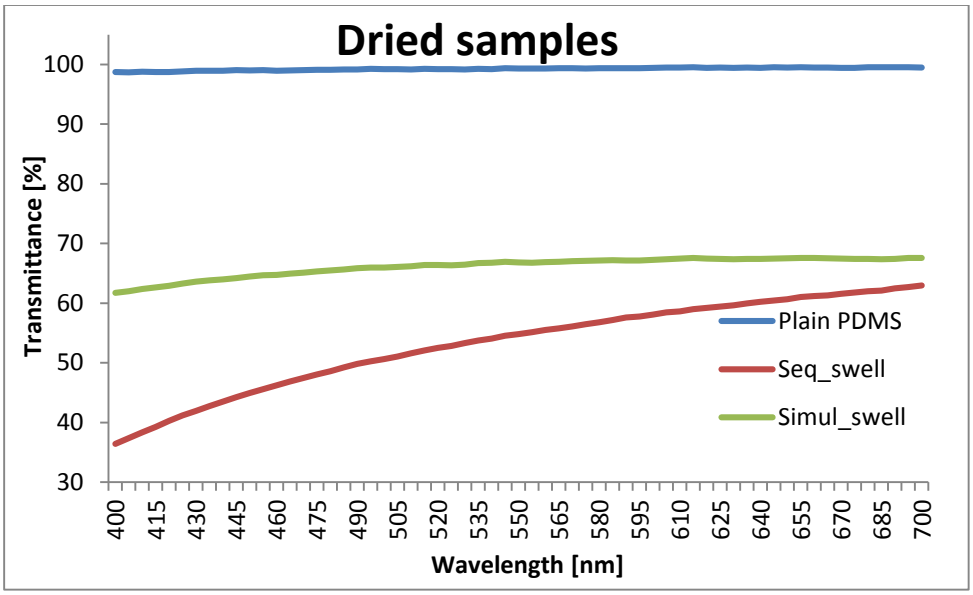

Figure 3.3: Plot summarizing the optical transmittance of plain PDMS and HA-treated PDMS when dried.

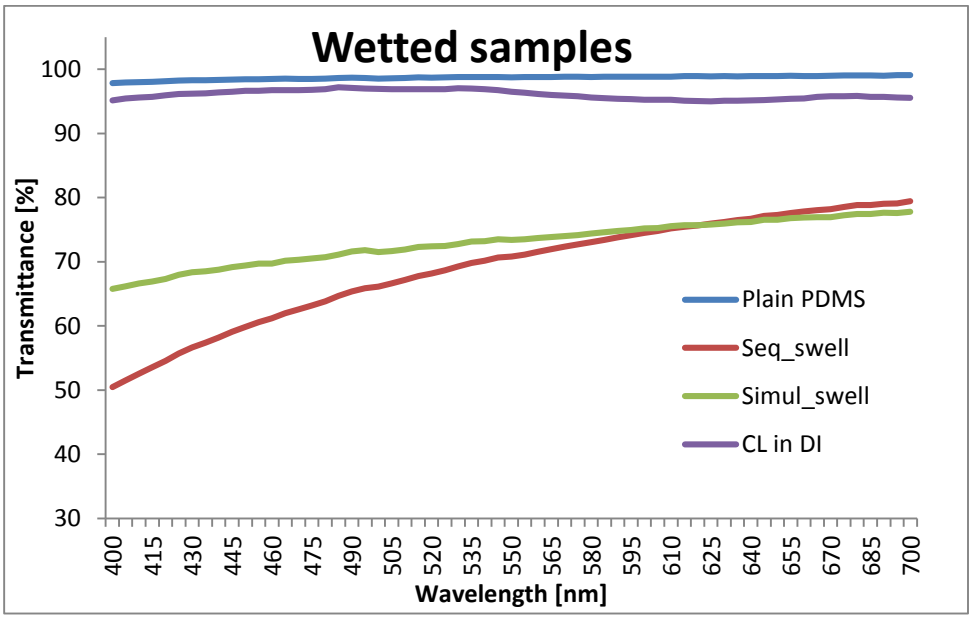

Figure 3.4: Plot summarizing the optical transmittance of plain PDMS, HA-treated PDMS, and a commercially available silicone hydrogel contact lens (CL) (Biofinity, Coopervision) when in DI water.

3.3.2 Oxygen gas permeability

The results of the oxygen gas permeability are summarized in Figure 3.5 below. The oxygen gas permeability (Dk) for the untreated PDMS and HA-treated PDMS were found to be 795.5±24.2 Barrer and 722±16.6 Barrer, respectively. These values are not statistically significantly different from each other ($p=0.08$ at $\alpha=0.05$). This indicates that the treatment does not have a statistically significant impact on the Dk of the PDMS material used in this work. Furthermore, both of these values dwarf literature values for standard silicone hydrogel SCLs which are reported as high as 160 Barrer [10]. This indicates that not only do the HA-treated PDMS films made in this work have higher oxygen Dk values than silicone hydrogels, they are also comparable to that of the unmodified PDMS material.

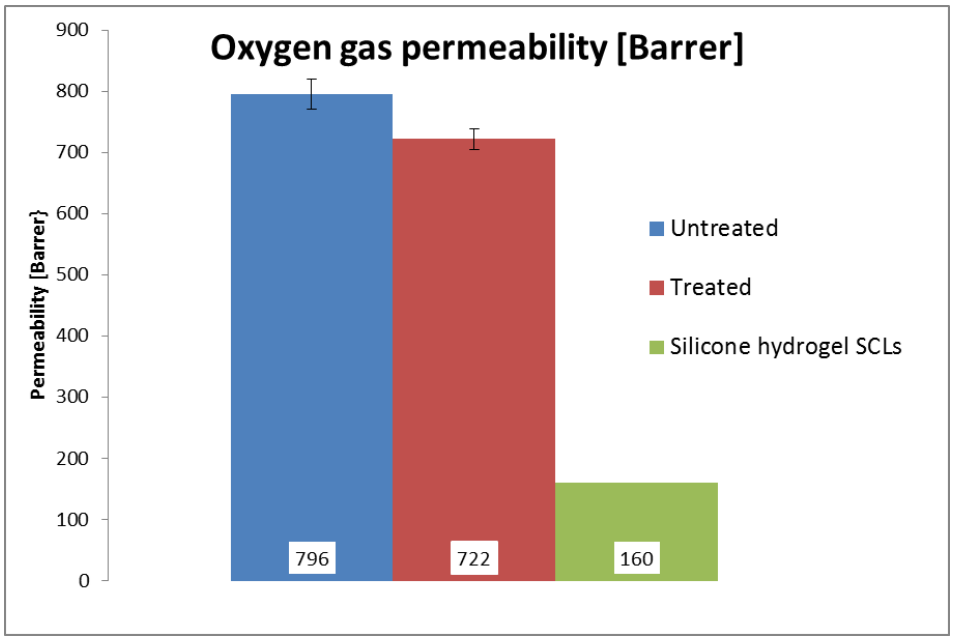

Figure 3.5: Plot summarizing the results of the oxygen gas permeability of untreated PDMS, HA-treated PDMS, and the literature value for a commercially available silicone hydrogel lens (Focus Night & Day; CIBA Vision) [10].

3.3.3 Platelet adhesion/activation

The results of the platelet adhesion and activation studies are presented and discussed here. This discussion begins with the calcein stained samples.

3.3.3.1 Calcein staining

Table 3.3 contains select example fluorescent microscopy images for calcein stained untreated PDMS, treated PDMS, and TCPS pucks. Larger versions of the images contained in this table can be found in the appendix section of this chapter. The primary trend that can be gleaned from the images in this table is the increase in fluorescing entities on the untreated PDMS samples as compared to both the treated PDMS and TCPS controls. This seems to imply that fewer cells are adhering to the treated PDMS and TCPS control samples. This is congruent with literature knowledge of unmodified silicone materials inciting protein adsorption [1, 2].

However, particle counts using an image analysis software (ImageJ, National Institutes of Health) showed no statistically significant difference between the groups. This implies that there is no difference between the counted particles in each of the images when normalized to area. This seems to contradict the visual observations, however it is possible that this is due to the lesser intensity of the fluorescing objects on the treated PDMS and TCPS samples. These images had to have a much lower threshold for separating fluorescing objects from the background. It is likely that this included many particles in these counts that would have been left out in the plain PDMS counts. Attempts to use the same threshold for all groups resulted in either blending together or loss of fluorescing objects depending on the threshold used.

3.3.3.2 SEM imaging of fixed samples

Table 3.4 contains select example fluorescent microscopy images for SEM fixed untreated PDMS, treated PDMS, and TCPS pucks. Larger versions of the images contained in

this table can be found in the appendix section of this chapter. The immediate trend that was noticed during SEM imaging of the fixed samples was that both the untreated PDMS and TCPS control samples were virtually barren of cells. The most noteworthy features on the untreated PDMS were perfectly spherical structures sitting on the surface (pictured upper right and left in Table 3.4). There were very few locations on those samples which showed anything worth mentioning. This is starkly contrasted by one of the treated PDMS films (shown in the middle left image of Table 3.4) which had many surface features as well as many platelets of varying degrees of activation. This seems to contradict the results from the calcein staining in which the untreated PDMS films showed far more platelet adhesion than the treated PDMS or TCPS. Further confounding issues, is that another treated PDMS film (pictured middle right in Table 3.4) had surface features normally seen on treated surfaces but had far less platelet presence and activation compared to the aforementioned sample.

One possible explanation for this contradiction relates to the fixing and drying process. Glutaraldehyde (which was used in the SEM fixing procedure) is known to react with (crosslink) hyaluronan [12, 13]. It is possible that the platelets could have been anchored to the HA-treatment domains of the treated PDMS surface by the glutaraldehyde, thereby causing the treated samples to retain more platelets than the untreated samples even if there were originally more on the latter. Alternatively, this issue could also have been the result of the dehydration process. Specifically the culprit is believed to be the HMDS drying step since HMDS swells PDMS to a significant degree. This could explain the surprising lack of platelets on the untreated PDMS as the stress of the substrate to which they were bound deformed so greatly. It is no great leap of logic to think that this could have dislodged a great many platelets that were previously adhered to the surface.

Perhaps the most likely explanation is that it was both. The platelets would be far less susceptible to dislodging from the substrate if they are chemically cross-linked to a portion of it. Whereas in the case of the untreated PDMS, which has a surface that does not react with the glutaraldehyde and is smooth down to the nanometer level, would leave little for the platelets to grip if the surface were to deform. Furthermore, similar deformation of the HA-treated surface has been seen on other materials such as ePTFE fixed under this sample protocol (unpublished work). The wrinkled surface that seems to be triggering more platelet activation, as seen in the middle left image of Table 3.4, is not typical of the samples treated under the methods described in Chapter 2.

Worthy of further discussion is the difference in platelet presence and activity between the two treated PDMS samples (pictured middle left and right in Table 3.4). Other than the platelets, the two samples display very different background morphologies. Whereas the sample pictured on the left has a surface characterized by wrinkled plate-like features and larger superstructures of spherical globules, the sample pictured on the right has smaller, more independent spherical surface features which appear more integrated into the surface. Discussion was made in Chapter 2 about the observed correlation between samples which presented the surface morphology of the latter and improved surface wetting and general hydrophilicity. The apparent reduction in adsorption and activation of platelets only furthers the theory that more refinement of the treatment process can more reliably create that type of surface and thereby create more hydrophilic samples. Additionally, while it may seem like the surface has a large amount of exposed PDMS, hyaluronan has extraordinary swelling tendencies when hydrated: even reaching up to 1000 times its previous molecular volume [14]. This bloom of HA could

create a mask over the PDMS surface such that the cells do not interact with the host polymer surface.

Table 3.3: Comparison of untreated PDMS, treated PDMS, and tissue culture polystyrene control. Larger versions of these images can be found in the appendix section.

Untreated PDMS	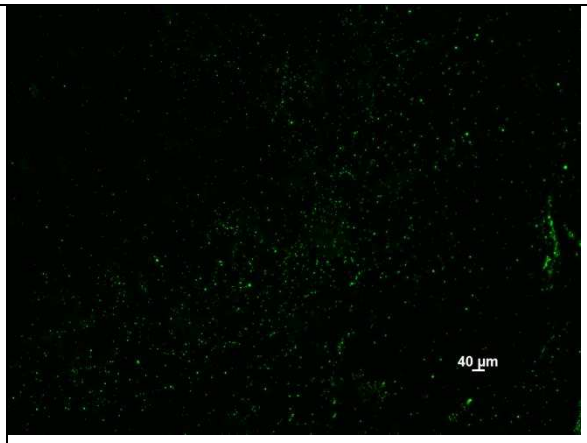	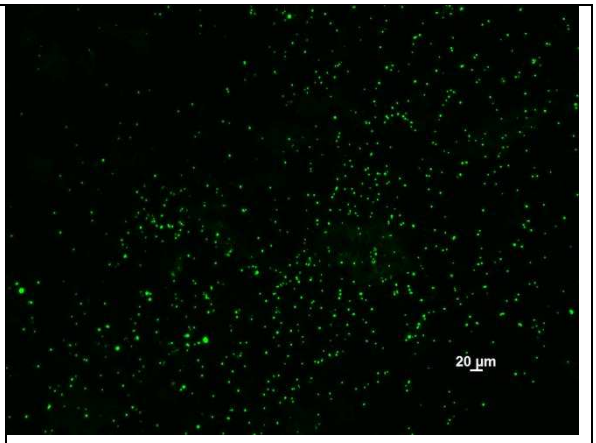
Treated PDMS	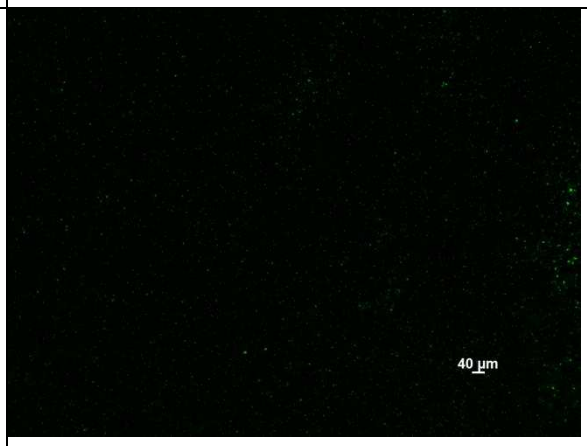	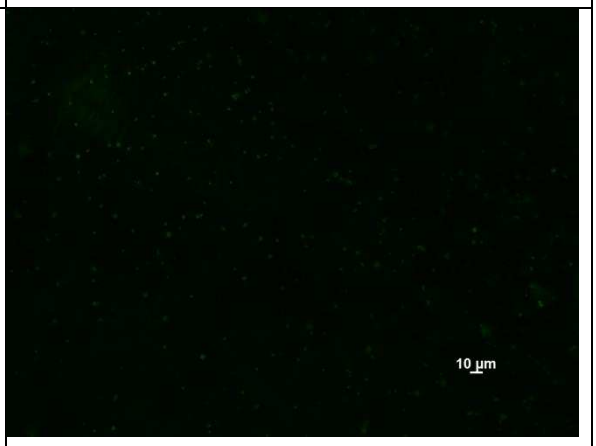
TCPS control		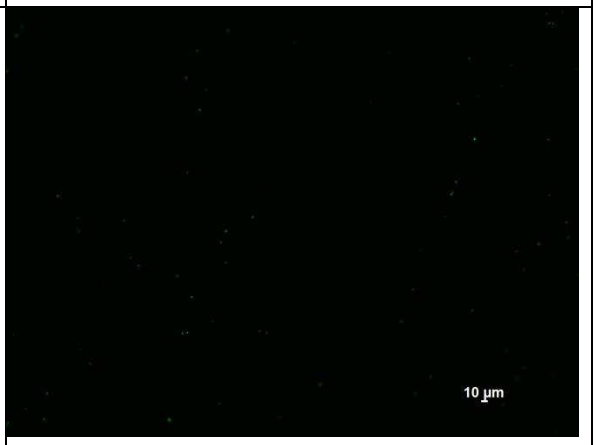

Table 3.4: Comparison of untreated PDMS, treated PDMS, and tissue culture polystyrene control. Larger versions of these images can be found in the appendix section.

Untreated PDMS	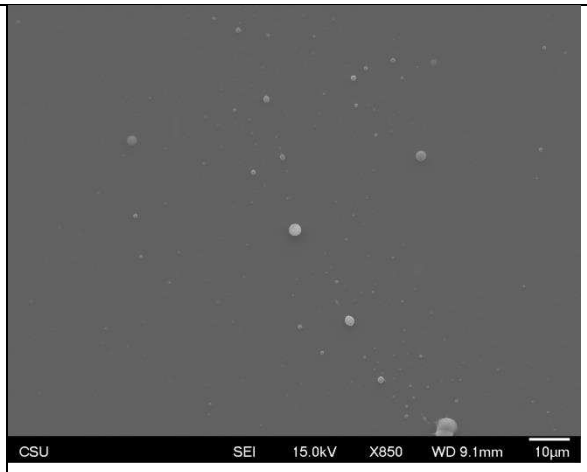	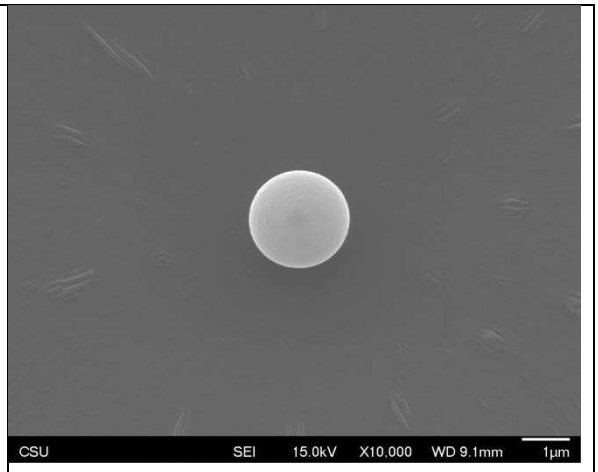
Treated PDMS	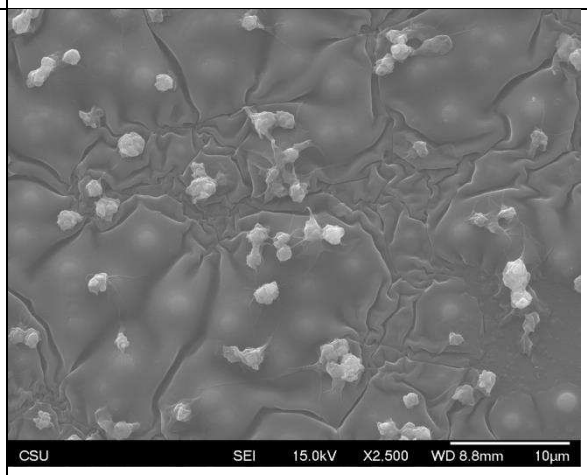	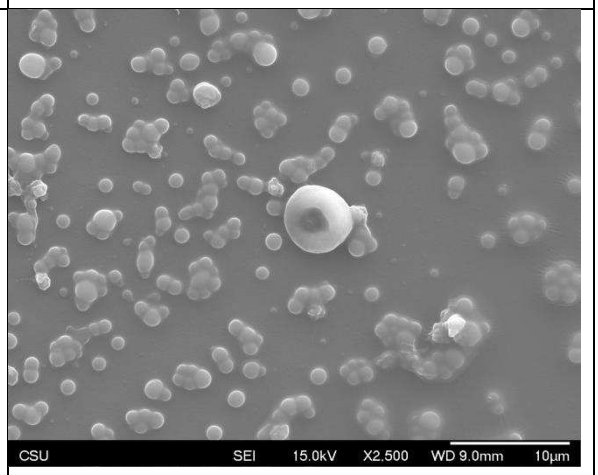
TCPS control	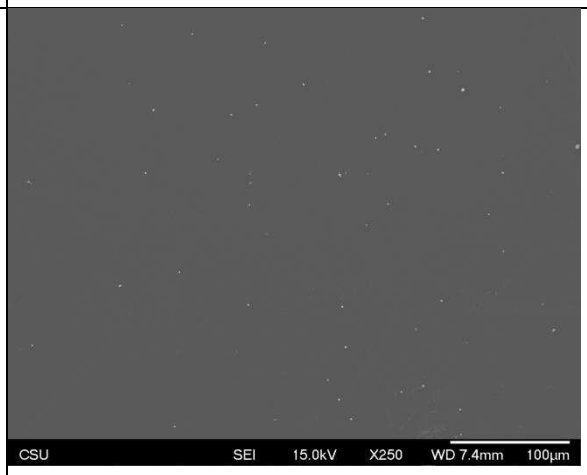	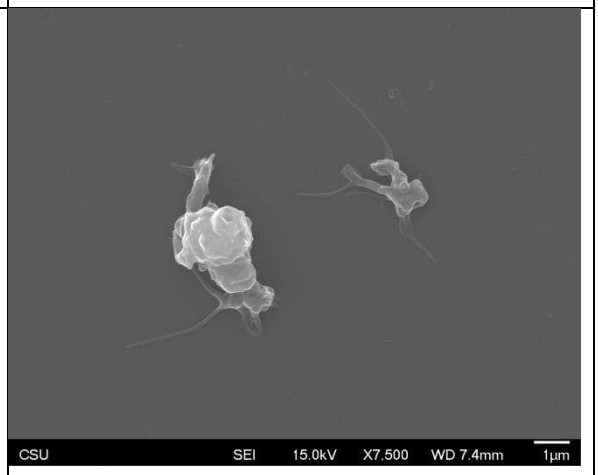

3.3.4 Cytotoxicity (LDH assay)

The results for the cytotoxicity (LDH assay) study are summarized in Figure 3.5 below. In short, there was no statistical difference between the TCPS control, untreated PDMS, or treated PDMS (at α=0.05). This indicates that both the untreated and treated PDMS were no more cytotoxic than tissue culture polystyrene pucks. That the treated samples demonstrated a cytotoxicity comparable to TCPS, which is known to be particularly conducive to cell growth, indicates that the treated materials are not cytotoxic.

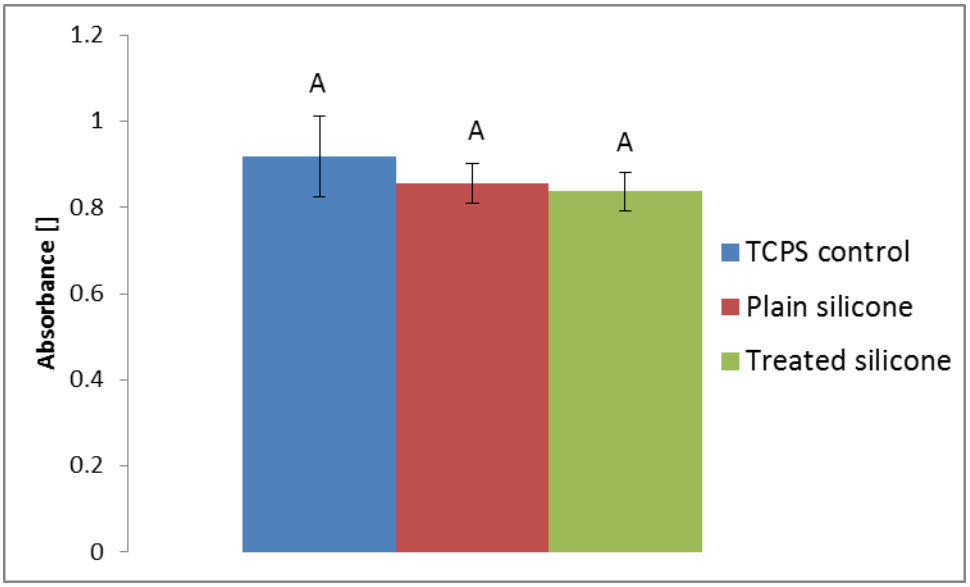

Figure 3.5: Plot summarizing the results of the cytotoxicity (LDH) assay. There was no significant difference between any group at α=0.05.

3.3.5 Whole Blood Clotting

The results of the whole blood clotting study showed no significant difference in absorbance between the treated and untreated PDMS films with the only exception being at the 15 min time point ($p<0.05$ and α=0.05). Figure 3.6 below contains a plot of the average absorbance values for the PDMS films as well as the control (blood placed directly into a well of

DI water). This indicates that the treated PDMS films as thrombogenic as the untreated PDMS films.

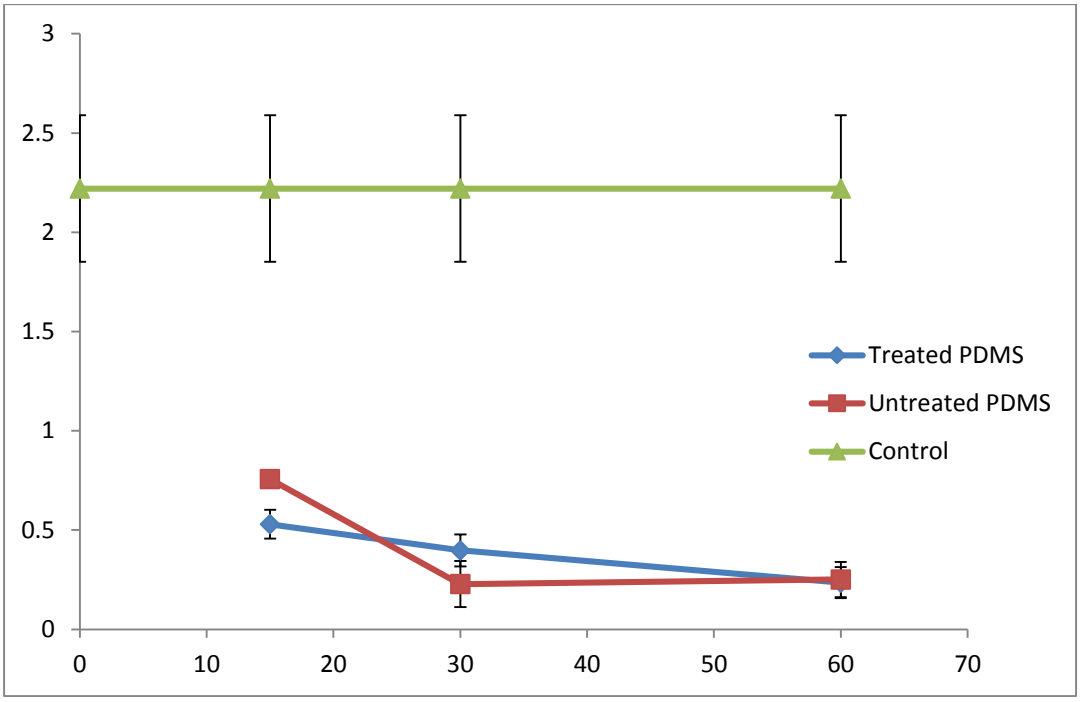

Figure 3.6: Plot of the absorbance values for the whole blood clotting study. The error bars are ±1 standard deviation.

However, it was observed that the drop of blood spread out on the treated samples but not on the untreated samples. This is likely due to the increased hydrophilicity of the treated samples. Similar spreading is seen for water drops during sessile drop contact angle measurements. Figures 3.7 and 3.8 below show examples of this spreading. This implies that there was more surface contact with the treated samples than there was on the untreated samples. It is suspected that this increase in surface contact may have resulted in increased clotting. Adding to this suspicion is that this result contradicts blood clotting results obtained in earlier pilot studies. In this early study, the treated and untreated PDMS samples had statistically different absorbance values after the 15 min time point. Figure 3.8 contains the plot of the

absorbance values from this early study. Given this, more accurate blood clotting results may be obtainable from dynamic flow hemocompatability testing.

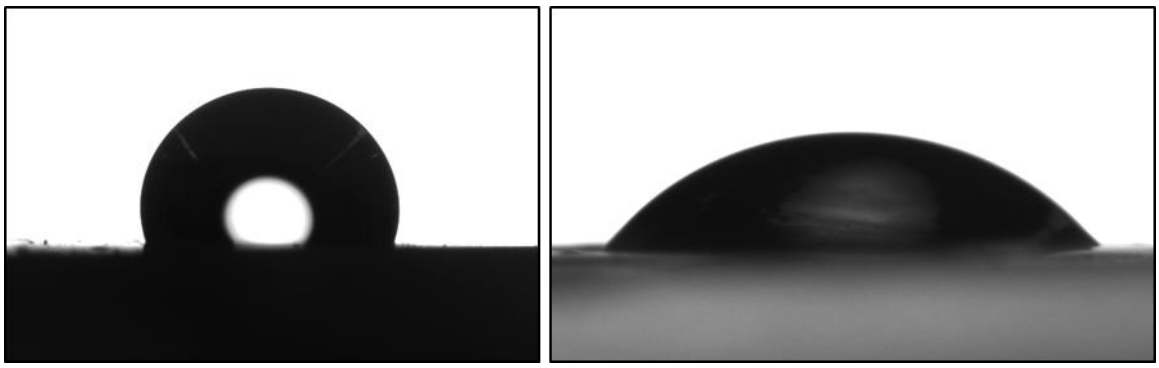

Figure 3.7: Contrast profile images of water drops on untreated PDMS (left) and treated PDMS (right) films. This illustrates the spreading of the water drop on the treated sample's surface.

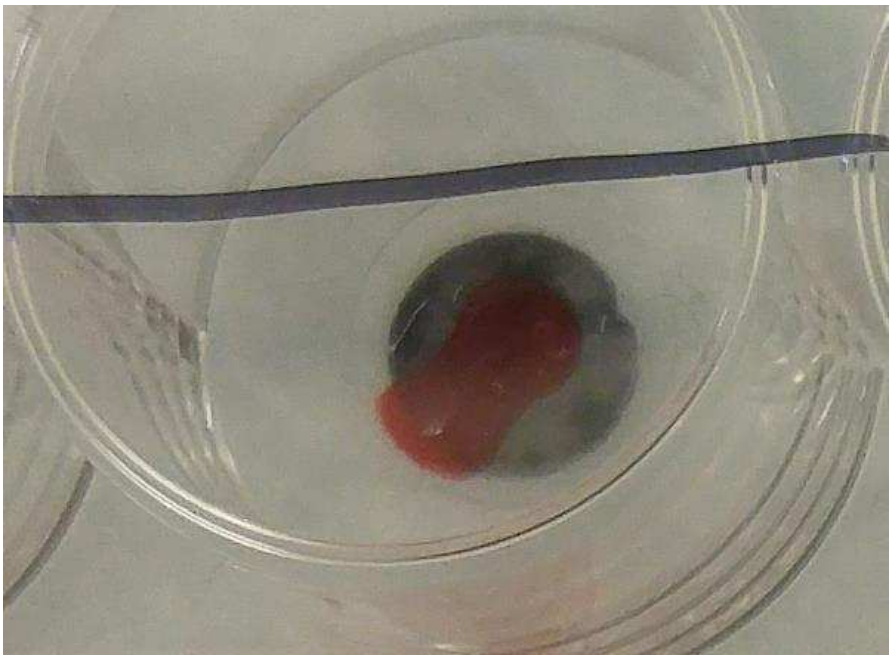

Figure 3.8: Picture showing an example of the blood spreading on the surface of a treated sample. The sample pictured is one of the 60 min time point treated samples and is dry.

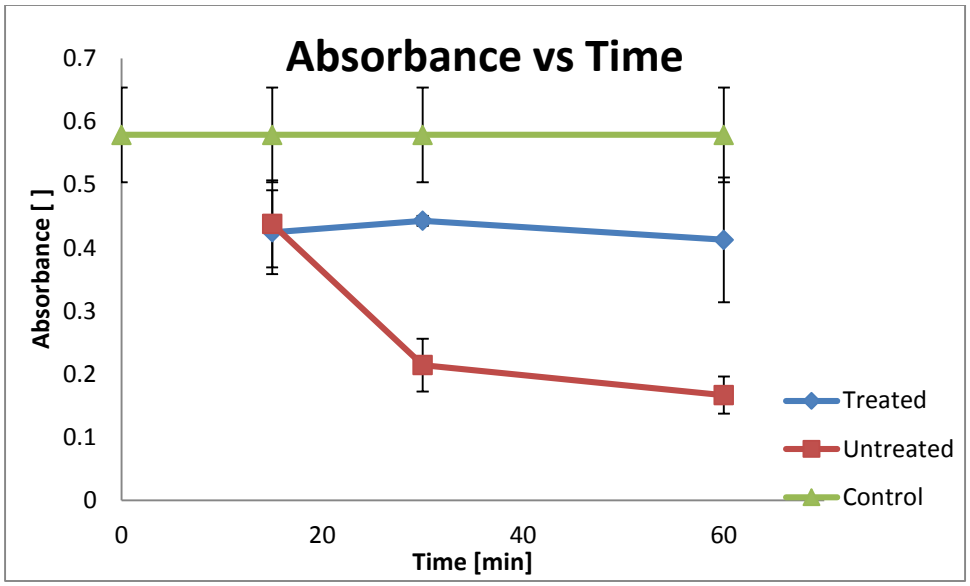

Figure 3.8: Plot of the absorbance values for the mentioned past whole blood clotting study. The error bars are ±1 standard deviation.

3.4 Conclusions

The results of the cytotoxicity (LDH assay) and gas permeability showed favorable aspects of the HA-treated PDMS materials for use in ocular lenses. The LDH assay showed that the treated PDMS materials were no more cytotoxic than tissue culture polystyrene (TCPS) for platelets in isolated human blood plasma. Oxygen gas permeability measurements showed that there was no statistically significant difference between Dk values for treated and untreated PDMS films. Furthermore, both the plain PDMS and HA-PDMS films show much higher oxygen permeability than commercial hydrogel contact lenses.

However, SEM imaging of fixed platelets showed a large number of activated platelets on some of the treated samples but very few on untreated PDMS and TCPS controls. This is likely an artifact of the SEM fixation process and deserves further study. Additionally, measurements of optical transmittance showed that treated films had reduced optical transmittance compared to untreated PDMS. This increase in opacity was also noted during

handling of the treated samples. Worthy of note: samples made under both treatment methods increased in optical transmittance when measured while hydrated. Finally, a whole blood clotting study performed on treated and untreated PDMS films showed no decrease in the clotting tendency from normal PDMS.

The above discussion demonstrates the HA-PDMS IPN materials created under specific aim 1 have great potential to be a new biomaterial; however, more optimization is still needed to regularly produce samples with the desired micron-scale morphology, consistent hydrophilicity and optical clarity.

REFERENCES

[1] M.B. Habal, The biologic basis for the clinical application of the silicones: A correlate to their biocompatibility, 119(7) (1984) 843-848.

[2] H. Chen, M.A. Brook, H. Sheardown, Silicone elastomers for reduced protein adsorption, 25(12) (2004) 2273-2282.

[3] H.J. Davidson, V.J. Kuonen, The tear film and ocular mucins, Veterinary Ophthalmology 7(2) (2004) 71-77.

[4] P.N. Dilly, Structure and Function of the Tear Film, Springer US, Boston, MA, 1994, pp. 239-247.

[5] S.G. Hu, C.H. Jou, M.C. Yang, Protein adsorption, fibroblast activity and antibacterial properties of poly(3-hydroxybutyric acid-co-3-hydroxyvaleric acid) grafted with chitosan and chitooligosaccharide after immobilized with hyaluronic acid, 24(16) (2003) 2685-2693.

[6] S. Verheye, C.P. Markou, M.Y. Salame, B. Wan, S.B. King, K.A. Robinson, N.A.F. Chronos, S.R. Hanson, Reduced Thrombus Formation by Hyaluronic Acid Coating of Endovascular Devices, Arteriosclerosis, Thrombosis, and Vascular Biology 20(4) (2000) 1168-1172.

[7] B. Holden, G. Mertz, Critical oxygen levels to avoid corneal edema for daily and extended wear contact lenses., Investigative Ophthalmology and Visual Science 25 (1984) 1161-1167.

[8] D.M. Harvitt, J.A. Bonanno, Re-Evaluation of the Oxygen Diffusion Model for Predicting Minimum Contact Lens Dk/t Values Needed to Avoid Corneal Anoxia, Optometry & Vision Science 76(10) (1999).

[9] V. Leszczak, *POLYCAPROLACTONE NANOWIRE SURFACES AS INTERFACES FOR CARDIOVASCULAR APPLICATIONS* Ph.D. Dissertation, Colorado State University, Fort Collins, CO, Summer 2014.

[10] N. Efron, P.B. Morgan, I.D. Cameron, N.A. Brennan, M. Goodwin, Oxygen Permeability and Water Content of Silicone Hydrogel Contact Lens Materials, Optometry & Vision Science 84(4) (2007).

[11] BioAssay-Systems, "QuantiChrom LDH Cytotoxicity Assay Kit (C2LD-100)", https://www.bioassaysys.com/Datasheet/C2LD.pdf, 2015.

[12] P.A. Ramires, E. Milella, Biocompatibility of poly(vinyl alcohol)-hyaluronic acid and poly(vinyl alcohol)-gellan membranes crosslinked by glutaraldehyde vapors, 13(1) (2002) 119-123.

[13] K. Tomihata, Y. Ikada, Crosslinking of hyaluronic acid with glutaraldehyde, 35(16) (1997) 3553-3559.

[14] M. Zhang, *Surface modification of ultra high molecular weight polyethylene with hyaluronan for total joint replacement application*, Ph.D. Dissertation, Colorado State University, Fort Collins, CO, 2004.

CHAPTER 4: RESEARCH SUMMARY, LIMITATIONS, AND FUTURE WORK

4.1 Summary of Research

Methods for the fabrication of sequential IPNs of poly(dimethyl siloxane) (PDMS) and hyaluronan (HA) were successfully developed. Samples were prepared under both the proposed methods: sequential and simultaneous swelling. HA-PDMS IPN materials created under these methods were characterized for hydrophilicity via contact angle goniometry (CAG) and for changes to surface chemistry/morphology via ATR/FTIR, SEM imaging, and XPS spectroscopy. Following this, treated HA-PDMS IPN materials were also evaluated in terms of biocompatibility as an ocular lens material: optical transmittance; oxygen gas permeability; cytotoxicity; platelet adhesion/activation; and whole blood clotting.

CAG analysis indicated increase in hydrophilicity by a decrease in sessile drop angle (especially in the receding angle) and an increase in the captive bubble angle when compared to untreated samples. CAG was also used to demonstrate the large hysteresis (difference between receding and advancing contact angles). This large hysteresis suggests significant surface rearrangement of the substrate when transitioning from dried to wetted states.

New chemical bonds and species were detected in treated PDMS materials that were absent in untreated PDMS under ATR/FTIR and XPS analysis. This included the appearance of FTIR peaks about 1320, 1600, and 3400 cm^{-1}, which correspond to carboxyl groups, NH bonds, and OH bonds respectively. None of which appear in untreated PDMS but are found in cross-linked HA. Elemental composition analysis using XPS demonstrated that the surfaces of the treated PDMS materials had more carbon, oxygen, and nitrogen content than untreated PDMS

materials. This again implies the incorporation of HA into the PDMS material for the formation of an HA-PDMS IPN material.

Scanning electron microscopy (SEM) of the samples showed the introduction of new surface features on HA-treated samples that did not appear on untreated or sham PDMS samples. These new features varied in detail with the treatment method, but were generally characterized by aggregates or loose communities of spherical micro-globules believed to be phase-separated cross-linked HA domains. Additionally, correlations were noticed between hydrophilicity, opacity, and these spherical micro-domains. When the micro-domains were mostly contained in tightly packed superstructures, the materials were hydrophilic, but also strongly opaque. This is in comparison to samples which had these micro-domains more evenly distributed across the surface in looser communities. These samples demonstrated good hydrophilicity while being notably clearer than the former.

From the above, it can be seen that the treated materials are HA-PDMS IPNs with improved hydrophilicity when compared to untreated PDMS. However, the mentioned trends noticed in conjunction with SEM images indicate that there is still room for improvement. It is believed that with further refinement of the treatment methods, samples which are even more clear and hydrophilic may be possible.

The biocompatibility studies told a mixed story about the HA-PDMS IPNs' suitability as ocular lens materials in their current state. Cytotoxicity (LDH assay) demonstrated the the HA-treated PDMS materials were no more cytotoxic than the tissue culture polystyrene (TCPS) control pucks. This is promising in that TCPS is known for its low cytotoxicity and tendency to encourage cell attachment and proliferation. Oxygen gas permeability values (Dk) for treated PDMS was found to be not statistically different from untreated PDMS (at $\alpha=0.05$) with

untreated PDMS and treated PDMS have Dk values of 795.5±24.2 Barrer and 722±16.6 Barrer respectively. These values fall in line with expected values of PDMS oxygen gas permeability which range from 600~800 Barrer, depending on the form of the PDMS [1-3]. Fluorescent microscopy of samples with calcein stained cells showed fewer cells on the surface of the treated PDMS films indicating a lower platelet adhesion.

However, the SEM images taken of samples which were incubated in human blood plasma tell a different story. The TCPS control and untreated silicone were largely barren of fixed platelets, save for an anomalous spot or two. In contrast, one of the treated samples had a large degree of platelets adhered to the surface and of varying degrees of activation. To confound the issue even more, another treated PDMS sample under the same analysis had very little platelet adhesion. More discussion on this can be found in Chapter 3. In brief, it is believed that this is due largely to a combination of two factors: the SEM fixing protocol; and differences in background surface morphology of the treated samples.

In summary, this work was inspired by a yet unmet need for ocular lens materials which could address both the issues of dehydrating and reducing oxygen delivery to the lens wearer's eyes. Spurred by this, a hydrophilic PDMS IPN material which had no water in its bulk was envisioned and then created. The presented work represents the exploration of countless variations to treatment parameters and puts forth two methods for creating an IPN of hyaluronan and poly(dimethyl siloxane).

4.2 Limitations and Future Work

4.2.1 Molecular weight of hyaluronan used

The hyaluronan used in this work had an average molecular weight of 750 kDa. This was a legacy decision influenced primarily by the success of previous work [4-6]. While there are

commercial sources for different molecular weight hyaluronan, this was considered beyond the scope of the current work. However, lower molecular weight HA has been considered for this application since its conception and holds promise. Additionally, a review of the literature shows no other work published on making sequential IPNs with a guest polymer of this size: 750kDa. In fact, the majority of the published work with sequential IPNs is done using monomers which are polymerized and cross-linked in the host polymer *in situ* [7]. Unfortunately, there is currently no known method for fully artificial synthesis and *in situ* polymerization of hyaluronan.

4.2.2 Photo-crosslinkable Hyaluronan

Other published work in successful IPN formation utilizes a photo-crosslinkable guest polymer [8]. The benefit in this method as compared to the present methods is that the guest polymer can be allowed to swell to equilibrium without having to be constrained by time or reactions occurring during uptake into the host polymer. This contrasts the sequential swelling method used in this work in that a photo-crosslinking system would not allow the impregnated hyaluronan to be displaced during the uptake of the chemical cross-linker solution. The photo-crosslinking system would also alleviate the issues of precise temperature and humidity control needed in the simultaneous swelling method. This is especially appealing for materials like PDMS due to their inherent high degree of chain mobility. The current work suggests that guest polymer displacement during film drying, swelling, and crosslinking affected treatment success. Modification of hyaluronan such that is it photo-crosslinkable to itself is not a novel concept and published work on this exists in the literature. An example modification which would, in theory, not interfere with the ability to further process the hyaluronan into silyl-HA-CTA is methacrylation of the hyaluronan [9, 10]. Similar to work with lower molecular weight HA, this is something that had been considered since the early stages, but was ultimately decided to be

outside the scope of this work. That being said, it is believed that there is great potential in the usage of photo-crosslinkable hyaluronan as opposed to the separate chemical cross-linker used in this study.

4.2.3 Alternative Solvents

During the course of this work, xylenes (racemic mixture) were used as the solvent for swelling the PDMS network, dissolving silyl-HA-CTA, and dissolving the crosslinker. This was a legacy decision influenced primarily by the success of previous work [4-6]. While xylenes did serve as an excellent solvent for expanding the PDMS network, it was only a fair solvent for the cross-linker, poly(hexamethylene diisocyanate) (pHMDI) and a decent solvent for silyl-HA-CTA. Consideration has been given to using other solvents based on their affinity for their respective components. Ultimately, these alternatives were not thoroughly pursued and xylenes remained the default solvent due to constraints on time. Some example solvents which have been considered are: hexamethyl disilizane (HMDS) as it swells both the PDMS network well and is a strong solvent for silyl-HA-CTA; acetone or acetone/xylenes mixture for dissolving the cross-linker as acetone is a far better solvent for pHMDI than xylenes and acetone/xylenes mixtures still swell the PDMS network (albeit to a weaker degree based on decreasing xylenes amount).

4.2.4 Ultrasonic Bath Assisted Swelling

The inclusion of an ultrasonic bath (a “sonicator”) to the treatment protocol is believed to be able to increase treatment success. This is believed to be able to aid treatment success by encouraging the more thorough dispersion of the modified hyaluronan derivative throughout the PDMS elastomer. This extra agitation during swelling may result in smaller, more evenly dispersed micro-domains of crosslinked hyaluronan in the treated samples.

REFERENCES

[1] L. Jones, C. May, L. Nazar, T. Simpson, In vitro evaluation of the dehydration characteristics of silicone hydrogel and conventional hydrogel contact lens materials, 25(3) (2002) 147-156.

[2] N. Efron, P.B. Morgan, I.D. Cameron, N.A. Brennan, M. Goodwin, Oxygen Permeability and Water Content of Silicone Hydrogel Contact Lens Materials, Optometry & Vision Science 84(4) (2007).

[3] G. Erdodi, J.P. Kennedy, Water-swollen highly oxygen permeable membranes: Analytical technique and syntheses, 43(16) (2005) 3491-3501.

[4] M. Zhang, *Surface modification of ultra high molecular weight polyethylene with hyaluronan for total joint replacement application*, Ph.D. Dissertation, Colorado State University, Fort Collins, CO, 2004.

[5] H. Dean, *Development of BioPoly® materials for use in prosthetic heart valve replacements* Master's Thesis, Colorado State University, Fort Collins, CO, Spring 2012.

[6] N.R. Lewis, *HYALURONIC ACID ENHANCEMENT OF EXPANDED POLYTETRAFLUOROETHYLENE FOR SMALL DIAMETER VASCULAR GRAFTS* Master's Thesis, Colorado State University, Fort Collins, CO, Summer 2014.

[7] J.S. Turner, Y.L. Cheng, Preparation of PDMS−PMAA Interpenetrating Polymer Network Membranes Using the Monomer Immersion Method, Macromolecules 33(10) (2000) 3714-3718.

[8] A. Hillerström, B. Kronberg, A two-step method for the synthesis of a hydrophilic PDMS interpenetrating polymer network, 110(5) (2008) 3059-3067.

[9] S.A. Bencherif, A. Srinivasan, F. Horkay, J.O. Hollinger, K. Matyjaszewski, N.R. Washburn, Influence of the degree of methacrylation on hyaluronic acid hydrogels properties, 29(12) (2008) 1739-1749.

[10] J. Baier Leach, K.A. Bivens, C.W. Patrick Jr, C.E. Schmidt, Photocrosslinked hyaluronic acid hydrogels: Natural, biodegradable tissue engineering scaffolds, 82(5) (2003) 578-589.

APPENDICES

Appendix I: Protocols

1. HA complexation to HA-CTA
2. HA-CTA silylation to silyl-HA-CTA

Appendix II: Data and figures

1. XPS output
2. Larger images from Calcein stained samples
3. Larger images from SEM fixed samples
4. LDH assay kit product insert (manual)

Appendix I: Protocols

HA-CTA Complexation

Objective
Hydrophobic modification of hyaluronan for reaction in anhydrous solvents

Materials and Equipment
- Sodium hyaluronan (NaHA)
- Cetyltrimethylammonium bromide (CTAB)
- Fresh Deionized water (DI H_2O)
- 1000 ml beaker or flask
- 500 ml beaker or flask
- Magnetic stir bars
- Stir plates
- Freezer mill/Cryogrinder
- Liquid nitrogen
- Hyaluronan-cetyl trimethylammonium complex (HA-CTA)
- Vacuum oven
- Vapor trap
- Vacuum pump
- Thermal gloves
- Safety glasses
- Buckner funnel
- Filter paper
- Erlenmeyer flasks

Procedure
1. Prepare a 0.30% w/v solution of sodium hyaluronan in DI H_2O. Minimize large clumps when adding NaHA.
   a. Example: 1.5g NaHA in 500 ml DI H_2O
   b. Stir the reaction at room temperature until the NaHA is completely dissolved. This can take several hours depending on the molecular weight of the NaHA. Stir for 15 hours to 3 days. Parafilm the beaker.
   c. When fully dissolved, the solution is clear.
   d. To get the NaHA into solution, turn the stir bar RPMs high enough to get a vortex on the top part of the stir bar for at least 5 mins. Then, turn the RPMs down to a low setting to form a little vortex.
   e. Record the following in lab notebook:
      - Date, Time, Mass of NaHA (g) used, Volume of DI H_2O (mL) used, Dissolve Time (from start of mixing to when CTAB is added), Manufacturer, Lot Number, Part Number, and when the bottle of NaHA was opened.
2. Prepare a 1.00% w/v solution of CTAB in DI H_2O.
   a. Example: 1.69 g CTAB in 169 ml DI H_2O

b. Stir the reaction at 40°C until the CTAB is completely dissolved. When dissolved, the solution will be clear. This takes 10-15 mins.
c. Record the following in lab notebook:
   - Date, Time, Mass CTAB (g) used, Volume DI H_2O (mL) used, Dissolve time, Manufacturer, Lot Number, Part Number, and when bottle of CTAB was opened.

3. Slowly add the CTAB solution to the NaHA solution while under magnetic stirring. Parafilm the beaker. The mixture will become increasingly opaque as the CTAB solution is added. When the reaction is complete, a white precipitate forms and the supernatant is clear. Varying the addition rate affects the size of the precipitate (a slower addition rate produces a smaller precipitate). Stir for 15 hours – 36 hours.
   a. Record the following in lab notebook:
      - Date, and Time of addition.
4. The precipitate is HA-CTA. Collect and wash the HA-CTA to remove excess CTAB using a Buckner funnel. Use a vapor trap on the oven.
   a. Set up a Buckner funnel to two Erlenmeyer flasks. (pic)
   b. Place filter paper on the funnel and wet it using DI H_2O.
   c. Pour the HA-CTA/DI H_2O solution into the Buckner funnel slowly to prevent HA-CTA from getting under the filter paper.
   d. Rinse the HA-CTA with 500 ml DI H_2O.
   e. Use a spatula to scrape the HA-CTA into an Erlenmeyer flask with 300 ml DI H_2O.
   f. Cover the Erlenmeyer flask with a serum stopper and shake it for 30 seconds.
   g. Pour the contents of the Erlenmeyer flask in the Buckner funnel and vacuum off the water.
   h. A second time, rinse the HA-CTA with 500 ml DI H_2O.
   i. A second time, use a spatula to scrape the HA-CTA into an Erlenmeyer flask with 300 ml DI H_2O.
   j. Cover the Erlenmeyer flask with a serum stopper and shake it for 30 seconds.
   k. Pour the contents of the Erlenmeyer flask in the Buckner funnel and vacuum off the water.
   l. A third time, rinse the HA-CTA with 500 ml DI H_2O.
   m. A third time, use a spatula to scrape the HA-CTA into an Erlenmeyer flask with 300 ml DI H_2O.
   n. Cover the Erlenmeyer flask with a serum stopper and shake it for 30 seconds.
   o. Pour the contents of the Erlenmeyer flask in the Buckner funnel and vacuum off the water.
   p. A fourth time, rinse the HA-CTA with 500 ml DI H_2O.
   q. A fifth time, rinse the HA-CTA with 500 ml DI H_2O.
   r. Move the HA-CTA to the center of the filter paper, and carefully place the filter paper inside a petri dish. Spread the HA-CTA out.
   s. Place the petri dish and filter paper in a vacuum oven to dry at 50°C for 3 days. Occasionally wipe the water off the inside of the oven door. Be sure to watch vapor traps to make sure they don't fill and are functioning correctly. <<note: combine with 5 below>>
   t. Record the following in lab notebook:
      - Date, Process Start Time, Process End Time, and Oven in Time.
5. Dry HA-CTA in a vacuum oven (-25 in Hg, 50°C) for 3 days or until no change in weight is observed. A yield of about 2.5 g HA-CTA is expected for a starting NaHA weight of 1.5 g.
6. Grind the dried HA-CTA to a powder using a freezer mill/cryogrinder.

a. Wear thermal gloves and safety glasses.
b. Slowly fill the cryogrinder with liquid nitrogen to the fill line. This typically requires about 5L of liquid nitrogen and will cool the cryogrinder down. Close the top cover and let the cryogrinder sit until vapor stops coming out of the rear vent.
c. Weigh the HA-CTA and record the weight.
d. Place the bottom cap on a cryogrinder tube, and place half of the HA-CTA into the tube with a magnet.
e. Place the top on the cryogrinder tube, with the slotted end towards the outside so that it can be removed using the "tool".
f. Insert the cryogrinder tube into the cryogrinder so that the cap slot is aligned with the end of the tube chamber.
g. Use a low impact frequency for a total of 3 mins.
h. Collect the HA-CTA powder in a 50 ml centrifuge tube.
i. Repeat the previous steps to cryogrind the remaining half of the HA-CTA.
j. Periodically check the liquid nitrogen level and add more if needed.
k. Clean cryogrinder tubes with 2% Liquinox and DI H_2O. **Do not use solvents, including acetone**. Clean metal caps and magnet with 2% Liquinox, DI H_2O, and acetone.
l. Record the following in lab notebook:
    - Date, Process Start Time, Grind Time, Process End Time, and Oven in Time

7. Dry the ground HA-CTA in a vacuum oven (-25 mm Hg, 50°C) for 24 hours or until no change in weight is observed.
8. When dry, HA-CTA should be stored in a dessicator. Save a sample for FTIR analysis.

Notes

- Rinse all stir bars and spatulas with acetone and let air dry prior to use.
- Log lot numbers, etc. in documentation

Revision by NL (09/19/2013) – ADD MORE HERE. Changed "HA" to "NaHA." Changed sodium hyaluronate abbreviation in Materials and Equipment to match the procedure. Added abbreviation for DI H_2O to Materials and Equipment. Clarified wording. Changed bullets to numbers and changed formatting to match required thesis formatting guidelines.

Revision by CD (11/16/11) – Changed concentration of CTAB:DIH_2O and CTAB:NaHA to match SBM protocol.

References

Zhang, M. and James, S.P., (2005). *Silylation of hyaluronan to improve hydrophobicity and reactivity for improved processing and derivatization*. , **46**(11):3639-3648.

1.9.1 HA-CTA Silylation

HA-CTA Silylation

Objective
Hydrophobic modification of hyaluronan for reaction in anhydrous solvents

Materials & Equipment
- Hyaluronan-cetyl trimethylammonium complex (HA-CTA)
- Dimethyl sulfoxide ≥99.9% ReagentPlus (DMSO)
- Hexamethyldisilazane ≥99.9% ReagentPlus (HMDS ≥ 99.9% ReagentPlus)
- Hexamethyldisilazane ≥97.0% (HMDS ≥ 97.0%)
- 500 ml Round Bottom Flask (RBF)
- Graduated cylinders
- Serum stoppers
- Copper wire
- Needle nose pliers
- Keck clips
- Condenser
- Dry Nitrogen (N_2) gas
- Magnetic stir bars
- Stir plates
- Vacuum oven
- Vapor trap
- Vacuum pump

Procedure
Glassware preparation
Wash glassware with 2% liquinox, then rinse with DI H_2O, and then rinse with acetone. Place glassware in oven (125℃) for 24 hours. Remove glassware from oven and let cool. When cool, silylate glassware with HMDS ≥ 97.0% for at least 5 mins. Swish the HMDS around, making sure to contact the surface that will contact the silyl HA-CTA, staying below the neck of a RBF or separatory funnel. Pour HMDS into hazardous waste, and rinse the glassware with acetone. Place the glassware back in the oven for 10 mins to dry the acetone. Remove the glassware from the oven and let it cool. The glassware is now ready to use.

Add DMSO
1. Silylate a 50 ml graduated cylinder and a 500 ml RBF.
2. Place a stir bar and the cryoground HA-CTA powder into a 500 ml single neck RBF.
    - Be sure a sample for FTIR was taken.
3. Cap the RBF and a graduated cylinder with rubber stoppers and copper wire. The copper wire should be tight and pinch into the rubber.
4. Turn on the dry nitrogen and adjust to a low flow rate.
5. Vent the RBF and graduated cylinder with dry N_2. Depending on the nitrogen flow, venting five times for five seconds each time is recommended.
6. Add 50 ml of DMSO for every 1.5g of starting NaHA to the RBF via a cannula and dry N_2. Maintain positive pressure in the graduated cylinder and RBF. Mark the number of punctures in tally form on the bottle.

1.9.1 HA-CTA Silylation

7. Swell the HA-CTA in the DMSO at room temperature until it is gel-like (about 4-12 hours).
8. Lower the RBF into a 50℃ oil bath and continue to stir until the starting material is fully dissolved (4-24 hrs).
    - **Make sure the thermocouple light on the hot plate is turned on.**
9. Record the following in lab notebook:
    - Date, Time, Manufacturer, Lot number, Part number, date the bottle of DMSO was opened, and time the heat was turned on.

Add HMDS

10. Silylate a 25 ml graduated cylinder.
11. Cap a graduated cylinder with a rubber stopper and copper wire. The copper wire should be tight and pinch into the rubber.
12. Vent the graduated cylinder with dry N_2 before adding HMDS. Depending on the nitrogen flow, venting five times for five seconds each time is recommended.
13. Add 25 ml of HMDS ≥dd 25 mReagentPlus for every 1.5g of starting NaHA to the RBF via a cannula and dry N_2 while maintaining positive pressure in the graduated cylinder and RBF. Increase the temperature of the oil bath to 75℃ for 48 hours. Vigourous stirring is important to mix the HMDS and DMSO layers. Mark the number of punctures in tally form on the bottle.
    - **Make sure the thermocouple light on the hot plate is turned on.**
14. Periodically check stirring and hot plate temperature. Stirring is important for mixing the DMSO and HMDS to increase the degree of silylation.
15. Record the following in lab notebook:
    - Date, Time, Manufacturer, Lot Number, Part Number, and when the bottle of HMDS was opened.

Separating and washing silyl HA-CTA

16. Cool the reaction to room temperature.
17. Silylate a separatory funnel and a crystallizing dish.
18. Pour the reaction mixture into a 250 ml separatory funnel, and let the two phases separate for 5 mins.
    a. The upper layer contains HMDS and silylated HA-CTA.
    b. The bottom layer is DMSO.
19. Let the DMSO drain into a beaker and dispose of the DMSO into a hazardous waste bottle.
20. Let the upper layer drain into the RBF that was used for silylation. This RBF now contains the silyl HA-CTA.
21. Close the separatory funnel stopper and add 10 ml of xylenes. Cap the funnel and swirl the xylenes to rinse the funnel. Collect the xylenes into the RBF containing the silyl HA-CTA. The purpose of this rinse step is to increase the yield of silyl HA-CTA.
22. Wash the silyl HA-CTA using a rotavap.
    a. Fill the bowl of the rotavap with DI H_2O.
    b. Heat the DI H_2O to 60-70℃. If the water heats to 75℃, cool it down to prevent degradation of the silyl HA-CTA.
    c. Apply vacuum grease to the two stopcocks, to the top surface of the cold finger, and to the inside surface of the RBF condenser as needed (see how to grease a stopcock by Mike).

1.9.1 HA-CTA Silylation

d. Place the cold finger inside the outer condensing column.
e. Place the rubber gasket flat against the rotavap arm as seen in Figure XX.
f. Screw the grey clamp partially on as seen in Figure XX.
g. Hold the edge of the coldfinger flat against the gasket and screw the grey piece until snug.
h. Attach the RBF condenser using a keck clip.
i. Fill the inner cold finger with ice.
j. Check vacuum tubing connection between the coldfinger and pump.
    i. Follow pump protocols taped to front of fume hood along with below.
        1. Make sure the exhaust port of the pump is not blocked by the back wall of the fume hood (or anything else).
        2. Run the pump for a few (2-3) minutes before connecting it to the rotovap until it has warmed up.
        3. Once finished rotovapping, let the pump run for three minutes disconnected from the system to make sure no vapors remain in the pump.
k. Lower the rotavap arm using the lever so that the RBF containing silyl HA-CTA is partially submerged in water but still able to rotate.
l. Turn the vacuum pump strength to low, and turn the pump on. Wait for the vacuum to pull through the system.
m. Set the rotation speed to 60RPM.
n. Slowly increase the strength of the vacuum until vapor is pulled into the cold finger. Be careful to avoid boiling the solution because this could decrease the yield of silyl HA-CTA by pulling it into the cold finger.
o. When the silyl HA-CTA is mostly dry, turn the rotation off, turn the vacuum pump strength down, and turn the vacuum pump off.
p. Raise the rotavap arm using the lever.
q. Release the vacuum from the system using the upper stopcock, and let air back into the tubing by opening and closing the stopcock a few times.
r. Gently twist and pull the RBF containing silyl HA-CTA off of the rotavap.
s. Add 40 ml of xylenes to the RBF, cover with a serum stopper, and dissolve the silyl HA-CTA by swirling the flask.
t. When dissolved, uncap the RBF and attach it to the rotavap using a keck clip.
u. Wash the xylenes as in the previous steps.
v. Add xylenes 4 more times and wash as described, for a total of 5 washes with xylenes (in addition to the first wash in HMDS).

. The sample should be allowed to crystallize on washes 2 and 4 and the time recorded for the sample to dissolve back into xylenes recorded.
w. On the last wash, leave a few milliliters (~5 ml) of xylenes in the flask.
x. Pour the silyl HA-CTA/xylenes into a silylated crystallizing dish.
y. Add 5 ml more xylenes to the RBF to dissolve any remaining silyl HA-CTA, and pour it into the same crystallizing dish.
23. Dry the silyl HA-CTA at 50℃ using a vapor trap until no weight change is observed. Save a sample for FTIR analysis. A yield of 2.0-2.5 g of silyl HA-CTA is expected when starting with 1.5 g NaHA.
24. Record the following in lab notebook:

1.9.1 HA-CTA Silylation

- Date, Time, Oven in Time, Oven out Time, and Final Weight.

Note

- Cannula transfers should be done with at least two people. Never try a cannula transfer alone.

Protocol History

Revision by NL (09/19/2013) – ADD MORE HERE. Updated Materials and Equipment. Added glassware preparation procedure. Added nitrogen venting for glassware. Updated separating and washing procedure. Changed HMDS stir time from 72-96 hours to 48 hours. Changed "HA" to "NaHA." Changed sodium hyaluronate abbreviation in Materials and Equipment to match the procedure. Added abbreviation for DI H_2O to Materials and Equipment. Clarified wording. Changed bullets to numbers and changed formatting to match required thesis formatting guidelines.
Revision by JG (02/21/2013)
Originator: CD

References

Kurkowski, R. *The chemical crosslinking, compatibilization, and direct molding of ultra high molecular weight polyethylene and hyaluronic acid microcomposites*, M.S. thesis, Colorado State University Department of Mechanical Engineering, Fort Collins, CO (2007).
Zhang, M. and James, S.P., (2005). *Silylation of hyaluronan to improve hydrophobicity and reactivity for improved processing and derivatization*. , **46**(11):3639-3648.

Appendix II: Data and figures

XPS outputs

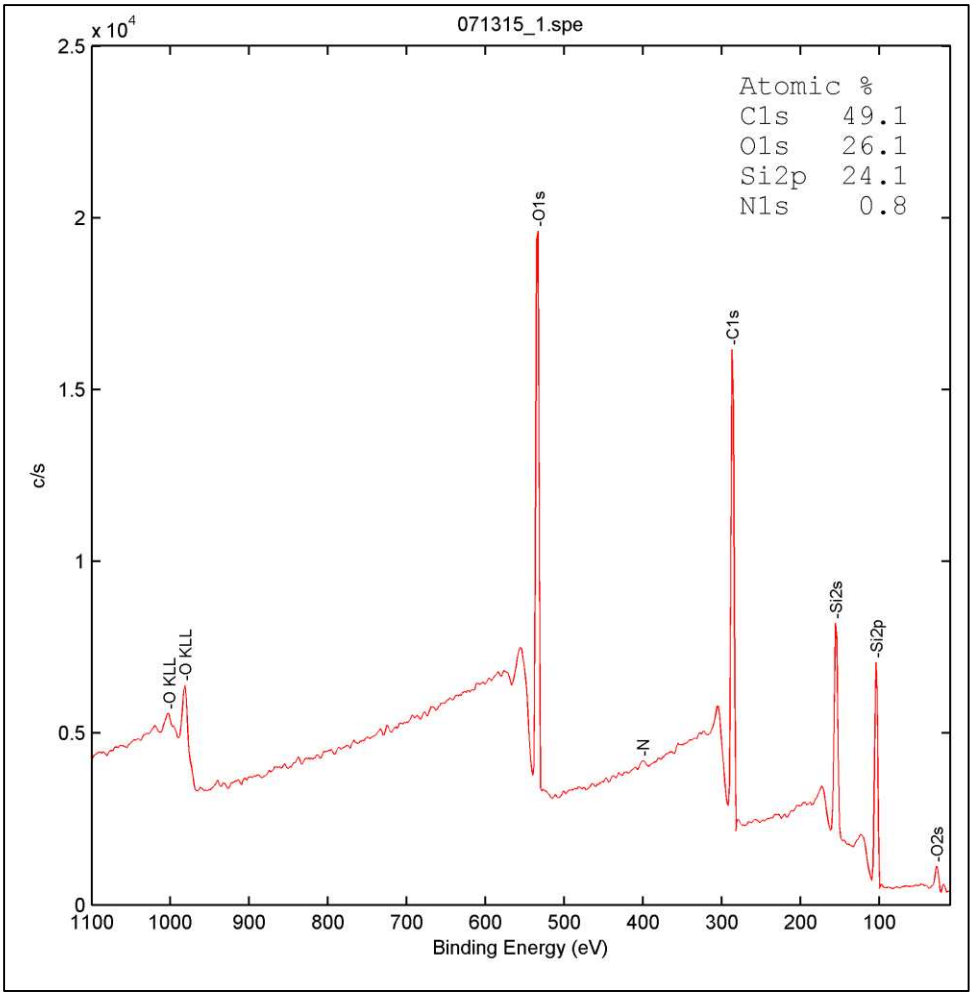

Figure A.1: XPS analysis output for a sham silicone film. The approx. 2:1:1 ratio of C:O:Si is expected and implies a lack of modification to the sample. The small amount of detected nitrogen is likely either noise or contamination.

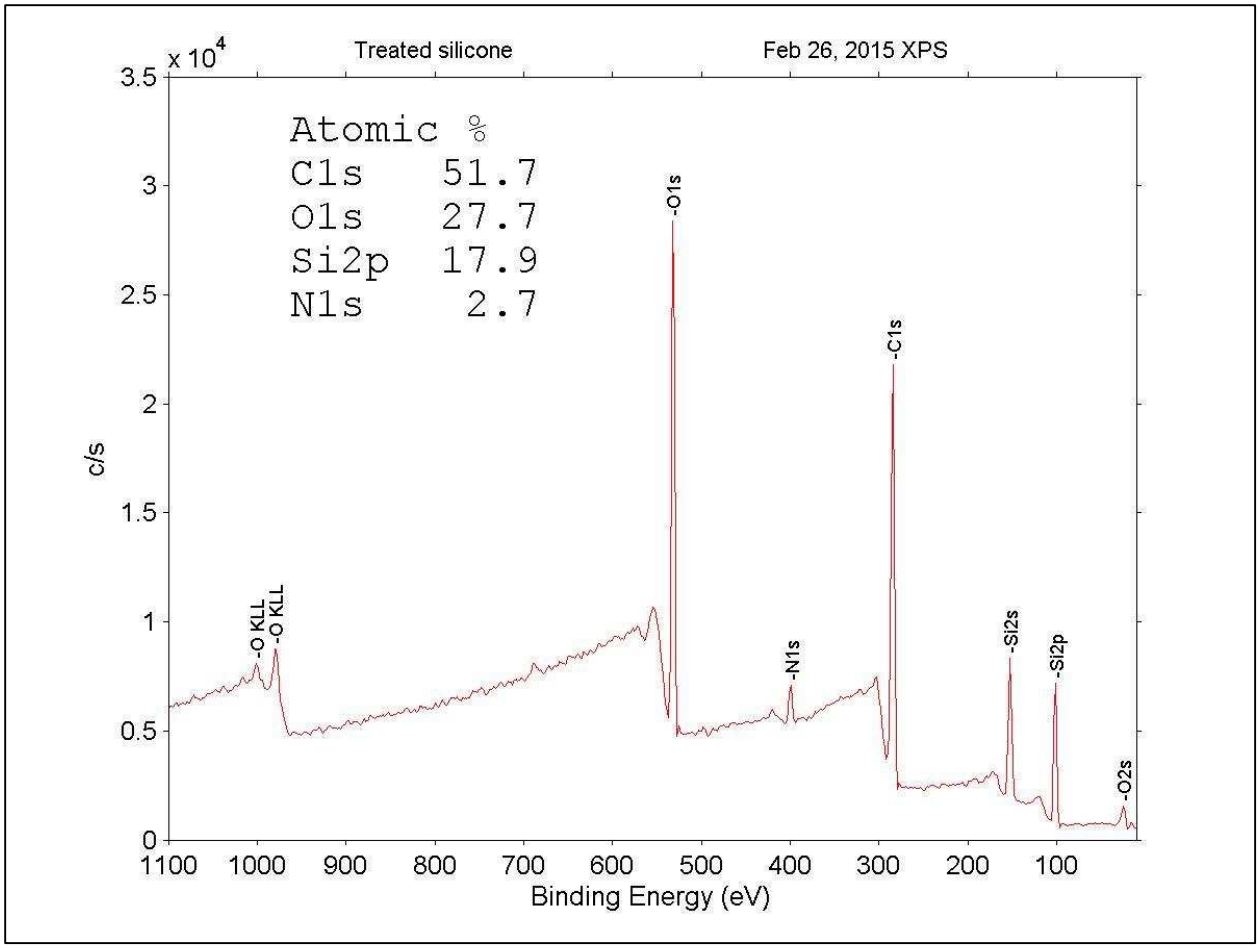

Figure A.2: XPS output for an HA treated silicone film. Note shift in the C:O:Si atomic ratio in favor of more carbon and oxygen, as would be expected from the inclusion of hyaluronan. Additionally, the presence of nitrogen also indicates HA inclusion to the surface.

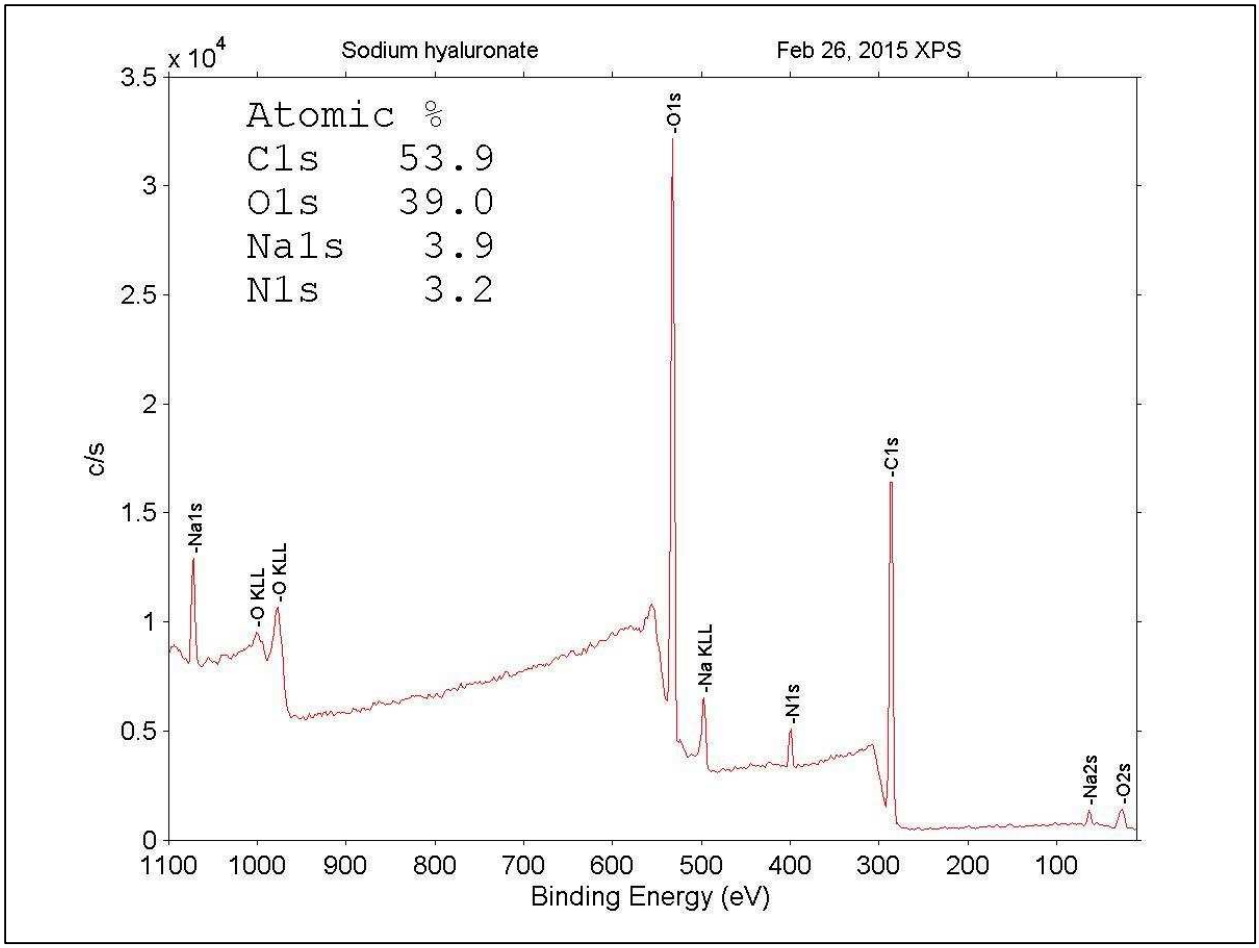

Figure A.3: XPS output for pure powdered sodium hyaluronate, as received by the manufacturer (Lifecore Biomedical, LLC).

Larger images from Calcein stained samples

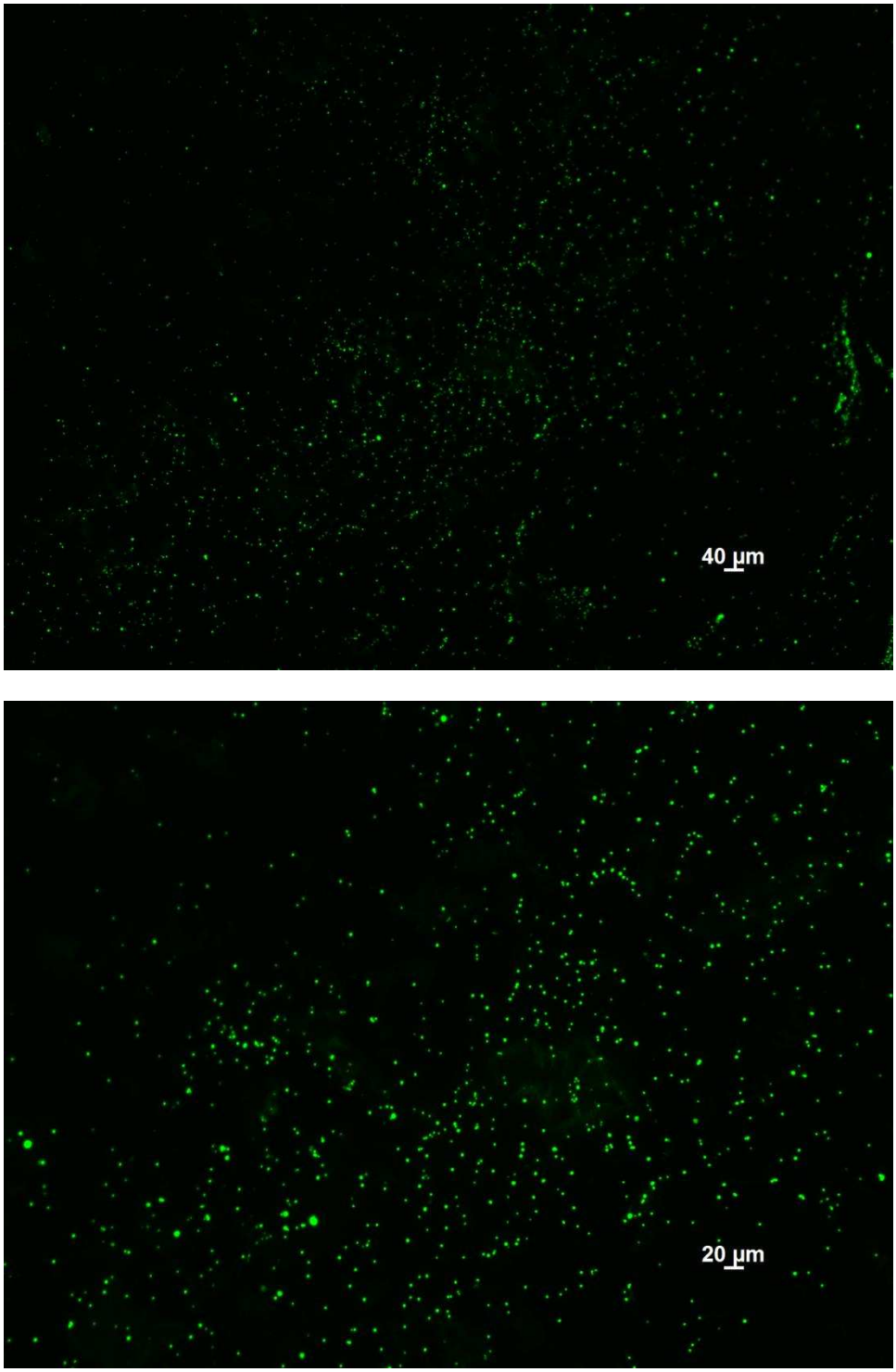

Figure A.4: Fluorescent microscopy of Calcein stained, untreated PDMS. 5x (top) and 10x (bottom) magnification

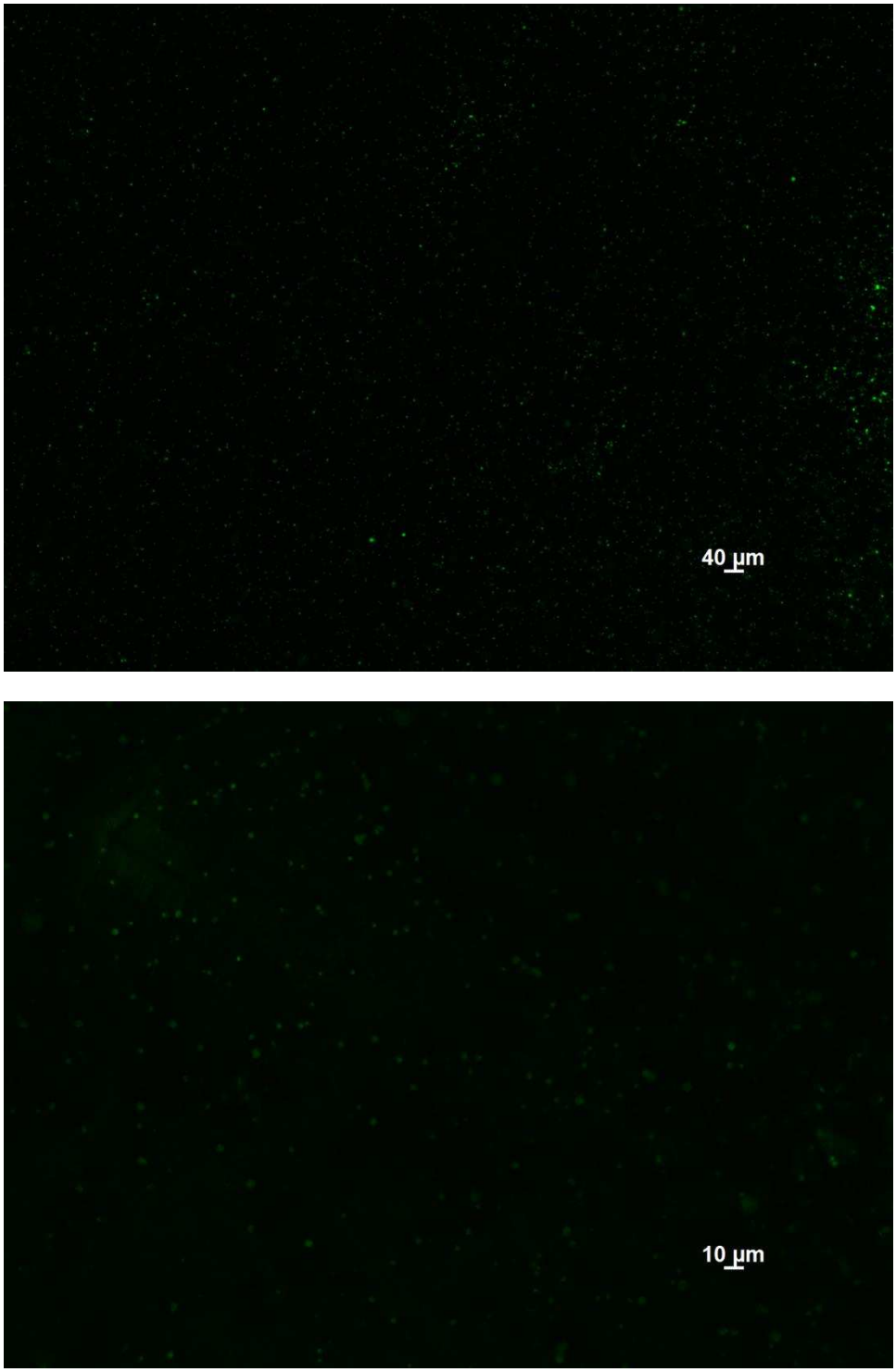

Figure A.5: Fluorescent microscopy of Calcein stained, treated PDMS. 5x (top) and 20x (bottom) magnification

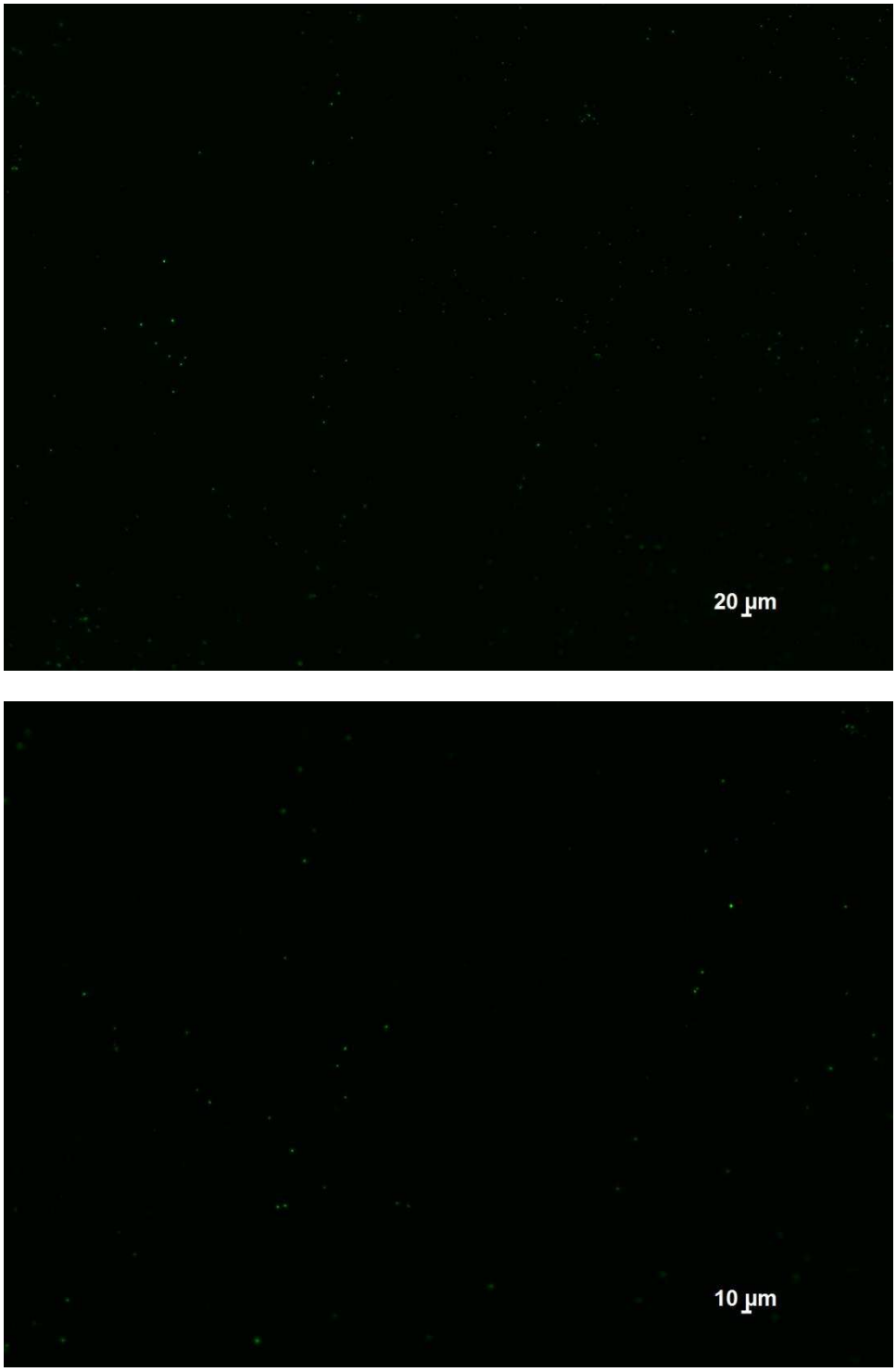

Figure A.6: Fluorescent microscopy of Calcein stained, Tissue Culture Polystyrene (TCPS). 10x (top) and 20x (bottom) magnification

Larger images from SEM fixed samples

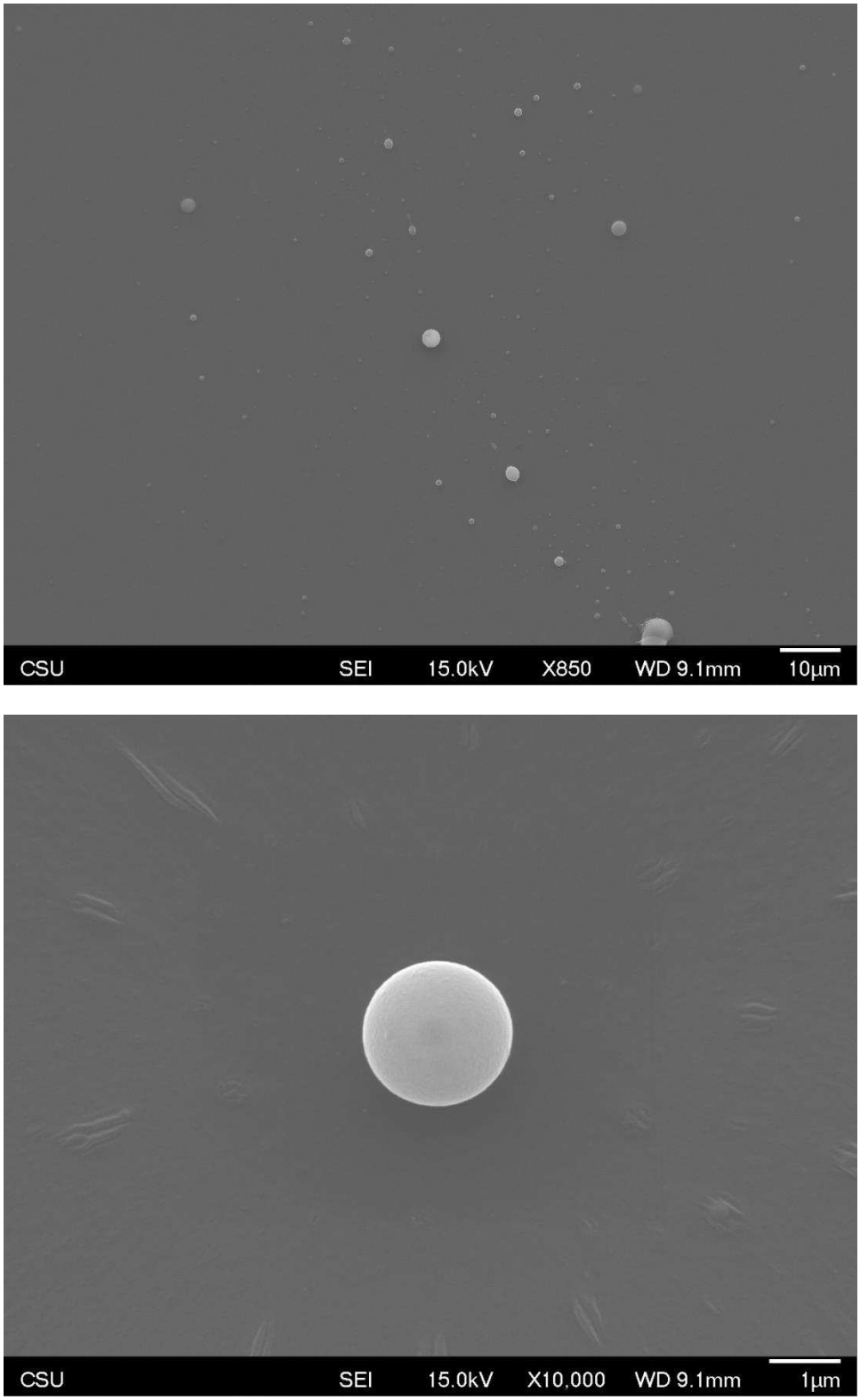

Figure A.7: SEM images of glutaraldehyde fixed untreated PDMS sample

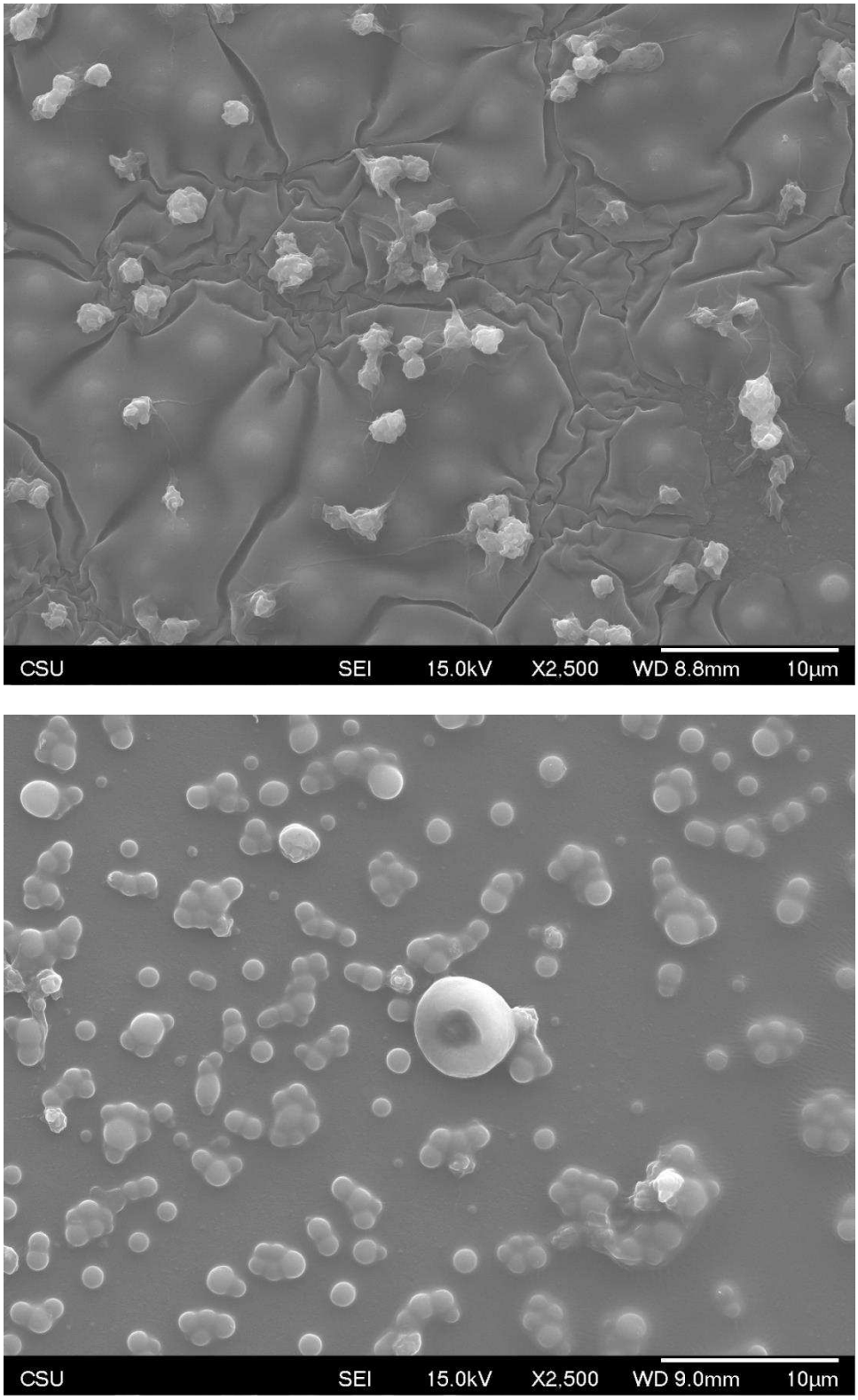

Figure A.8: SEM images of glutaraldehyde fixed treated PDMS sample

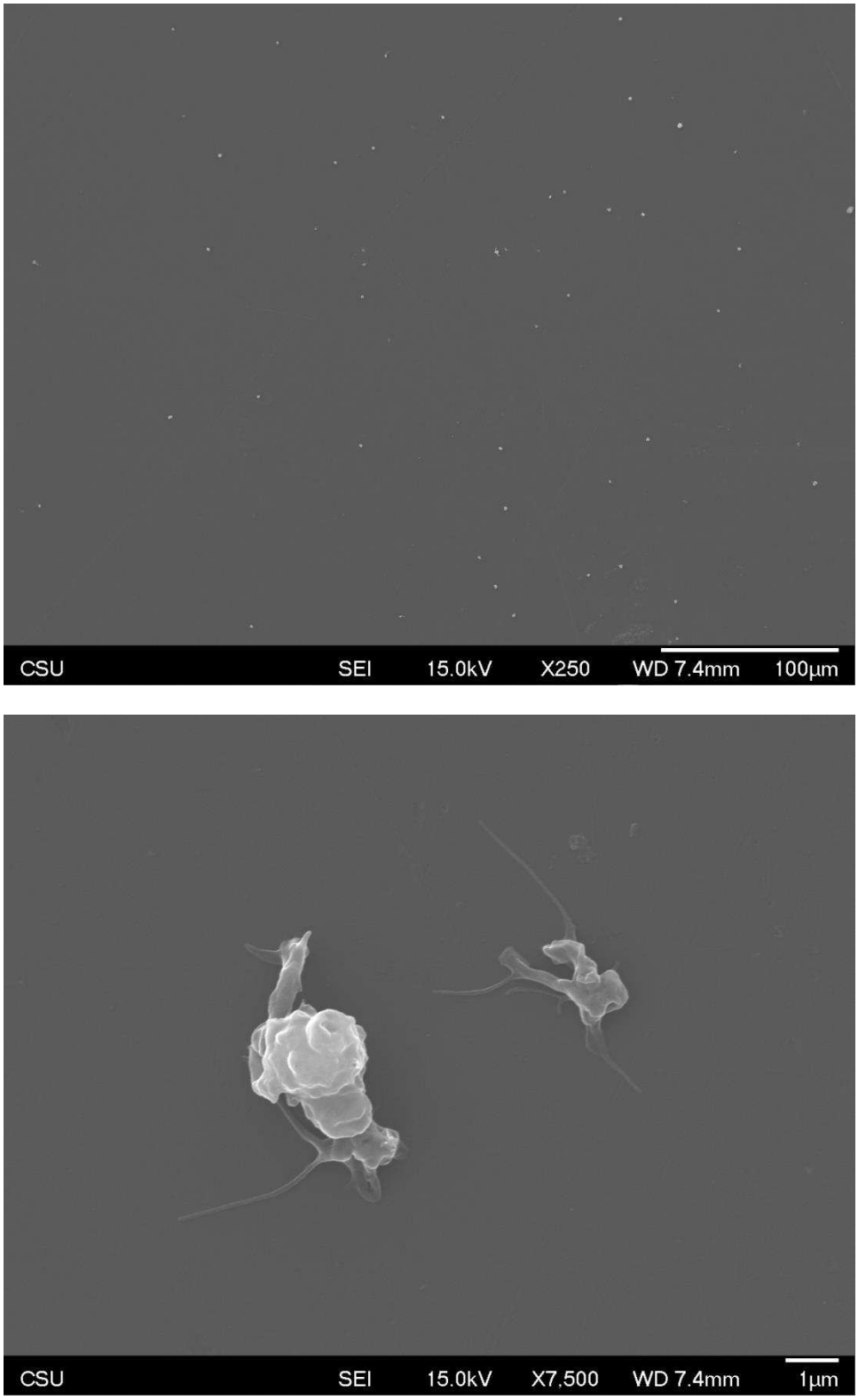

Figure A.9: SEM images of glutaraldehyde fixed TCPS control sample

LDH assay kit product insert (manual)

QuantiChrom™ LDH Cytotoxicity Assay Kit (C2LD-100)

Quantitative Colorimetric Assay of LDH Released in Cell Culture Medium

DESCRIPTION

LACTATE DEHYDROGENASE (LDH) is an oxidoreductase which catalyzes the interconversion of lactate and pyruvate. Cytotoxic compounds often compromise cell membrane integrity by inducing apoptosis or necrosis. LDH is a stable cytosolic enzyme that upon membrane damage is released into the cellular environment. Therefore, LDH is often measured to evaluate the presence of tissue or cell damage. The colorimetric LDH release assay is a simple and robust method to assess cytotoxic effects on cells by measuring the activity of LDH in cell culture supernatant. The assay is based on the reduction of a tetrazolium salt to a formazan dye.

KEY FEATURES

Safe. Non-radioactive assay.

Fast. Single reagent assay. High-throughput assay using 96-well plates allows simultaneous processing tens of thousands of samples per day.

Homogeneous and convenient. "Mix-incubate-measure" type assay. No wash steps are involved.

Robust and amenable to HTS. Can be readily automated with HTS liquid handling systems.

APPLICATIONS

Cytotoxicity and Apoptosis: evaluation of toxic compounds, toxins, detergents, environmental pollutants etc.

Drug Discovery: high-throughput screen for drug toxicity.

KIT CONTENTS (100 Tests in 96-Well Plate)

Reagent: 20 mL **Triton X-100:** 1 mL 20%

Storage conditions. The kit is shipped at room temperature. Store kit at 2-8°C upon receiving. Shelf life: 12 months after receipt.

Precautions: Reagents are for research use only. Normal precautions for laboratory reagents should be exercised while using the reagents. Please refer to Material Safety Data Sheet for detailed information.

PROCEDURE

Sample Preparation: Cells should be in logarithmic growth phase for the assay. Subculture cells 2 days before the experiment. Medium containing 10% FBS is compatible with the assay: it is not necessary to subculture cells in FBS free medium.

1. Plate and culture cells (100 µL per well) in a 96-well tissue culture plate. Assays can be performed on either adherent cells or cells in suspension. The number of cells can vary with cell type, but a range between 10,000 and 40,000 cells per well for adherent cells and between 40,000 and 160,000 suspension cells will be appropriate for most mammalian cell types. In addition to the test samples, one must include extra wells of cells without treatment (Control) and wells of cells treated with Triton X-100 (Total Lysis).
2. Add 10 µL test compounds to sample wells, 10 µL dH_2O to Control wells, and 10 µL 20% Triton X-100 to the Total Lysis control wells, and incubate cells for four hours or desired period of time at 37°C. It is recommended that assays be run in duplicate or triplicate.
3. Equilibrate reagent to room temperature. Add 160 µL of Reagent per well and incubate at room temperature for 10 minutes.
4. Measure OD_{500nm} for each well in an absorbance plate reader. The suitable absorbance range for the formazan dye is between 490 and 510 nm. We recommend reading at 500 nm.

CALCULATION

Cytotoxicity is calculated as the percentage of the maximum LDH release in the Total Lysis wells in the Sample wells, as follows:

$$\text{Cytotoxicity} = \frac{OD_{Sample} - OD_{Control}}{OD_{Total\ Lysis} - OD_{Control}} \times 100\ (\%)$$

Where OD_{Sample}, $OD_{Control}$ and $OD_{Total\ Lysis}$ are absorbance values of the sample, the no treatment control and the Triton X-100 treated cells respectively.

MATERIALS REQUIRED, BUT NOT PROVIDED

Pipetting devices and accessories, clear flat-bottom 96-well tissue culture plates (e.g. Sigma cat# M0812), microplate reader.

EXAMPLE

Dose Response: PANC-1 cells were seeded at 20,000 cells per well and allowed to settle overnight. Test compounds (Triton X-100, Saponin, Tween 20) were diluted in complete medium (RPMI1640, 10% FBS) and incubated with cells for 4 hours. Cytotoxicity of test compounds was assayed as increased release of LDH into the culture media.

Time Response: PANC-1 cells were seeded at 20,000 cells per well and allowed to settle overnight. 0.025% Triton X-100 was diluted in complete medium, then added to cells at the appropriate time. Cytotoxicity of test compounds was assayed as increased release of LDH into the culture media.

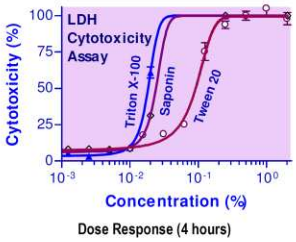

Dose Response (4 hours)

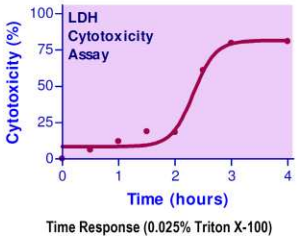

Time Response (0.025% Triton X-100)

LITERATURE

1. Korzeniewski C. and Callewaert DM. (1983). An enzyme-release assay for natural cytotoxicity. J Immunol Methods 64(3): 313-320.
2. Weidmann E. et al. (1995). Lactate dehydrogenase-release assay: A reliable, nonradioactive technique for analysis of cytotoxic lymphocyte-mediated lytic activity against blasts from acute myelocytic leukemia. Ann Hematol 70(3): 153-158.
3. Kawai et al. (1992). Additive effects of antitumor drugs and lymphokine-activated killer cell cytotoxic activity in tumor cell killing determined by lactate-dehydrogenase-release assay. Cancer Immunol Immunother 35(4):225-229.